

Diss. ETH. NO. 28924

**Generation of functional xenogeneic germ and muscle  
stem cells via interspecies chimerism**

A thesis submitted to attain the degree of  
DOCTOR OF SCIENCES  
(Dr. sc. ETH Zurich)

presented by

Joel Moran Zvick  
MSc ETH in Health Sciences and Technology, ETH Zurich  
Born on 31.07.1987

Accepted on the recommendation of  
Prof. Dr. Ori Bar-Nur  
Prof. Dr. Micha Drukker  
Prof. Dr. Francesco Saverio Tedesco  
Prof. Dr. Ferdinand von Meyenn

2023



## Summary

Pluripotent stem cells (PSCs), including embryonic and induced pluripotent stem cells (ESCs and iPSCs) can contribute to all germ layers of the developing embryo when injected into host blastocysts, which results in chimeric animals. These properties can be harnessed to generate donor PSC derived cells and tissues across species boundaries. Blastocyst complementation is a promising technique exploiting this observation, wherein the host blastocysts carry mutations hindering the formation of specific cells, allowing the injected PSCs to populate this developmental niche and generate cells or tissues exclusively derived from the donor PSCs.

Generation of male gametes *in vitro* is investigated not only for the study of how germ cells are formed, but also for potential species conservation efforts. However, it often relies on testes of the species of interest being available, which is not feasible for rare species. To overcome this limitation, in the first study, we aimed to generate exclusively donor PSC derived spermatozoa via blastocyst complementation with mouse-to-mouse intra- and rat-to-mouse interspecies chimeras. To this end, we injected the donor cells into mouse *Tsc22d3*-knockout (KO) blastocysts, which carried a defect in meiosis I, causing male sterility in non-complemented animals. Resultant intraspecies chimeras harbored exclusively allogeneic donor mouse PSC derived spermatozoa, and were fertile upon natural mating with female mice. In addition, injection of rat rESCs into *Tsc22d3*-KO blastocysts resulted in mouse-rat chimeras, and analysis of testes and spermatozoa revealed exclusive generation of xenogeneic donor rESC derived germ cells, which was further confirmed by single-cell RNA-sequencing. Fertilizing rat oocytes using chimera derived rat spermatozoa led to the generation of blastocysts *in vitro*, and implantation sites and embryos *in vivo*, although no offspring was generated.

In the second project, blastocyst injections were utilized to generate muscle stem cells, also termed satellite cells, conferring the skeletal muscle's immense capacity for regeneration, which is lost in muscular dystrophies. We generated iPSCs from a muscular dystrophy mouse model, gene-corrected the present mutation using CRISPR/Cas9 and utilized the iPSCs to generate intraspecies chimeras. The host blastocysts carried a satellite cell specific ablation system allowing for exclusive generation of donor cell derived satellite cells. Upon isolation of the iPSC derived satellite cells, and *in vitro* propagation, the resulting myoblasts were transplanted into the *Tibialis anterior* muscles

of dystrophic mice, where they expressed dystrophin. Further, we generated interspecies chimeras via injection of the iPSCs into rat blastocysts. We were able to purify mouse satellite cells from these chimeras, expanded and characterized them *in vitro*, and we observed contribution of the myoblasts to dystrophin expression *in vivo* in dystrophic recipient muscles.

These results show that generation of interspecies chimeras carries the potential to not only generate xenogeneic germ cells, potentially capable of aiding in species conservation, but also adult muscle stem cells, which could help in paving the way to treat muscular dystrophies in human patients.



## Zusammenfassung

Pluripotente Stammzellen (PSZ), inklusive embryonaler und induzierter pluripotenter Stammzellen (ESZ und iPSZ), können zu allen Keimblättern des sich entwickelnden Embryos beitragen wenn sie in Empfänger-Blastozysten injiziert, was zur Bildung von chimären Tieren führt. Diese Eigenschaften können genutzt werden, um speziessübergreifend Spender-PSZ abgeleitete Zellen oder Gewebe zu generieren. Blastozysten-Komplementierung ist eine vielversprechende Technik welche diese Beobachtung nutzt, wobei die Empfänger-Blastozysten Mutation in sich tragen, welche die Genese bestimmter Zellen unterbindet, und dadurch den Spender-PSZ ermöglicht, eine Entwicklungsnische zu besiedeln, und Zellen und Gewebe welche ausschliesslich von den Spender-PSZ stammen zu bilden.

Die Generierung von männlichen Gameten *in vitro* wird nicht nur für das Studium der Keimzellbildung verwendet, sondern auch für potenzielle Anstrengungen im Artenschutz. Jedoch sind oft Testes der Spezies von Interesse nötig, was für seltene Spezies nicht machbar ist. Um diese Einschränkung zu überwinden, hatten wir in der ersten Studie zum Ziel, ausschliesslich Spender-PSZ abgeleitete Spermatozoen via Blastozysten-Komplementierung mit Maus-zu-Maus intra- und Ratte-zu-Maus interspezifischen Chimären zu bilden. Dazu haben wir die Spenderzellen in Maus *Tsc22d3*-ausgeschaltetet (KO) Blastozysten injiziert, welche einen Defekt in Meiose I in sich tragen, was zu Sterilität in allen nicht komplementierten Männchen führt. Die daraus resultierten intraspezifischen Chimären hatten Spermien welche ausschliesslich von den Spender-PSZ abgeleitet waren, und waren fruchtbar bei natürlicher Verpaarung mit weiblichen Mäusen. Weiter haben wir Ratten ESZ in *Tsc22d3*-KO Blastozysten injiziert, wodurch Maus-Ratten Chimären gebildet wurden, und Analyse derer Testes und Spermatozoen zeigte auf, dass nur xenogeneische von den Spender-rESZ abgeleitet Keimzellen gebildet wurden, was auch mittels Einzelzell-RNA-Sequenzierung bestätigt wurde. Die Befruchtung von Ratten-Oozyten mittels von Chimären abgeleiteten Rattenspermatozoen führte zur Bildung von Blastozysten *in vitro*, und Nidationsstellen und Embryos *in vivo*, jedoch wurden keine Nachkommen geboren.

Im zweiten Projekt, wurden Blastozysten-injektionen dazu benutzt um Muskelstammzellen zu generieren, auch Satellitenzellen genannt, welche ursächlich sind für die beachtliche Regenerationskapazität von Skelettmuskeln, welche im Falle von

Muskeldystrophien verloren geht. Dazu haben wir iPSZ eine Mausmodelles von Muskeldystrophie generiert, in diesen mittels CRISPR/Cas9 gen-korrigiert und diese iPSZ verwendet, um intraspezifische Chimären zu generieren. Die Empfänger-Blastozysten haben eine Mutation in sich getragen, welche die gezielte Abtragung ihrer Satellitenzellen ermöglicht, und wodurch ausschliesslich Spenderzellen abgeleitete Satellitenzellen gebildet werden. Auf die Isolation der iPSZ abgeleiteten Satellitenzellen und deren *in vitro* Vermehrung folgend, wurden die daraus gebildeten Myoblasten in die *Tibialis anterior* Muskeln von dystrophischen Mäusen transplantiert, woraufhin sie Dystrophin exprimierten. Weiter haben wir interspezifische Chimären gebildet mittels Injektion der iPSZ in Ratten-Blastozysten. Wir konnten Maus-Satellitenzellen aus diesen Chimären aufreinigen, diese *in vitro* Vermehren und Charakterisieren, und wir konnten einen Beitrag der Myoblasten zur Dystrophin Expression *in vivo* in dystrophischen Empfängermuskeln beobachten.

Diese Resultate zeigen auf, dass die Bildung von interspezifischen Chimären nicht nur das Potenzial hat, xenogeneische Keimzellen zu bilden, welche Möglicherweise im Artenschutz verwendet werden können, sondern auch adulte Muskelstammzellen, welche den Weg hin zur Behandlung muskulärer Dystrophien in humanen Patienten pflastern können.

## Abbreviations

BCI	Blastocyst complementation
BMP	Bone morphogenetic protein
CRISPR	Clustered regularly interspaced short palindromic repeats
DMD	Duchenne muscular dystrophy
E	Embryonic day
EpiLC	Epiblast like cells
EpiSC	Epiblast stem cell
FACS	Fluorescence activated cell sorting
<i>Gilz</i>	Glucocorticoid-induced leucine zipper
GSK3	Glycogen synthase kinase-3
hESC	Human embryonic stem cells
hiPSC	Human induced pluripotent stem cells
hPSC	Human Pluripotent stem cells
ICM	Inner cell mass
ICSI	Intracytoplasmic sperm injection
KO	Knockout
LIF	Leukemia inhibitory factor
mESC	Mouse embryonic stem cells
miPSC	Mouse induced pluripotent stem cells
mPSC	Mouse Pluripotent stem cells
MEK	Mitogen-activated protein kinase kinase
<i>MyoD</i>	Myoblast determination protein 1
rESC	Rat embryonic stem cells
riPSC	Rat induced pluripotent stem cells
rPSC	Rat Pluripotent stem cells
P	Day post-partum
PCR	Polymerase chain reaction
PGCLC	Primordial germ cell like cell
ROSI	Round spermatid injection
<i>Pax3</i>	Paired box protein 3
<i>Pax7</i>	Paired box protein 7
<i>Prdm1</i>	PR domain zinc finger protein 1
<i>Prdm14</i>	PR domain zinc finger protein 14

<i>Pdx1</i>	Pancreatic and duodenal homeobox 1
<i>Sox9</i>	SRY-Box Transcription Factor 9
<i>Sry</i>	Sex determining region Y
SSC	Spermatogonial stem cell
SSCT	Spermatogonial stem cell transplantation
<i>Tcfap2</i>	Transcription factor activator protein AP-2
TE	Trophectoderm
TESE- ICSI	Testicular sperm extraction ICSI
XEN	Extraembryonic endoderm stem cells

# Table of Contents

Summary .....	i
Zusammenfassung .....	iii
Abbreviations.....	v
Table of Contents .....	vii
Chapter 1. General Introduction .....	1
1.1.1 Pluripotency .....	1
1.1.2 Induced pluripotency .....	2
1.1.3 Blastocyst complementation .....	3
1.2 Germline .....	5
1.2.1 From stem cells to spermatozoa .....	5
1.2.2 In vitro gametogenesis .....	8
1.2.3 The formation of spermatogenic niches .....	10
1.2.4 Generation of xenogeneic germ cells.....	10
1.3 Muscle .....	11
1.3.1 Skeletal muscle regeneration .....	11
1.3.2 Duchenne Muscular Dystrophy .....	13
1.3.3 Treatment approaches for DMD.....	14
Chapter 2. Aims of the thesis .....	17
Chapter 3. Exclusive generation of rat spermatozoa in sterile mice utilizing blastocyst complementation with pluripotent stem cells .....	18
Chapter 4. Interspecies generation of functional muscle stem cells .....	61
Chapter 5. Discussion .....	90
5.1 Exclusive generation of rat spermatozoa in sterile mice.....	90
5.2 Interspecies generation of functional muscle stem cells.....	95
5.3 Blastocyst complementation in a human context.....	99
Chapter 6. Appendix.....	104
6.1 Supplemental Figures .....	104
Acknowledgements.....	105
Bibliography.....	106
Curriculum Vitae .....	<b>Error! Bookmark not defined.</b>

# Chapter 1. General Introduction

---

## 1.1.1 Pluripotency

Every mammalian life relying on sexual reproduction begins with the fertilization of the female gamete, the oocyte, with a male gamete, the spermatozoon. It is this crucial process which gives rise to the diploid and totipotent zygote, a single cell out of which all the embryonic as well as extra-embryonic tissues develop, ultimately leading to the generation of a whole organism.

Soon after fertilization, the 8-cell-stage embryo, made of equally totipotent blastomeres, is compacting into the morula<sup>1</sup>. The spherical morula consists of 16 to 32 cells, and the outer layer is made of polar cells developing towards the extraembryonic trophoblast (TE) lineage, which will go on to form the placenta, and the inner apolar cells, which will give rise to the inner cell mass (ICM) of the blastocyst<sup>1,2</sup>. At embryonic day 3.5 (E3.5) on the inside of the early blastocyst a cavity called the blastocoel is beginning to form. The cells of the ICM express markers either for the pluripotent epiblast stem cells (EpiSC), such as Nanog and Oct4, or for the primitive endoderm (PrE), such as Gata6<sup>1,2</sup>. The EpiSCs will contribute to the whole developing embryo, whereas the PrE cells will commit their fate towards the yolk sack and the extraembryonic endoderm. The cells continue to organize themselves, and in the late blastocyst stage the EpiSCs are packed between the TE cells towards the outside, and the PrE cells towards the blastocoel<sup>1,2</sup>. Up to this point, the cells have already undergone two cell fate decisions, between ICM and TE, and PrE and EpiSC, but many more are to follow during embryogenesis until birth<sup>3</sup>. To continue embryonic development, the blastocyst implants into the uterine wall between E4.75 to E5<sup>4</sup>.

From the ICM of pre-implantation blastocysts, embryonic stem cells (ESCs) can be isolated for further *in vitro* culture<sup>5</sup>. Before the isolation of mouse ESCs (mESCs) in 1981, embryonal carcinoma cells were the only pluripotent stem cells available<sup>6-8</sup>. However, it is also possible to isolate extra-embryonic endoderm stem cells (XEN) from the PrE and trophoblast stem cells (TSCs) from the trophoblast<sup>9,10</sup>. First reports of human ESCs (hESCs) followed in 1998<sup>11</sup>. For another common research animal, the rat, it took another decade to generate rat ESCs (rESCs) in 2008<sup>12,13</sup>. The two key hallmarks of pluripotency are self-renewal and the potential to differentiate into any cell type of the three embryonic germ layers<sup>14</sup>. One of the gold standards of evaluating pluripotency of ESCs is the teratoma formation assay, in which ESCs are injected into immunodeficient

mice and give rise to teratomas, which contain all three germ layers of the endo-, meso- and ectoderm<sup>15</sup>. More importantly, ESCs have the capability to give rise to all tissues of the developing embryo, including the germline, upon injection into blastocysts<sup>14</sup>. A more stringent evaluation of ESC functionality is tetraploid complementation, a method allowing for generation of animals derived only from donor cells<sup>14</sup>. Tetraploid 4n embryos are generated by electrofusion of 2-cell zygotes and upon culture to the blastocyst stage, PSCs can be injected. While the tetraploid cells are restricted towards the extraembryonic lineage, the donor PSCs develop to the embryo proper<sup>14,16,17</sup>

While mouse and rat ESCs are maintained in a naïve state (i.e. resembling the ICM of pre-implantation blastocysts), hESCs are more closely matching peri- and post-implantation EpiSCs which are primed for specification into a cell lineage<sup>18</sup>. Thus, they also differ in their culture conditions and dependence on support from feeder cells, cytokines or small molecules to maintain pluripotency<sup>18</sup>. For example, mESCs were commonly cultured on mitotically inactivated feeder cells in medium containing serum and leukemia inhibitory factor (LIF) to inhibit differentiation. However, in recent years more defined serum-free media formulations containing the GSK3 inhibitor CHIR99021 and the MEK inhibitor PD0325901 have been reported, with some even claiming vastly superior chimera formation efficiency, while contrasting publications reported on prolonged MEK inhibition negatively affecting chimera formation efficiency<sup>19-21</sup>. Unlike mESCs, rESCs are exclusively maintained in serum free conditions, with only very minor differences in media composition<sup>12,13</sup>.

### 1.1.2 Induced pluripotency

In 2006, a seminal study performed by Takahashi and Yamanaka showed the feasibility of generating pluripotent stem cells termed induced pluripotent stem cells (iPSC) from somatic cells<sup>22</sup>. Via overexpression of the pluripotency associated transcription factors and oncogenes Oct4, Klf3/4, Sox2 and c-Myc, mouse fibroblasts were reprogrammed to pluripotency, exhibiting ESC morphology, and also matching ESCs in terms of gene expression very closely, however the epigenetic state is more disputed<sup>23,24</sup>. Akin to ESCs, iPSCs also contribute to the developing embryo and can give rise to chimeric animals, exhibiting germline transmission potency and giving rise to entirely iPSC derived animals upon tetraploid complementation<sup>25</sup>. The generation of iPSCs has not only opened up many opportunities for basic research, but also for regenerative medicine<sup>26-28</sup>. It holds promise for the generation of patient derived iPSCs,

which can be generated from easily obtainable skin biopsies or blood<sup>29,30</sup>. These could be utilized for *in vitro* disease modelling and drug testing, allowing to find drugs best suited for a specific patient, and could also be used to generate autologous cells from *in vitro* differentiated hPSCs<sup>30</sup>. It could also be envisioned that human autologous cells or tissues could be derived via blastocyst complementation with large mammal hosts<sup>31</sup>.

### 1.1.3 Blastocyst complementation

Blastocyst complementation (BCI) has been pioneered in a groundbreaking study by Chen and colleagues in 1993<sup>32</sup>. Recombination-activating gene 2 (RAG-2) is crucial for the formation of mature B and T cells, and mice lacking the gene are devoid of lymphocytes, rendering them immunodeficient. However, upon injection of donor mouse ESCs into a RAG-2 *-/-* blastocyst, followed by transplantation of the embryo into a foster mother, all the lymphocytes of the resulting chimeras were derived from the donor cells, also resolving the immunodeficiency of the chimeras<sup>32</sup>. This publication was the first to take advantage of an empty developmental niche in blastocysts harboring knockout (KO) mutations, precluding the formation of specific cells, tissues or organs. Since competition for these niches from host cells is eliminated, the injected donor ESCs can complement the niche during embryogenesis, eventually generating entirely the specific cell population or even an organ in the animal post-partum<sup>32</sup>.

It was not until a decade later that this approach was utilized to study the development of a whole organ, namely the pancreas<sup>33</sup>. An inducible system to ablate *Pdx1* expressing cells was used, since *Pdx1* is indispensable for the formation of the pancreas, generating a donor cell derived pancreatic epithelium. This study also established the number of progenitor cells as one of the key determinants of organ size. However, the focus was on embryonic development, and no live birth of chimeric animals was reported<sup>33</sup>.

After the discovery of rat PSCs, the next step was to trial interspecies blastocyst complementation. First steps towards the generation of interspecies chimeras were taken in the 1970s, when different approaches were trialed to generate rat-to-mouse chimeras. By aggregation of mouse and rat morulae, and injections or aggregations of rat ICM cells into mouse blastocysts, chimeric embryos were formed<sup>34-36</sup>. This was followed up by combining bank vole (*Clethrionomys glareolus*) morulae together with mouse morulae, culturing them to the blastocyst stage *in vitro* and transplantation into recipient female mice<sup>37</sup>. Only two normal looking embryos developed until E9 and E10, respectively, and



both showed only low chimeric contribution<sup>37</sup>. It was not until 1980 that viable interspecies chimeras between *Mus musculus* and *Mus caroli* were generated<sup>38</sup>. In a landmark study in 2010, Kobayashi and colleagues confirmed the feasibility of inter-specific BCI between mouse hosts, and rat iPSC donor cells<sup>39</sup>. Capitalizing on a *Pdx1*-KO mouse blastocyst, which in an uncomplemented state leads to embryonic lethality, they injected rat iPSCs and brought the animals to term. Strikingly, this resulted in interspecies chimeras being born. Several findings were of importance in this study. First, the rat donor iPSCs can complement the embryo, and rescue the lethal phenotype. Second, the animals were of host animal size and overall appearance. Third, all the endocrine and exocrine tissues in the chimeric pancreas were rat-derived, yet the pancreas was of mouse size. Interestingly, they also observed contribution of rat PSCs to interspecific gallbladders, hinting towards 'unlocking' of a developmental program in a xenogeneic environment, since rats do not have gallbladders<sup>39</sup>.

In the years since then, multiple tissues and organs have been generated in mouse intraspecies chimeras, such as kidneys, forebrain, liver, lung, and bone amongst others, but also in pig intraspecies chimeras<sup>20,40-46</sup>. Additionally, numerous studies have also generated interspecific organs via BCI. In rat and mouse interspecies chimeras, generation of thymi, blood vasculature, kidneys, and also mouse germ cells in rat hosts have been reported on<sup>47-49</sup>. There are just few publications about chimerism between primates, such as humans or monkeys, with other species, and even fewer about BCI<sup>50-57</sup>. However, it is important to note that the contribution of primate PSCs to the resulting chimeras were either minute, or that the chimeric embryos were not brought to term.

The most facile way to assess contribution of donor cells to chimeras is based on coat color chimerism if the fur of donor and host cells is encoded by different genes<sup>38</sup>. An interesting finding in rat-to-mouse chimerism is that rat PSCs appear to preferentially contribute to the anterior part of the chimeras, however the reason is as of yet unknown<sup>39,58</sup>. Depending on the amount of contribution, the weight and size of the animal is affected as well. While at birth interspecies chimeras exhibit size comparable to the host species, during later development the size is skewed to some extent towards the donor species, dependent on the amount of contribution<sup>39,58</sup>. However, chimeras with a very high amount of donor cell contribution are rarely observed. Considerable xenogeneic contribution causes high embryonic lethality, and chimeras being born often suffer from various malformations, likely due to mismatches between the two species<sup>58,59</sup>. This

finding, in extension, might also imply future challenges in utilizing BCI between species more distant than rat and mouse<sup>57</sup>.

## 1.2 Germline

### 1.2.1 From stem cells to spermatozoa

Germ cells are the only cells which can transmit genetic information to offspring and are essential for sexual reproduction. Since the focus of this project lies with the male germline, pathways pertaining to the female germline will not be covered in this thesis.

In mice, the primordial germ cells (PGCs), the gamete's precursors, specialize early during embryogenesis in the proximal epiblast<sup>60,61</sup>. At around E6 the bone morphogenic proteins (BMP) BMP4 and BMP8b secreted from the extraembryonic mesoderm direct the PGC precursors to segregate in their development from somatic cells and develop towards the germ cell lineage via signaling through the Smad1/5 pathway<sup>62-64</sup>. At E6.25, *Blimp1* (also known as *Prdm1*) serves as a marker for the germ cell lineage, and is detected in a few precursor cells, acting together with other key regulators for PGC specification called *Prdm14* and *Tcfap2c*, a downstream target of *Blimp1*<sup>65-67</sup>. A lack of these transcription factors has been shown to impair PGC formation as the somatic program is not sufficiently suppressed, or genes required for maintenance of the PGCs do not reactivate<sup>65-68</sup>. At E7.25, the PGCs form the first identifiable cluster making up the founder population, consisting of about 40 cells specifically expressing *Stella* and staining positive for alkaline phosphatase<sup>60,69</sup>.

Shortly thereafter, the PGCs need to migrate to the correct location in the developing embryo in order to populate the gonads. At E7.75 the PGCs start to migrate along the hindgut endoderm towards, and eventually start to colonize, the genital ridges between E10 and E11<sup>70-72</sup>. Once the genital ridges have been colonized, the PGCs undergo a rapid increase in numbers, until they reach approximately 25,000 cells<sup>73</sup>.

PGCs are bipotential, being able to give rise to the female as well as the male germline. Thus, they are reliant on external cues from the gonads to initiate sex determination. In XY gonads, the Y-linked gene *Sry* is upregulated at E10.5 and initiates male gonad determination, but its expression is brief and is downregulated by E12.5<sup>74,75</sup>. *Sry* acts to differentiate the pre-Sertoli cells via initial activation of *Sox9*<sup>76,77</sup>. *Sox9* then leads to an upregulation of *Fgf9*, establishing an FGFR2 mediated *Sox9-Fgf9* positive feedback loop, leading to an *Sry* independent maintenance of *Sox9* expression in PGCs<sup>76</sup>. Aside from a role in expression of *Sox9*, *Fgf9* is also important for proliferation

of pre-Sertoli cells<sup>76-78</sup>. This feedback loop establishes *Sry*, *Fgf9* and FGFR2 as necessary to inhibit specification of granulosa cell and the formation of female ovaries, and instead direct the pre-Sertoli cells to differentiate towards Sertoli cells<sup>77</sup>. At around E11.5 to E12.5, formation of the testis cords takes place<sup>79,80</sup>. Testis cords are the precursors of the seminiferous tubules and are formed by Sertoli cells enclosing germ cells. Sertoli cells are the only cells present inside the seminiferous tubules apart from germ cells. They are commonly described as ‘nurse’ cells for the male germ cells, secreting a number of proteins and hormones essential for spermatogenesis<sup>81</sup>. They also secrete Cyp26b1, which metabolizes retinoic acid and thus ensures inhibition of meiosis until post-partum<sup>82</sup>. Another important role of Sertoli cells is the formation of tight junctions to maintain the blood-testis-barrier, affording immune privilege to the developing germ cells<sup>83</sup>. In rodents, testis cords are also surrounded by one layer peritubular myoid cells, smooth muscle-like cells important for transportation of the not yet motile spermatozoa<sup>79</sup>.

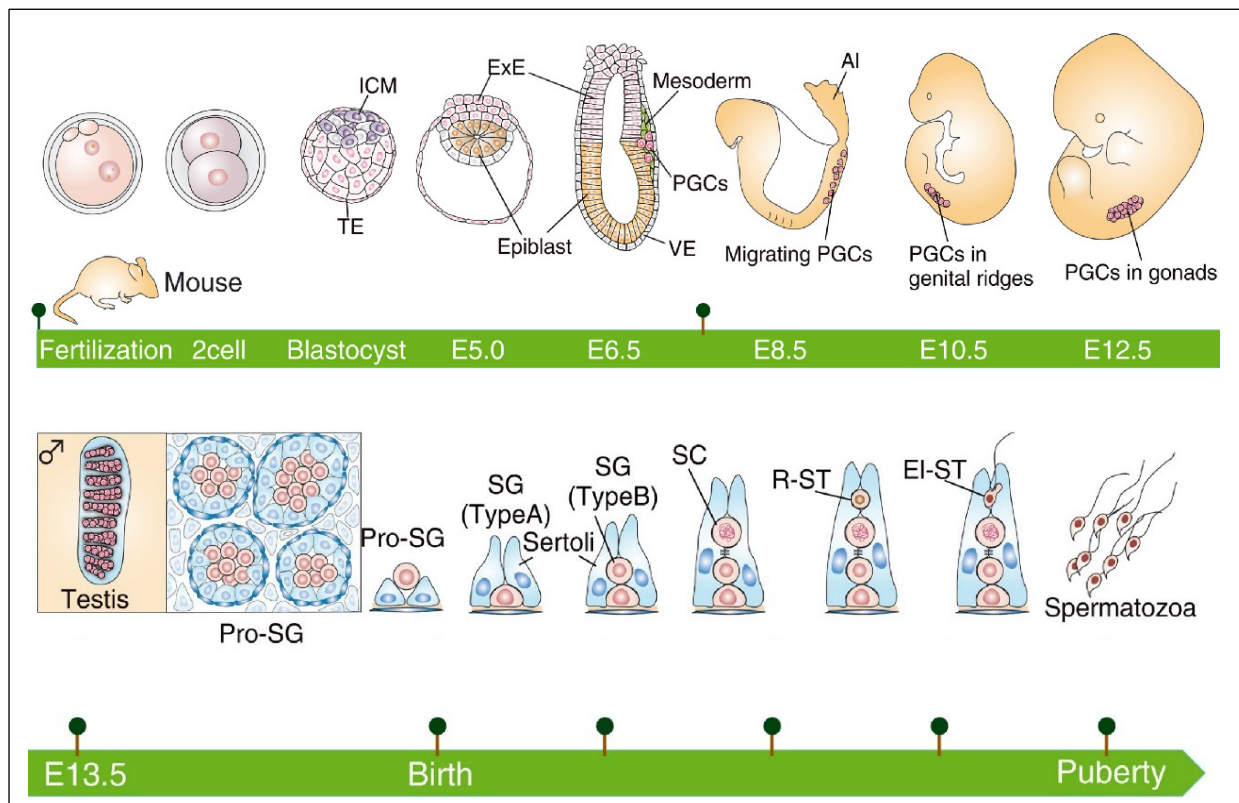


**Figure 1.1: Schematic for germ cell development.** During embryonic development, at around E6.5 PGCs arise at the most proximal. After migration to the genital ridges, they colonize the gonads, undergo sex differentiation and form testis cords with Sertoli cells. After birth, meiosis commences and via spermatogenesis gives rise to mature spermatozoa. ICM, inner cell mass. TE, trophoblast. ExE, extraembryonic ectoderm. VE, visceral endoderm. AI, allantois. PGCs, primordial germ cells. Pro-SG, prospermatogonia. SG, spermatogonia. SC, spermatocyte. R-ST, round spermatids. EI-ST, elongating spermatids. [Adapted from <sup>84</sup>]

The formation of testis cords also defines the interstitial space, which contains fibroblasts, vasculature and fetal Leydig cells<sup>80</sup>. The fetal Leydig cells are dependent on PDGF signaling to migrate and differentiate from their precursors. Once established, they produce androstenedione which is converted to testosterone by Sertoli cells, directing masculinization of genitalia<sup>80,85</sup>. Fetal Leydig cells diminish in numbers shortly after birth, however, and the adult Leydig cells capable of producing testosterone start to differentiate and contribute to the regulation of spermatogenesis<sup>85</sup>. Around the time of testis cord formation, the male germ cells undergo mitotic arrest, remaining in the G0/G1 cell cycle phase as primary transitional T1 prospermatogonia<sup>86</sup>.

After birth, between day 0 and 3 post-partum (P0-P3), T1 prospermatogonia enter the cell cycle again, migrate towards the basal lamina and convert into secondary transitional T2 prospermatogonia<sup>87-89</sup>. Once at the correct location under the basement membrane, between P4 to P6 they give rise to two cell populations; one is transient, lacks self-renewal and is responsible for the first wave of spermatogenesis, while the other gives rise to spermatogonial stem cells (SSCs), which are the germ cell specific stem cells responsible for spermatogenesis after sexual maturity has been reached<sup>87,89</sup>. SSCs are also called Type A Single ( $A_s$ ) spermatogonia. They can either undergo symmetrical divisions, resulting in generation of two progenitor cells committed to spermatogenesis or two daughter SSCs, or asymmetrical division, giving rise to a single SSC and a committed progenitor each<sup>90</sup>. However, it has not been resolved whether symmetrical divisions occur in adult testes, or whether they are only relied on during testis morphogenesis, and then switch to asymmetric<sup>91,92</sup>. The committed progenitor spermatogonia, Type A paired ( $A_{pr}$ ) undergo a series of 8-10 mitotic divisions to give rise to Type B spermatogonia<sup>90</sup>. After a final mitotic division, the preleptotene primary spermatocytes are formed<sup>90</sup>.

While primary spermatocytes are diploid with 46 sister chromatids, the mature spermatozoa are haploid with only 23 single chromatids each. In order to reduce the number of chromatids, the spermatocytes have to undergo two meiotic divisions. In rodents exactly every 8.6d an increase in retinoic acid initiates spermatogonial differentiation as well as meiotic initiation, indicating the length of a seminiferous cycle<sup>93</sup>. The first burst of retinoic acid is derived from the Sertoli cells, while later on they act in concert with primary pachytene spermatocytes to regulate retinoic acid levels and progression through spermatogenesis<sup>93</sup>. After passing through Meiosis I, a single primary spermatocyte has given rise to two secondary spermatocytes. The two secondary spermatocytes then undergo Meiosis II and generate four haploid round spermatids. The

round spermatids already carry the capacity to generate offspring via Round Spermatid Injections (ROSI), but in a process termed spermiogenesis will have to undergo dramatic changes in order to become spermatozoa<sup>94,95</sup>.

Spermiogenesis in the mouse consists of four phases and sixteen steps<sup>96</sup>. Starting with the Golgi phase, the trans-Golgi network forms pro-acrosomic granules, which accumulate and fuse with each other to form a singular acrosomal granule<sup>95</sup>. During the cap phase, the enlarged acrosomal granule flattens, spreading over a third of the nucleus. It is attached to the nucleus by the acroplaxome, which ensures that acrosome and nucleus do not separate in the following acrosomal phase<sup>95</sup>. The spermatid is now elongating, the shape of the nucleus and the acrosome changing drastically towards falciform. To accommodate the paternal DNA in a spermatozoon, a small cell, histones are replaced by protamines, allowing for stabilization and condensation of the DNA, however, rendering the spermatozoon transcriptionally silent with only a fraction of RNAs present<sup>97-99</sup>. In the last phase of spermiogenesis, the maturation phase, the nucleus further condenses, and the acrosome undergoes final maturation<sup>95</sup>. The remaining excess cytoplasm and organelles are shed as residual bodies, which are then digested by the Sertoli cells<sup>95</sup>. During the last step of spermiogenesis, the mature elongated spermatids, at this point still connected to the Sertoli cells, need to be released into the lumen of the seminiferous tubules<sup>95</sup>. Throughout the spermiogenesis, the components of the tail develop, ultimately conferring motility in mature and capacitated spermatozoa<sup>100</sup>.

In the event spermatogenesis, spermiogenesis and spermiation succeed, the spermatozoa transit through the epididymis towards the cauda epididymis, where they are stored until needed to fertilize an oocyte. During this transition, they acquire the first part of their fertilization competence and gain motility, but also undergo further maturation<sup>101</sup>.

### 1.2.2 In vitro gametogenesis

In an effort to study gametogenesis in more depth *in vitro*, in 2003 Toyooka and colleagues built on the observation that co-culture of isolated epiblasts with extra-embryonic ectoderm fragments, or cells expressing BMP4 and BMP8b, led to the formation of cells resembling PGCs<sup>102-104</sup>. They expanded these findings to mouse ESCs, which upon aggregation together with BMP4 expressing cells gave rise to PGCs. Following transplantation of the PGCs into recipient testes, they underwent complete spermatogenesis<sup>104</sup>. Of note, capacity of these spermatozoa to fertilize oocytes or give

rise to offspring was not evaluated<sup>104</sup>. A few years later, the first offspring generated from EpiSC derived primordial germ cell-like cells (PGCLCs) was born<sup>105</sup>. After induction of PGCLCs from EpiSCs in a floating culture with addition of BMP4, the cells were transplanted into testes of nude mice which have been busulfan treated to ablate all spermatogonia. The transplanted cells then successfully committed to spermatogenesis, resulting in spermatozoa which gave rise to pups after Intracytoplasmic sperm injection (ICSI), an artificial reproductive technique<sup>105,106</sup>. However, since EpiSC culture is more demanding, and ESCs and iPSCs are more readily available, the protocol was extended to generate offspring from *in vivo* transplanted PGCLCs generated from PSCs via either a cytokine-induced transient EpiLC state, or via overexpression of *Prdm14* in EpiLCs<sup>107,108</sup>. To circumvent the need for an *in vivo* host for the PGCLCs, the system was further optimized to generate completely *in vitro* derived spermatid-like cells, by co-culture of PGCLCs with neonate sterile Kit<sup>w</sup>/Kit<sup>w-v</sup> testis cells, or aggregation with embryonic testicular somatic cells with subsequent air-liquid interface culture<sup>109-111</sup>. These findings were only recently replicated with rat ESC derived PGCLCs, which gave rise to offspring upon ROSI and Testicular Sperm Extraction (TESE-) ICSI<sup>112-114</sup>. Generation of human PGCLCs and prospermatogonia has been reported on, however, these trials will be scrutinized to a higher extent due to associated ethical concerns<sup>84,115-117</sup>.

Transplantations of spermatogonial stem cells (SSCT) have also been explored, resulting in the first successful mouse-to-mouse transplantations which gave rise to spermatozoa able to generate offspring<sup>118</sup>. Intraspecies SSCT leading to spermatogenesis, has been described also for dogs, cattle, pigs and macaques, however in these trials no generation of offspring was reported<sup>119,120</sup>. In addition, the generation of offspring from intraspecies SSCT has been recorded not only for mice, but also for rats, goats, and sheep<sup>121-124</sup>. The idea of SSCT was also adapted for xenogeneic SSCs, namely by transplantation of rat or Syrian golden hamster SSCs into non-sterile, but spermatogonia-ablated mouse testes, where donor cell spermatogenesis was observed, although malformations were present in hamster spermatozoa, and fertilization capacity was not evaluated<sup>125,126</sup>. It was later confirmed that indeed rat spermatozoa generated via interspecies SSCT into mice were able to give rise to rat offspring<sup>121</sup>. The reverse experiment was also performed, whereby mouse germline stem cells were injected into *ex vivo* E14.5 rat embryonic testes and the testes explants transplanted into immune compromised and spermatogonia-ablated nude mice<sup>127</sup>. Upon ROSI and ICSI with mouse oocytes, successful generation of offspring was observed<sup>121</sup>.

### 1.2.3 The formation of spermatogenic niches

Generation of mature spermatozoa is a highly regulated process, and perturbations to genes important for formation of precursor germ cells or spermatogenesis can result in sterility, as has been shown previously with *BMP4*, *c-kit*, *Prdm14*, *Nanos2/3*, *Blimp1*, or *Tcfap2*<sup>62,65-67,120,128-131</sup>. For obvious reasons, these animals cannot be maintained on a homozygous background, resulting in only 25% of homozygous sterile animals from heterozygous matings. There are several reports about intraspecies germ cell blastocyst complementation, either utilizing ablation of *VASA* expressing germ cells via diphtheria-toxin, or a knockout of *Nanos3* in mouse hosts<sup>132,133</sup>. A mutation in a gene indispensable for spermatogenesis, the X-chromosome linked *Tsc22d3*, has been generated via the Cre/loxP system<sup>134</sup>. *Tsc22d3* (also known as glucocorticoid-induced leucine zipper, *Gilz*) is required for inhibition of proliferation of undifferentiated spermatogonia, and its absence causes defects in spermatogonia differentiation. Further, lack of *Tsc22d3* leads to increased spermatogonial apoptosis upon re-initiation of meiosis post birth<sup>130,135-137</sup>. Apart from spermatogonia, *Tsc22d3* is also expressed in primary spermatocytes, but not at later stages of meiosis, indicating a crucial role in the pachytene phase of prophase I of meiosis I. A KO of the gene leads to a complete lack of any spermatogenic cells past meiosis I, including spermatozoa, and male sterility<sup>130,135-137</sup>. This model has been utilized to generate exclusively donor-derived spermatozoa in intraspecies mouse chimeras from ESCs<sup>134</sup>. Of note, while males are sterile, females are not affected and are fertile. The loss of all cells of the spermatogenic lineage results in reduced testis size and weight. In addition, the seminiferous tubules are devoid of any cells aside from Sertoli cells, and there is an increased number of Leydig cells present in the interstitium<sup>130,135</sup>.

### 1.2.4 Generation of xenogeneic germ cells

In a surprising finding, in testes of a rat-to-mouse chimera mature rat spermatozoa were found<sup>138</sup>. This observation was further substantiated by the finding that rat spermatozoa generated in rat-to-mouse chimeras could be used for the generation of rats via ICSI and even transmit transgenes<sup>139,140</sup>. It is important to note that the mouse host blastocysts did not carry a mutation rendering them sterile, such that time-consuming visual identification and separation of the rat spermatozoa from the mouse spermatozoa was required, also relying on fluorescent reporters which could interfere with the intended use of the inter-species chimera derived rat sperm<sup>139,140</sup>. To improve on these results, rat

*Prdm14*-KO blastocysts lacking PGCs were complemented with mouse ESCs, generating exclusively donor derived germ cells<sup>141</sup>. This finding could potentially be extended to more diverse species than mice and rats to generate xenogeneic germ cells.

A key motivation to generate xenogeneic gametes is the sixth mass extinction of species, which describes the massive loss of biodiversity caused by human actions<sup>142</sup>. Urgent measures are needed to counter the rapid loss of, not only, mammalian species. One way to conserve and potentially even de-extinct species, while concomitantly maintaining genetic diversity, could be stem cell technology<sup>143-146</sup>. However, it is not possible to obtain ESCs from most endangered species, but cell banks containing cells from hundreds of animals could provide a resource for the generation of gametes of endangered animals via iPSCs via interspecies germline complementation to aid in conservation efforts<sup>146,147</sup>.

## 1.3 Muscle

### 1.3.1 Skeletal muscle regeneration

Skeletal muscle tissue comprises 35%-45% of the normal human body mass and is the most abundant tissue. Approximately 600 individual muscles, each exhibiting different contraction properties, allow for force generation, thus enabling postural support and act in concert to also generate highly precise movements<sup>148,149</sup>. In order to contract in an efficient way, it consists of several distinct units, organized hierarchically to form a functional muscle<sup>148-150</sup>. Multinucleated muscle fibers, termed myofibers and containing post-mitotic myonuclei, are made up of myofibrils, themselves containing the myosin and actin filaments which convert energy into movement. Myofibers are connected to bones via tendons and osteotendinous junctions, and together they form intricate levers<sup>148,149</sup>. However, as myonuclei are post-mitotic, other cells in the form of muscle stem cells are responsible for muscle adaptation and regeneration<sup>148-150</sup>.

These unique muscle stem cells termed satellite cells are localized in a niche underneath the basal lamina and above the cell membrane, and carry a prodigious capacity to functionally repair muscle upon injury, disease or during normal growth<sup>149</sup>. Remarkably, satellite cells have transplantation potential when isolated and re-injected back into pre-injured skeletal muscles<sup>149,151,152</sup>. While under homeostatic conditions, satellite cells are usually in a quiescent state, characterized by high expression of the key transcription factor paired box protein 7 (*Pax7*)<sup>153</sup>. However, the quiescent satellite cell population is not homogeneous, as some are in an alert state, allowing for rapid



activation, and others are in a more in committed state<sup>154,155</sup>. Upon activation cues in the form of tissue insult or growth, satellite cells undergo asymmetric divisions, forming daughter stem cells that can replenish the satellite cell pool in addition to committed myogenic progenitors termed myoblasts that can further differentiate into fusion-competent myocytes and myofibers<sup>156</sup>. During the proliferation phase, myoblasts express high levels of the transcription factors *Pax7* and *Myf5* and express high levels of MYOD mRNA which is sequestered awaiting translation, and following differentiation into myocytes they downregulate *Pax7* expression. Concomitantly, other Myogenic Regulatory Factors (MRFs) and Myogenin are hierarchically expressed until the myocytes either fuse to each other to form new myofibers, or to damaged muscle fibers to regenerate the tissue<sup>148</sup>. *Pax7* has been reported to be indispensable for satellite cell function, and therefore to muscle growth and regeneration<sup>153,157,158</sup>. Newborn mice lacking *Pax7* show severe growth retardation, exhibit a considerable small size relative to wild type littermates, and typically die within a few weeks post birth<sup>153,157</sup>. Deletion of the *Pax7* gene in adult mice results in progressive loss of nearly all satellite cells due to

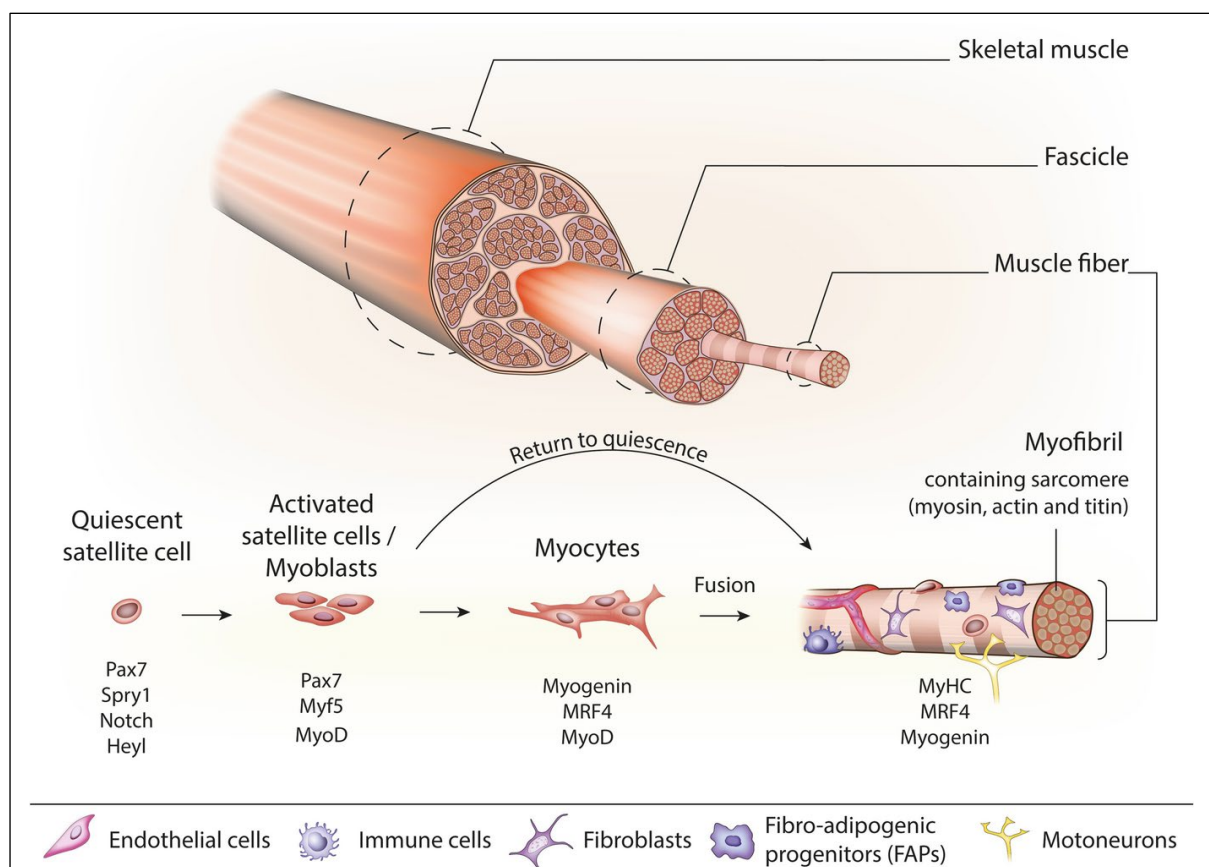


**Figure 1.2: Structure of skeletal muscle.** Schematic to show the structure of skeletal muscle (top). During regeneration, quiescent satellite cells, marked by high expression of *Pax7*, become activated and express the MYOD protein. Their differentiate into myocytes, which can then fuse with myofibrils. [From <sup>159</sup>]

their inability to self-renew, leading to severely impaired muscle regeneration upon injury<sup>158</sup>. Interestingly, a few cases of human Pax7 mutations have been described in the literature. The patients, often of consanguineous heritage, presented with a severe clinical phenotype, however, have been reported to survive at least into their second decade of life<sup>160-162</sup>.

### 1.3.2 Duchenne Muscular Dystrophy

Although skeletal muscle has a remarkable plasticity and capacity for regeneration, both can be hampered by genetic mutations in key genes necessary for muscle function, leading to muscular degenerative disorders. The most common hereditary muscle disease, Duchenne Muscular Dystrophy (DMD), occurs in approximately 1 in 5000 male births<sup>163,164</sup>. It is marked by progressive muscle weakening, leading to first signs of the disease during early childhood, presenting with difficulties walking and general ambulation is often lost at early adolescence, requiring a wheelchair<sup>164</sup>. Since muscles supporting breathing are affected as well, leading to respiratory insufficiency, patients are also often dependent on assisted ventilation<sup>164</sup>. Eventually, patients succumb to respiratory or cardiac failure around the third to fourth decade of life<sup>164,165</sup>.

DMD is caused by a loss of function mutation in the Dystrophin gene, the largest gene in the human genome, which encodes for a structural protein that plays a crucial role in the dystrophin-associated glycoprotein complex (DGC)<sup>165</sup>. The DGC consists of four binding domains and links the F-actin of the muscular cytoskeleton to the muscle's extracellular matrix<sup>166,167</sup>. Most commonly, large deletions account for the defect, however duplications, point mutations and small deletions also occur frequently and can generate premature stop-codons<sup>164,168</sup>. Since the majority of mutations occur between dystrophin exons 45 and 55, it is often regarded as mutational 'hotspot' region<sup>168</sup>. As the gene is X-chromosome linked, it mainly affects males, however, females can be carriers of the mutation, most often without exhibiting a phenotype<sup>169,170</sup>.

In absence of a functional dystrophin protein, a loss of stability of the muscle's plasma membrane ensues, leading to fragile muscle fibers being damaged by contractions<sup>165,166,171</sup>. In turn, this causes muscle degeneration and necrosis through excessive reactive oxygen species, functional ischemia, and an overload in intracellular calcium<sup>164,166</sup>. The resulting muscle wasting, accompanied by fibrosis and replacement of muscle tissue with fat, cannot be repaired by the satellite cells, which led to the idea that the satellite cell pool is exhausted via constant degeneration and regeneration,

indicating that DMD is not only a disease of the DGC, but also of the satellite cells<sup>172-174</sup>. It has been shown that satellite cells express dystrophin, which governs asymmetric cell divisions. A lack of dystrophin protein in satellite cells leads to a reduction in asymmetric divisions, contributing to satellite cell dysfunction, exacerbated satellite cell exhaustion, and to an overall perturbed myogenic regeneration program<sup>172,174,175</sup>. While DMD mainly affects skeletal and cardiac muscle tissue, tissues such as eyes and brain can also be affected, leading to impairments of vision and cognition<sup>164,166</sup>.

### 1.3.3 Treatment approaches for DMD

To date, there is no effective cure for most muscular dystrophies<sup>163,176,177</sup>. Most treatments available focus on symptoms, for example by providing respiratory support, management of urological or gastrointestinal issues, or neurological impairments<sup>178,179</sup>. Therapies also aim to maintain muscle function, for example physiotherapy or treatments with glucocorticoids<sup>179</sup>. However, especially glucocorticoids can cause severe side-effects such as osteoporosis, increasing the risk of fractures, but also affecting metabolism or the gastrointestinal tract<sup>178</sup>. It is thus paramount to find treatments to tackle DMD at the root of the cause: defective dystrophin protein expression. First allogeneic myoblast transplantations for the treatment of DMD in the 1990s did not prove to be successful<sup>180,181</sup>. It was assumed that several factors such as low graft survival, poor migration of transplanted myoblasts, immune rejection or the inability of myoblasts to contribute to the muscle stem cell pool accounted for the poor functional outcomes<sup>182</sup>. However, later trials with improved injection protocols evidenced long-term expression of dystrophin emanating from donor cells<sup>182,183</sup>. Further, autologous myoblast transplantations did show functional improvements in patients suffering from Oculopharyngeal muscular dystrophy after a 2-year followup<sup>184</sup>.

Apart from cell transplantations, pharmacological agents inducing stop codon read through or skipping of the exons containing stop codons are currently being investigated or approved<sup>185,186</sup>. Other promising treatments aim to deliver and incorporate functional dystrophin genes into myonuclei<sup>187</sup>. However, in order to achieve a functional benefit, a large number of targeted muscles is needed, for example via systemic delivery of adeno-associated viruses (AAVs)<sup>187,188</sup>. Since dystrophin is a large gene, and AAVs typically have a small packaging capacity, micro-dystrophins have been generated, which are dystrophin variants containing only the most important parts of the gene<sup>187</sup>. In recent years, CRISPR/Cas9 has emerged as a powerful tool allowing for precise targeting of

mutations in genes, and has shown successful application in DMD animal models<sup>189,190</sup>. It has been shown that for example skipping the exon containing the stop codon can restore dystrophin expression and alleviate the disease phenotype *in vivo*<sup>191,192</sup>.

Myogenic cells potentially fit for therapeutic purposes can also be directly induced *in vitro* from PSCs. Since PSCs show rapid proliferation, and can be propagated *in vitro* to large numbers, generation of a sufficient amount of myogenic cells is rendered quicker. By harnessing the PSCs plasticity, overexpression of myogenic genes such as *Pax3* or *Pax7* can differentiate the PSCs towards the myogenic fate<sup>193,194</sup>. However, under the aspect of future application in human subjects, the use of transgenes might not be ideal. Protocols subjecting either mouse or human PSCs to growth factors in conjunction with small molecule treatment have also proven successful<sup>193,195-197</sup>. Of note, these protocols usually do not yield a homogeneous cell population, necessitating FACS purification.

Recently, teratomas have been identified as a potential source of satellite cells<sup>198</sup>. To this end, mouse ESCs were transplanted into hindleg muscles of recipient mice, where they formed teratomas. Sorting for the satellite cell surface maker ITGA7 and VCAM1 resulted in cells capable of contributing to muscle regeneration upon transplantation into recipient muscle, and sustaining muscle regeneration after re-injury of the muscle. A follow-up study further showed engraftment competence after an *in vitro* propagation step, and additionally a paper by the same group reported on formation of myogenic cells in hPSC derived teratomas, albeit not having been shown to carry transplantation potential<sup>199,200</sup>. However, it is unclear what confers this extraordinary capability to expand *in vitro* and still keep *in vivo* engraftment potential.

Based on the observation that mouse fibroblasts can be reprogrammed into post-meiotic myotubes via *MyoD* overexpression, a recent publication has expanded this finding by incorporating *MyoD* overexpression with treatment of the cells with three small molecules<sup>201,202</sup>. By addition of CHIR-99021, Forskolin and RepSox to the culture media, mouse embryonic fibroblasts readily reprogrammed into induced myogenic progenitor cells (iMPCs). These iMPCs contained not only myofibers expressing mature markers, but more importantly also *Pax7* expressing mononucleated cells. The iMPC cultures showed rapid *in vitro* expansion, and upon transplantation contributed to the satellite cell niche<sup>202</sup>. This finding was adapted to generate iMPCs from a DMD mouse model, and the iMPCs were subsequently edited to re-express dystrophin via a CRISPR/Cas9 exon-skipping approach. The gene-edited iMPCs were shown to contribute to the satellite cell pool upon transplantation into the muscles of DMD mice<sup>203</sup>.

Further, an attractive approach to restore dystrophin expression and remedy DMD symptoms is cell therapy by satellite cell transplantation<sup>203,204</sup>. The transplanted satellite cells contribute to the satellite cell niche, replenishing the cell pool, and also fuse with existing myofibers<sup>204</sup>. However, these cells are a rare population in muscles and as such only insufficient numbers can be isolated from allogeneic donors for transplantation via purification using satellite cell surface markers<sup>205</sup>. A further complication is that satellite cells convert into myoblasts when expanded *in vitro* and progressively lose their *in vivo* transplantation potential, rendering them ineffective for therapy<sup>204</sup>. A way to circumvent this limitation could be interspecies blastocyst complementation, harnessing mutations in genes of the myogenic lineage in host blastocysts. This might allow for generation of large numbers of donor cells in large mammals and direct transplantation of satellite cells. A first proof-of-concept and so far the only complementation in the myogenic lineage was recently reported for human-to-pig chimeras harboring a MYF5/MYOD/MYF6 -null mutation in the pig embryos. Of note, the embryos were not brought to term, and the functionality of the myogenic cells was not evaluated<sup>53,206</sup>. However, utilizing blastocyst complementation, it might be possible to generate autologous satellite cells which have been gene-edited to correct the dystrophin mutation.

If successful dystrophin restoration in patients is achieved, it is important bear in mind that this could also generate challenges in itself. Although many DMD patients have revertant fibers expressing dystrophin, the introduction of the dystrophin protein might elicit immune responses against the 'foreign' protein, potentially necessitating immunosuppression for some patients<sup>207-210</sup>.

## Chapter 2. Aims of the thesis

---

Currently, the world faces a mass annihilation of species, termed the sixth mass extinction. A potential way to help preserve endangered species is via generation of their gametes in interspecies chimeras. So far, there were reports about generation of rat spermatozoa in wildtype mouse hosts using wildtype blastocysts, but not on whether it's possible to generate exclusively rat donor ESC derived spermatozoa in sterile mouse hosts via blastocyst complementation. In Chapter 3, we aimed to elucidate on this by injecting mouse and rat PSCs into *Tsc22d3*-KO blastocysts, which are unable to undergo meiosis I and thus rendering all non-complemented males sterile, we generated mouse-to-mouse and rat-to-mouse chimeras. These chimeras were then further analyzed for presence of only donor PSC derived spermatozoa, and their potential fertilization capacity. This could serve as a proof-of-principle to exclusively generate xenogeneic germ cells of rare species in more common animal hosts, without time-consuming visual identification or fluorescent labelling of the germ cells for artificial reproductive techniques.

Animal life relies on movement to gather food and to reproduce. The key tissue involved in this is skeletal muscle, a multinucleated tissue harboring an exceptional regeneration capacity conferred by muscle stem cells, called satellite cells. However, in case of muscular dystrophies, this regeneration capacity is lost. To explore novel treatment strategies, in Chapter 4, we aimed to generate gene-corrected mouse iPSCs of the most common muscular dystrophy, Duchenne muscular dystrophy, and utilize them to generate intra- and inter-species chimeras. Via *in vitro* and *in vivo* characterization, we aimed to assess a potential therapeutic competence by restoration of dystrophin expression following cell engraftment, which could aid in treatment of Duchenne muscular dystrophy if recapitulated in the future in a human-animal chimera model.

## Chapter 3. Exclusive generation of rat spermatozoa in sterile mice utilizing blastocyst complementation with pluripotent stem cells

Authors: Joel Zvick<sup>1</sup>, Monika Tarnowska-Sengül<sup>1</sup>, Adhideb Ghosh<sup>1,4</sup>, Nicola Bundschuh<sup>1</sup>, Pjeter Gjonlleshaj<sup>1</sup>, Laura Hinte<sup>2</sup>, Christine L. Trautmann<sup>1</sup>, Falko Noé<sup>1,4</sup>, Xhem Qabrati<sup>1</sup>, Seraina A. Domenig<sup>1</sup>, Inseon Kim<sup>1</sup>, Thomas Hennek<sup>3</sup>, Ferdinand von Meyenn<sup>2</sup> & Ori Bar-Nur<sup>1#</sup>

### Affiliations:

<sup>1</sup> Laboratory of Regenerative and Movement Biology, Department of Health Sciences and Technology, ETH Zurich, Schwerzenbach, Switzerland.

<sup>2</sup> Laboratory of Nutrition and Metabolic Epigenetics, Department of Health Sciences and Technology, ETH Zurich, Schwerzenbach, Switzerland.

<sup>3</sup> ETH Phenomics Center, ETH Zurich, Zurich, Switzerland.

<sup>4</sup> Functional Genomics Center Zurich, ETH Zurich and University of Zurich, Zurich, Switzerland.

#Correspondence: Ori.bar-nur@hest.ethz.ch

### Contribution:

Joel Zvick and Ori Bar-Nur conceptualized the experiments, interpreted the results, and wrote the manuscript. Joel Zvick performed most experiments and analysis of results.

---

This article was published in Stem Cell Reports. This chapter is a reprint of the published article. The article and further supplementary materials can be found under: <https://doi.org/10.1016/j.stemcr.2022.07.005>

## Summary

Blastocyst complementation denotes a technique which aims to generate organs, tissues or cell types in animal chimeras via injection of pluripotent stem cells (PSCs) into genetically compromised blastocyst-stage embryos. Here, we report on successful complementation of the male germline in adult chimeras following injection of mouse or rat PSCs into mouse blastocysts carrying a mutation in *Tsc22d3*, an essential gene for spermatozoa production. Injection of mouse PSCs into *Tsc22d3*-KnockOut (KO) blastocysts gave rise to intraspecies chimeras exclusively embodying PSC-derived functional spermatozoa. Additionally, injection of rat embryonic stem cells (rESCs) into *Tsc22d3*-KO embryos produced interspecies mouse-rat chimeras solely harboring rat spermatids and spermatozoa capable of fertilizing oocytes. Furthermore, using single cell RNA-sequencing (scRNA-seq) we deconstructed rat spermatogenesis occurring in a mouse-rat chimera testis. Collectively, this study details a method for exclusive xenogeneic germ cell production *in vivo*, with implications that may extend to rat transgenesis, or endangered animal species conservation efforts.

## Introduction

Pluripotent stem cells in the form of ESCs or induced pluripotent stem cells (iPSCs) hold a unique propensity to differentiate into any cell type of the adult organism including germ cells<sup>211</sup>. Furthermore, injection of mouse or rat PSCs into blastocysts can produce adult chimeras that harbor PSC contribution to all cell types and organs including the germline, thus rendering genetically modified PSCs a commonly used method for the production of transgenic animals<sup>212</sup>. However, the quality of ESCs or iPSCs is oftentimes impaired due to genetic or epigenetic aberrations, precipitating reduced contribution to chimerism and to the germline. These undesirable attributes may complicate production of transgenic animal models which are reliant on germline transmission to establish animal colonies, warranting methods that augment PSC contribution to the germline highly valuable.

Blastocyst complementation is an innovative technology which enables production of specific cell types or organs in chimeras via injection of PSCs into blastocysts carrying organ or cell type-disabling genetic mutations, thereby unfolding a developmental niche receptive for exclusive generation of specific cell types or organs from injected PSCs<sup>212</sup>. A seminal study performed in the 1990s was the first to demonstrate injection of mouse



ESCs (mESCs) into recombination-activating gene-2 (RAG-2) mutated mouse blastocysts<sup>32,213</sup>. As RAG-2 deficient mice cannot produce mature lymphocytes, intraspecies chimeras harbored B and T cells that were solely derived from the injected ESCs<sup>32,213</sup>. Follow-up studies have recently reported on production of PSC-derived kidney, lung, bone, forebrain, and vascular endothelium utilizing blastocyst complementation in mice<sup>20,40-42,214,215</sup>. Similarly, recent studies have reported successes in utilizing intraspecies blastocyst complementation to produce tissues and organs in pigs<sup>43-45</sup>.

Animal chimeras carrying two distinct genotypes were first reported for two murine species, *Mus musculus* and *Mus caroli*<sup>38</sup>. Further, blastocyst complementation between mice and rats has been documented in groundbreaking studies which reported on xenogeneic pancreas formation in interspecies chimeras following injection of PSCs into *Pdx1*-KO blastocysts<sup>39,57,216</sup>. Additional studies have harnessed interspecies blastocyst complementation to exclusively generate blood vasculature, kidneys or thymi in mice or rats<sup>48,49,138</sup>.

Blastocyst complementation may further provide an attractive approach to generate germ cells solely from injected PSCs<sup>212</sup>. Notably, such method may aid in production of transgenic animals utilizing PSCs that do not contribute well to the germline, as a vacant germline niche may reduce competition with host germ cells and enable increased formation of gametes from the injected PSCs<sup>132,134,217</sup>. Additionally, intraspecies blastocyst complementation in mice may reduce the necessity to breed large numbers of chimeras to achieve germline transmission, thereby reducing animal husbandry costs and mitigating animal burden<sup>132,134</sup>. This method may also prove useful for interspecies blastocyst complementation in rats, which provide an excellent biomedical research model for a plethora of human conditions. Rat PSCs oftentimes do not contribute well to the germline, and transgenic techniques such as blastocyst injection and embryo transfer are not as widely established as with mice. As such, germline blastocyst complementation using genetically modified rat PSCs in sterile mice may enable exclusive production of transgenic rat gametes, thus assisting in the production of rat models for biomedical research.

Spermatogenesis is a complex biological process that manifests via spermatogonial stem cell differentiation into mature haploid spermatozoa in a unidirectional step-wise trajectory. Genetic mutations in genes that are critical for this differentiation process can lead to sterility and complete lack of mature spermatozoa in

adult animals<sup>64</sup>. For example, mutations in the X-linked glucocorticoid-induced leucine zipper gene (*Gilz*, also known as *Tsc22d3*), have been well-established to inflict sterility in male mice<sup>130,134-137</sup>. Absence of the TSC22D3 protein manifests in azoospermia and male infertility as a consequence of arrest in spermatogenesis during meiosis I, resulting in extensive atrophy of the testes and absence of spermatozoa in adult *Tsc22d3*-KO mice<sup>130,134-137</sup>. As a result, *Tsc22d3*-KO mice have been recently used to preferentially produce functional mouse spermatozoa from injected ESCs<sup>134</sup>. Building upon this finding, here we set out to explore whether injection of mouse iPSCs (miPSCs) or rESCs into *Tsc22d3*-KO blastocysts can overcome the sterility associated with the *Tsc22d3* mutation in male intra- or interspecies chimeras and produce functional spermatozoa which are solely derived from the injected PSCs.

## Results

### **Injection of mESCs into *Tsc22d3*-KO blastocysts produces intraspecies chimeras exclusively carrying functional mouse spermatozoa**

We commenced our investigation with injection of mESCs into *Tsc22d3*-KO blastocysts to assess whether injected cells can contribute to chimerism and generate functional mouse spermatozoa which are solely derived from injected ESCs as previously reported<sup>134</sup> (Figures 1A and S1A). The *Tsc22d3*-KO blastocysts were generated by crossing homozygous *Tsc22d3*-floxed females with homozygous *Rosa26-Cre* males<sup>134</sup>. As the *Tsc22d3* gene is located on the X chromosome, this mating strategy ensures that all male progenies are hemizygous *Tsc22d3*-KO and sterile, whereas females are heterozygous and fertile (Figure S1A). As donor PSCs, we utilized KH2-mESCs, a subclone of V6.5 ESCs, and transduced cells with lentiviruses encoding for a constitutive cytoplasmic and nuclear Red Fluorescent Protein (RFP) (Figure 1B)<sup>218</sup>. Prior to injections of cells into *Tsc22d3*-KO blastocysts, we confirmed that RFP<sup>+</sup>KH2-mESCs maintained a normal diploid karyotype and expressed well-established pluripotency genes (Figures S1B and S1C). Following fluorescence-activated cell sorting (FACS)-purification for RFP<sup>+</sup> cells and *in vitro* propagation, we injected 12-15 cells into *Tsc22d3*-KO blastocysts to produce RFP<sup>+</sup>KH2-mESC/*Tsc22d3*-KO chimeras, while concomitantly generating non-chimeric *Tsc22d3*-KO sterile male mice and fertile females (Figure 1C). Non-chimeric *Tsc22d3*-KO mice retained their albino fur color, whereas chimeric *Tsc22d3*-KO animals exhibited dark fur color emanating from the contribution of RFP<sup>+</sup>KH2-mESCs and

demonstrating a diverse degree of coat color chimerism (Figure 1C). *Tsc22d3*-KO adult male mice were of normal size and bodyweight, however their testes were significantly smaller and weighed less in comparison to wild-type (WT) mice (Figures 1E and S1D). In contrast, chimeras' testes size and weight were slightly smaller than WT mouse testes of a similar genetic background, and most notably weighing 4-5 times more than testes harvested from *Tsc22d3*-KO mice (Figure 1E). Of note, complemented testes exhibited strong RFP expression, suggesting that lentiviral promoter silencing did not occur in several testicular cell types (Figure 1F). Cross-section of *Tsc22d3*-KO testes followed by staining with Hematoxylin and Eosin (H&E) demonstrated extensive seminiferous tubule atrophy and lack of spermatozoa (Figure 1G). In contrast, testes of RFP<sup>+</sup>KH2-mESC/*Tsc22d3*-KO chimeras exhibited WT-like seminiferous tubule structures containing spermatozoa, albeit due to transgene silencing RFP expression was not detected in VASA<sup>+</sup> germ cells and was mostly confined to interstitial cells that expressed the Leydig cell marker HSD3B (Figures 1G and S1E-G). Notably, motile spermatozoa with intact tails and typical mouse sperm head-morphology were detected in the cauda epididymis of an RFP<sup>+</sup>KH2-mESC/*Tsc22d3*-KO chimera, however, were absent in the cauda of a *Tsc22d3*-KO mouse (Figure 1H and video S1). Natural mating of chimeras' F1 offspring with WT mice produced RFP<sup>+</sup> embryos, thus establishing the germline transmission potency of RFP<sup>+</sup>KH2-mESCs (Figure 1I). Last, *in vitro* fertilization (IVF) of oocytes from a Swiss Webster albino mouse strain with chimera spermatozoa only gave rise to progenies that had either a black or agouti fur coat color, emanating from the mixed C57BL/6 X 129/Sv genetic background of KH2-mESCs (Figure 1J). Based on these results, we confirmed that *Tsc22d3*-KO male mice embody a vacant developmental niche receptive for blastocyst complementation with mESCs as previously reported<sup>134</sup>. As such, *Tsc22d3*-mutated embryos can be employed to investigate blastocyst complementation of the male germline with other PSC types.

**Figure 1**

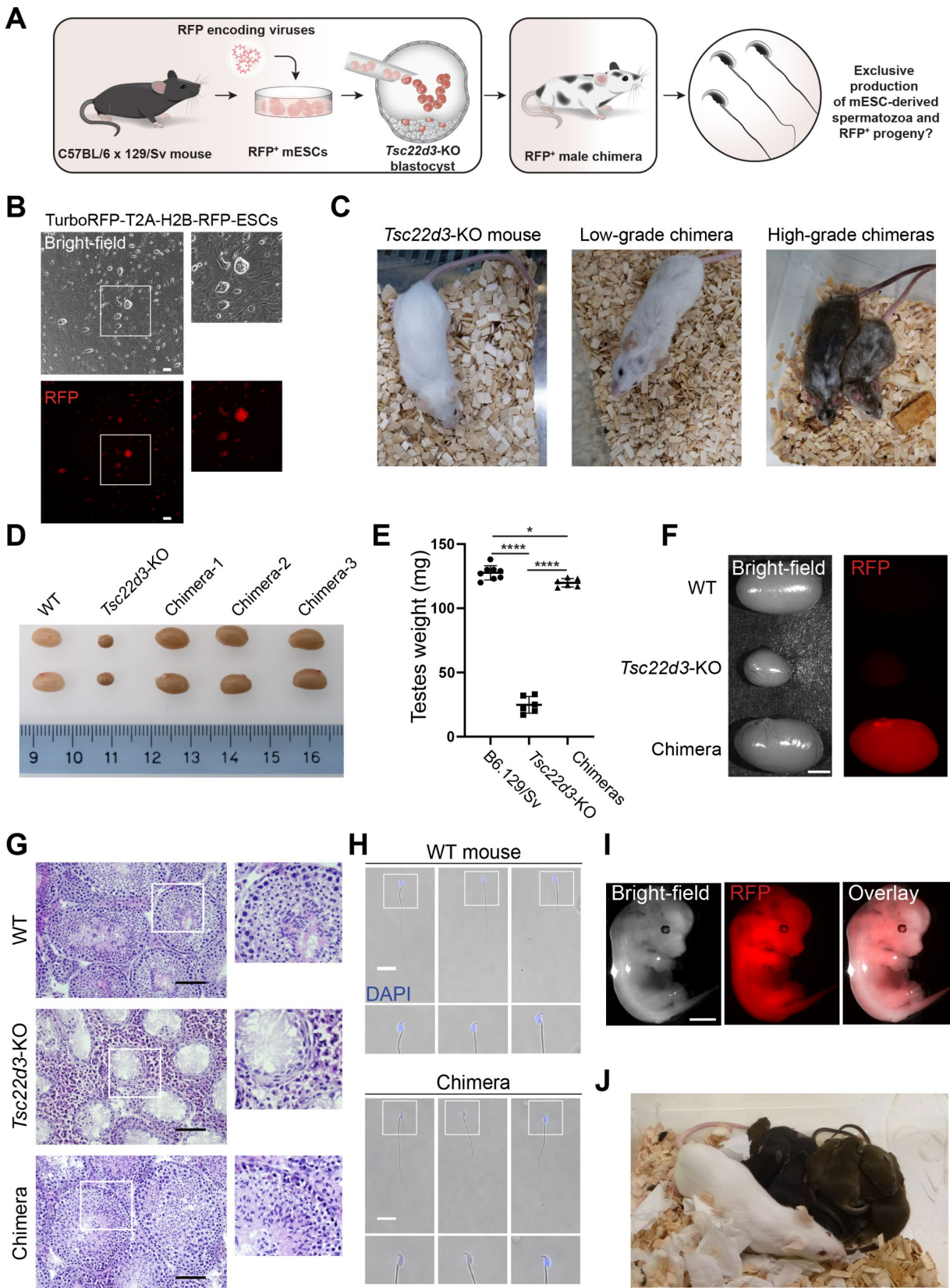


**Fig 2: (A)** A schematic illustrating experimental design. mESCs, mouse embryonic stem cells. RFP, red fluorescent protein, KO, KnockOut. **(B)** Representative bright-field and RFP images of KH2-mESCs transduced with lentiviruses encoding for constitutive *EF1 $\alpha$ -TurboRFP-T2A-H2B-*

*RFP* reporter expression. Scale bar, 100 $\mu$ m. **(C)** Representative photos of a *Tsc22d3*-KO mouse (left), a low-grade RFP<sup>+</sup>KH2-ESCs/*Tsc22d3*-KO chimera (middle) and high-grade RFP<sup>+</sup>KH2-ESCs/*Tsc22d3*-KO chimeras (right). **(D)** A representative photo of testes isolated from the indicated mouse strains. **(E)** Quantification of testes weight for the indicated mouse strains (n= 6-8 biological replicates; each dot represents a single testicle, one-way ANOVA test with Tukey Post-Hoc analysis was used, error bars denote SD, \*p<0.05, \*\*\*\*p<0.0001). **(F)** Representative bright-field and RFP images of mouse testes isolated from the indicated strains. Scale bar, 2mm. **(G)** Testes cross-sections of the indicated samples stained with H&E. Scale bar, 100 $\mu$ m. **(H)** Representative images of spermatozoa extracted from the cauda epididymis of the indicated animals. Scale bar, 20 $\mu$ m. **(I)** Representative images of an E13.5 embryo generated from a cross between the F1 male progeny of an RFP<sup>+</sup>KH2-mESCs/*Tsc22d3*-KO chimera and a WT female mouse. Scale bar, 2mm. **(J)** A photo showing mouse pups derived via IVF with spermatozoa extracted from an RFP<sup>+</sup>KH2-mESCs/*Tsc22d3*-KO chimera and oocytes of an albino Swiss Webster mouse.

### **Exclusive generation of miPSC-derived spermatozoa via blastocyst complementation**

ESCs are rarely available from most animal species, rendering iPSCs a more accessible PSC source to produce intra- or interspecies germ cells via blastocyst complementation. Therefore, our next goal was to investigate whether injection of transgenic mouse iPSCs into *Tsc22d3*-KO embryos can exclusively produce iPSC-derived functional spermatozoa in chimeras that carry a transgenic allele (Figure 2A). To this end, we reprogrammed to pluripotency embryonic fibroblasts carrying a *Pax7-nuclear GFP* (*Pax7-nGFP*) reporter, which fluorescently labels skeletal muscle stem cells termed satellite cells, thus allowing for genotyping in F1 progeny<sup>219</sup>. Reprogramming of *Pax7-nGFP* mouse embryonic fibroblasts into iPSCs was performed using lentiviral vectors carrying a polycistronic doxycycline-inducible mouse *STEMCCA* cassette, an *M2rtTA* cassette, and medium containing ascorbic acid and GSK-3 $\beta$  inhibitor as previously described<sup>220,221</sup>. *Pax7-nGFP* iPSCs were dome shaped, expressed pluripotency genes and maintained a normal diploid karyotype (Figures 2B, 2C, S2A and S2B). Injection of *Pax7-nGFP* iPSCs into *Tsc22d3*-KO blastocysts gave rise to several chimeras as judged by dark coat color (Figure 2D and table S2).

Testes weight and size of several *Pax7-nGFP* iPSC/*Tsc22d3*-KO chimeras were similar to those of *Tsc22d3*-KO mice, however three chimeras showed increased testicular size and weight (Figures 2E, 2F, S2C and table S2). Of note, the more variable and lower testicular weight of miPSC-chimeras in comparison to mESC-chimeras may be attributed to enhanced contribution of KH2-mESCs to chimerism and the germline in comparison with *Pax7-nGFP* iPSCs, as supported by increased contribution of KH2-mESCs to fur color (Figures 1C and 2D). Nonetheless, the *Pax7-nGFP* iPSC/*Tsc22d3*-

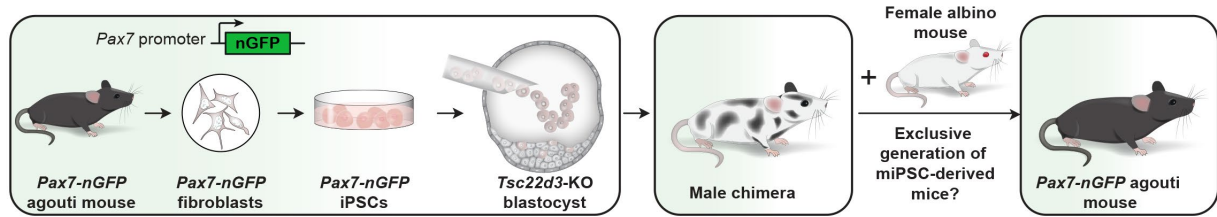
KO testes that were of bigger size and weight harbored intact seminiferous tubules containing spermatozoa, thus unveiling germline complementation (Figures S2D and S2E). Furthermore, we did not observe TSC22D3 or VASA protein expression in testes harvested from *Tsc22d3*-KO mice, whereas prominent expression of these germ cell-related proteins was documented in testes of a WT mouse and two complemented iPSC-chimeras (Figure 2G). Altogether, out of eight analyzed iPSC-chimeras we detected in the cauda epididymis of three animals mature and motile spermatozoa via percutaneous epididymal sperm aspiration (PESA) procedure or posthumous analysis (Figure S2E, table S2 and video S2). To better characterize the cell populations that are present in the cauda epididymis, we performed scRNA-seq of PESA biopsies extracted from a *Tsc22d3*-KO mouse and a *Pax7-nGFP* iPSC/*Tsc22d3*-KO chimera. This analysis revealed a germ cell population that was only present in the *Pax7-nGFP*-iPSC/*Tsc22d3*-KO chimera and expressed post-meiotic markers indicative of late-stage spermatogenesis such as *Prm1* and *Prm2* (Figures 2H, 2I, and S2F). In contrast, a PESA biopsy of a *Tsc22d3*-KO male mouse was devoid of cells expressing spermatid markers and was mainly composed of immune cells in the form of macrophages and B cells (Figures 2H, 2I, and S2F).

Next, we subjected PESA-derived cells from *Pax7-nGFP* iPSC/*Tsc22d3*-KO chimeras to FACS-purification for haploid cells based on DNA content and isolated mature spermatozoa (Figures S2G and S2H). PCR of genomic DNA extracted from the sorted spermatozoa demonstrated presence of the *Pax7-nGFP* transgenic allele (Figure S2I). Importantly, natural breeding of two complemented chimeras with albino female mice solely produced agouti F1 pups which all carried the *Pax7-nGFP* reporter allele, thus demonstrating the exclusive germline transmission of *Pax7-nGFP* iPSCs (Figures 2J and 2K). Last, FACS-purification of satellite cells from limb muscles of an F1 pup gave rise to a population of proliferative *Pax7-nGFP*<sup>+</sup> myoblasts that could further differentiate into multinucleated myotubes that were GFP negative (Figures S2J and S2K). Based on these results, and similar to mESCs, we conclude that transgenic miPSCs can reconstitute the male germline in intraspecies chimeras, giving rise via natural mating to mouse progeny that is exclusively iPSC-derived.

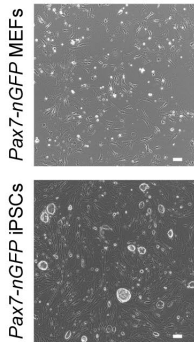


**Figure 2**

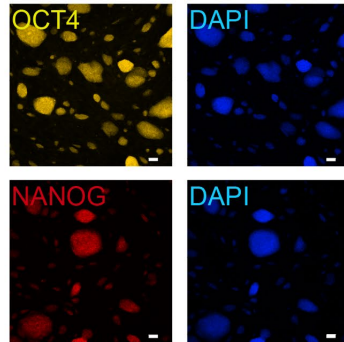
**A**



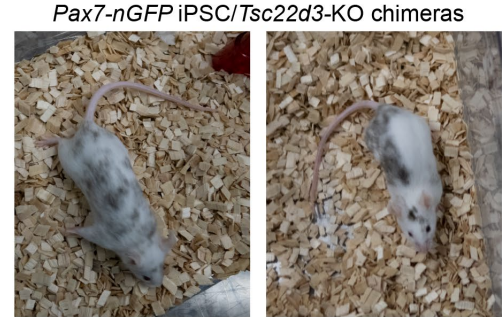
**B**



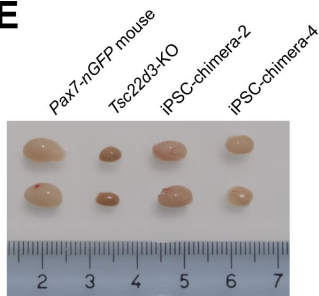
**C**



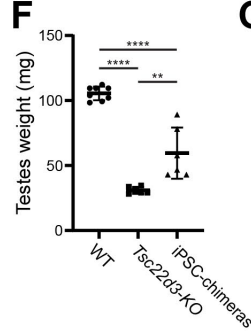
**D**



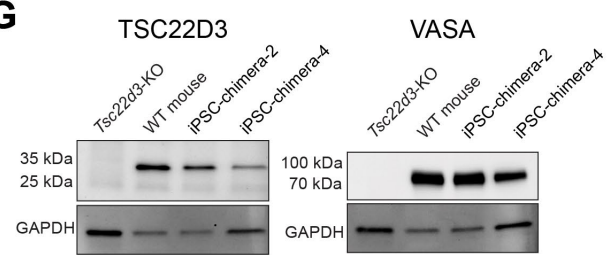
**E**



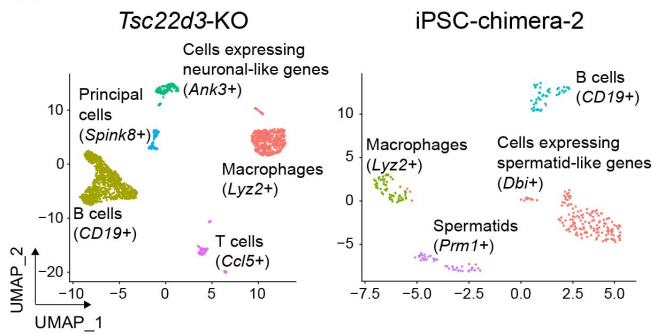
**F**



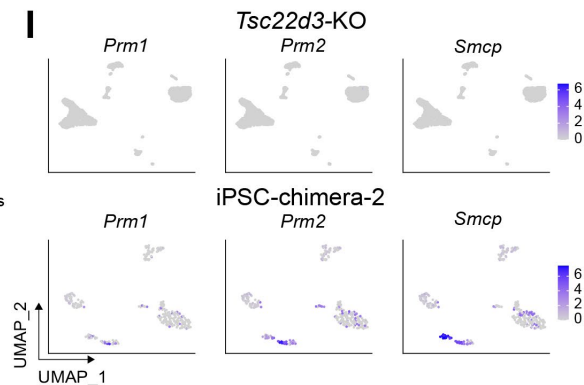
**G**



**H**



**I**



**J**



**K**

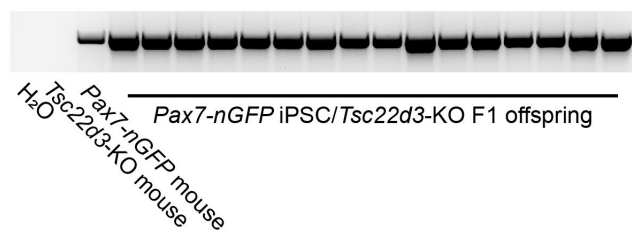


**Fig 2: Exclusive production of miPSC-derived functional spermatozoa in chimeras**

**(A)** A schematic illustrating experimental design. **(B)** Representative bright-field images of *Pax7-nGFP* fibroblasts (top) and derivative *Pax7-nGFP* iPSCs (bottom). Scale bar, 100 $\mu$ m. MEFs, mouse embryonic fibroblasts. **(C)** Representative immunofluorescence images of OCT4 and NANOG in *Pax7-nGFP* iPSCs. Scale bar, 100 $\mu$ m. **(D)** Representative photos showing two adult male *Pax7-nGFP*-iPSC/*Tsc22d3*-KO chimeras. Agouti coat color indicates contribution of *Pax7-nGFP* iPSCs to chimerism. **(E)** A photo of testes isolated from the indicated mouse strains. **(F)** A graph depicting testes weight from the indicated mouse strains (n=4-8 biological replicates; each dot represents a single testis, one-way ANOVA test with Tukey Post-Hoc analysis was used, error bars denote SD, \*\*p<0.01, \*\*\*\*p<0.0001). **(G)** Western blot analysis for TSC22D3 and VASA protein expression in the indicated samples. **(H)** UMAP projections showing all cells colored by different cell types in PESA-derived cauda epididymis biopsies from the indicated animals. Note presence of germ cells only in the iPSC-chimera. **(I)** UMAP projections for the indicated elongated spermatid markers showing presence only in the iPSC-chimera cell populations shown in (H). **(J)** A photo showing the progeny of natural breeding between a *Pax7-nGFP*-iPSC/*Tsc22d3*-KO male chimera and an albino female mouse. Note that all F1 pups have an agouti coat color, indicating exclusive germline transmission from *Pax7-nGFP* iPSCs. **(K)** PCR analysis for the transgenic *Pax7-nGFP* allele in the indicated mouse strains.

### **DAC8 rat ESCs contribute to multiple organs and tissues in mouse-rat chimeras**

Following the success in restoring fertility via intraspecies blastocyst complementation with mouse PSCs in male chimeras, we next wished to investigate whether injection of rat PSCs into *Tsc22d3*-KO mouse embryos can reconstitute the male germline niche and produce rat spermatozoa in mouse-rat chimeras. To this end, we set out to attempt production of adult mouse-rat chimeras utilizing DAC8 rat ESCs (DAC8-rESCs), a line that was previously shown to contribute to chimerism and germline transmission in rats (Figure 3A)<sup>12,222</sup>. As a first step, we transduced DAC8-rESCs with lentiviruses encoding for constitutive H2B-RFP expression followed by FACS-purification of RFP<sup>+</sup> cells to produce a homogeneous population of RFP<sup>+</sup>DAC8-rESCs for injections (Figures 3A and 3B). DAC8-RFP<sup>+</sup>rESCs expressed pluripotency markers and maintained a normal diploid male karyotype (Figures 3C and 3D). Furthermore, we confirmed via bulk RNA-seq analysis that DAC8-rESCs highly expressed, in comparison to rat fibroblasts, a suite of canonical markers indicative of pluripotency (Figure 3E). To assess the contribution of rESCs to chimerism in mice, we injected 12-15 RFP<sup>+</sup>DAC8-rESCs or DAC8-rESCs into *Tsc22d3*-KO blastocysts and transferred the embryos into the oviducts of foster mice. These efforts resulted in production of 16 mouse-rat chimeras as judged by visual inspection of fur color, exhibiting various degrees of coat color chimerism (Figure 3F and Table S3). Of note, we observed lower generation of interspecies mouse-rat chimeras in comparison to intraspecies chimeras, a finding which may be attributed to curtailed contribution of rat ESCs to mouse chimerism or increased embryonic lethality of



mouse-rat chimeras as previously reported<sup>58,59</sup>. Importantly, most of the mouse-rat chimeras appeared healthy and developed normally while exhibiting mouse size and weight (Figure S3A). However, a few chimeras exhibited reduced body size and weight, malocclusion or other abnormalities as reported by others (Figure S3A)<sup>58,59</sup>. Interestingly, one female mouse-rat chimera had reached over 1 year of age, suggesting that a chimera composed of XY-rat / XX-mouse cells can successfully reach an adult age (Figure 3F). We analyzed several internal organs for RFP expression and detected contribution of RFP<sup>+</sup>DAC8-rESCs to the heart, brain, kidney and spleen, and further confirmed presence of the RFP transgene (Figures 3G, 3H, 3I and S3B). We then subjected genomic DNA extracted from skin biopsies of chimeras to species-specific PCR using either mouse or rat specific primers and detected both mouse and rat DNA (Figure 3J). Taken together, we show that injection of DAC8 -rESCs into *Tsc22d3*-KO blastocysts gave rise to viable mouse-rat chimeras that predominately appeared normal and could reach adulthood. Contribution of rESCs was detected in the heart and brain, demonstrating a permissive environment for two distinct genotypes to coexist in important organs.

**Figure 3**

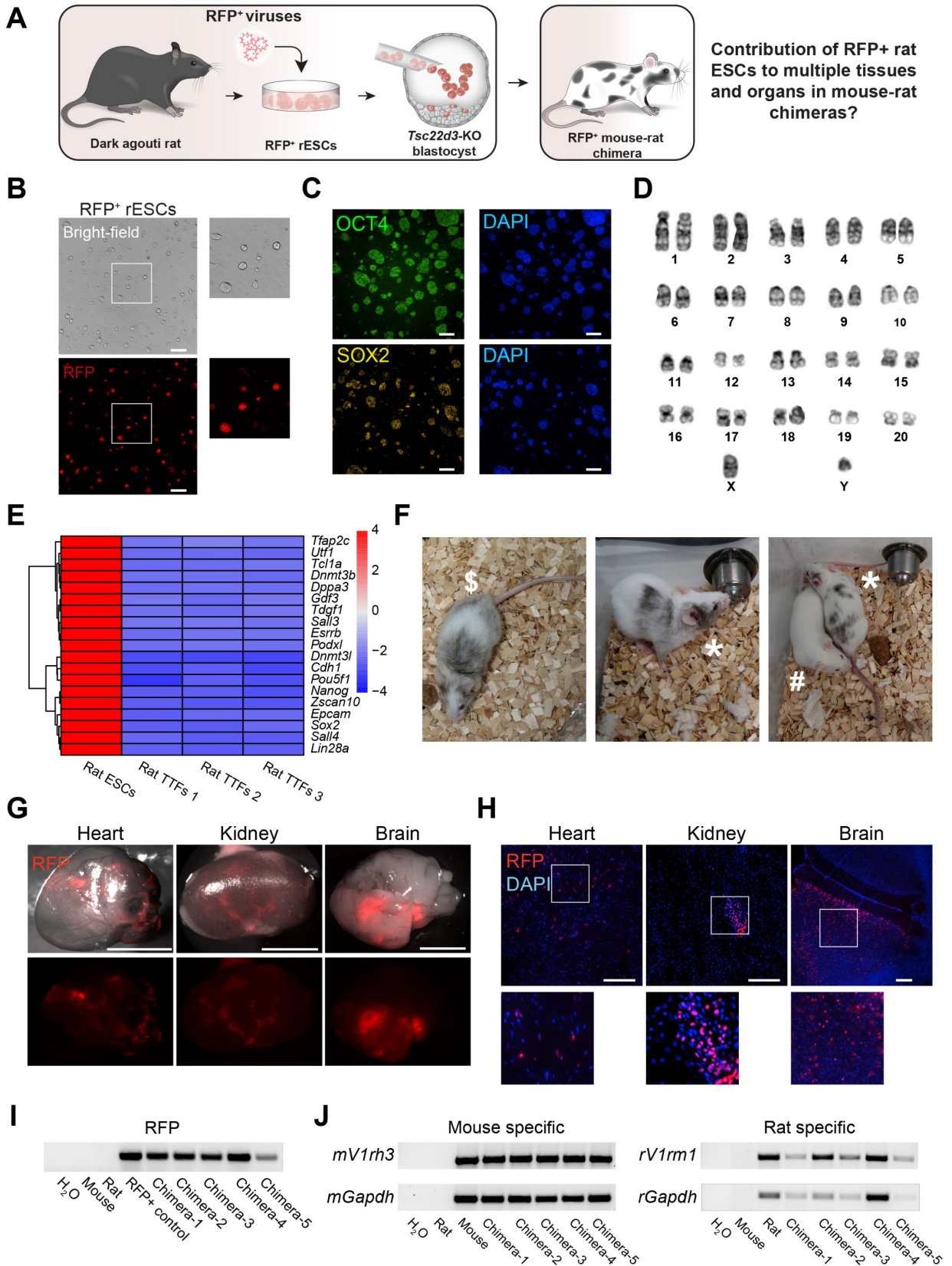


**Fig 3: Generation and characterization of mouse-rat chimeras**

(A) A schematic illustrating experimental design. (B) Representative bright-field and RFP images of RFP<sup>+</sup>DAC8 rESCs. Scale bar, 200µm. rESCs, rat embryonic stem cells. (C) Representative

immunofluorescence images of OCT4 and SOX2 in DAC8-rESCs. Scale bar, 200 $\mu$ m. **(D)** A karyogram of DAC8-rESCs showing a normal set of 42 chromosomes. **(E)** A heatmap depicting expression of pluripotency genes based on global RNA-seq of rESCs and three rat TTFs lines. TTFs, tail tip fibroblasts. **(F)** Representative photos of three adult mouse-rat chimeras demonstrating dark agouti fur color from the contribution of injected DAC8-rESCs. “#” denotes a non-chimeric *Tsc22d3*-KO mouse, “\*” denotes a male mouse-rat chimera, “\$” denotes a female mouse-rat chimera. **(G)** Representative bright-field and RFP images of the indicated organs that were harvested from mouse-rat chimeras. Scale bar, 5mm. **(H)** Representative cross-section images of the indicated organs harvested from RFP<sup>+</sup>DAC8-rESCs/*Tsc22d3*-KO chimeras and demonstrating RFP<sup>+</sup> reporter expression. Scale bar, 100 $\mu$ m. **(I)** A PCR analysis for presence of the RFP transgene in the indicated animals. **(J)** A gel depicting species-specific PCR for mouse (*mV1rh3*, *mGapdh*) or rat (*rV1rm1*, *rGapdh*) genes in the indicated animals.

### **Exclusive production of rESC-derived spermatozoa in interspecies chimeras**

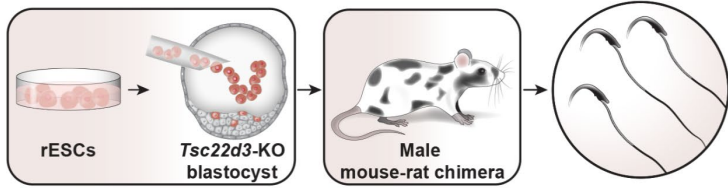
Following the success in production of adult mouse-rat chimeras, we next wished to investigate whether DAC8-rESCs or RFP<sup>+</sup>DAC8-rESCs can exclusively give rise to rat spermatozoa in interspecies mouse-rat chimeras (Figure 4A). To this end, we sacrificed and posthumously inspected an RFP<sup>+</sup>DAC8-rESC high-grade mouse-rat chimera-1 and documented a large testicular size in comparison to a non-complemented *Tsc22d3*-KO control (Figures S4A and S4B). Large testicular size was also observed in several other DAC8-rESC/*Tsc22d3*-KO chimeras (Figures 4B and 4C). A testis cross-section of mouse-rat chimera-1 showed strong nuclear RFP expression, emanating from RFP<sup>+</sup>DAC8-rESCs (Figure S4C). Most notably, the testis of a *Tsc22d3*-KO mouse exhibited atrophic seminiferous tubules, whereas the testis of a mouse-rat chimera demonstrated intact tubules containing spermatozoa (Figure 4D). We further detected presence of the germ cell and spermatid-associated proteins VASA and PNA in the testes of several DAC8-rESC/*Tsc22d3*-KO chimeras, whereas these germ cell markers were absent in the testes of *Tsc22d3*-KO mice (Figures 4E and 4F).

Immature spermatozoa gain motility and fertilization capacity as they transition from the testes through the epididymis, where they are stored in the cauda epididymis<sup>101</sup>. Spermatozoa extracted from the cauda epididymis of 2-3 months old mouse-rat chimeras contained elongated tails with a typical rat sperm head-morphology, whereas no spermatozoa were detected in the cauda epididymis of *Tsc22d3*-KO mice (Figures 4G and S4D). However, these spermatozoa were immotile, and we further detected in the cauda epididymis immature elongated spermatids containing intact tails albeit lacking the typical sperm head-morphology associated with mature rat spermatozoa (Figure S4D). To unequivocally confirm exclusive contribution of rESCs to the production of rat spermatozoa in mouse-rat chimeras, we subjected cells that were extracted from the

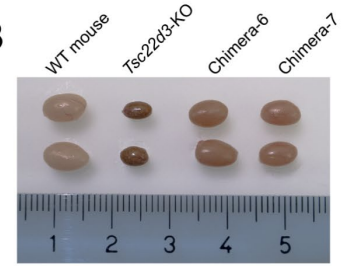
cauda epididymis of mouse-rat chimera-1 to FACS-purification for haploid cells based on DNA content (Figure 4H). Using this method, we purified spermatozoa containing elongated tails and a typical rat sperm head-morphology indicative of mature spermatozoa (Figure 4H). We then extracted genomic DNA from these spermatozoa and subjected it to species-specific PCR for the mouse and rat *Gapdh* and vomeronasal receptor genes (mouse *V1rh3* or rat *V1rm1*). We could only detect rat *Gapdh* and *V1rm1* PCR bands in the FACS-purified spermatozoa, and no PCR bands for mouse genes were detected (Figure 4I). Next, we subjected the PCR products to sequencing and documented complete matched read alignment only with the rat reference genome (Figures 4J and S4E). Collectively, these findings demonstrate that rESCs can overcome the germline differentiation defect attributed to lack of the TSC22D3 protein in sterile mice and exclusively produce haploid rat spermatozoa in interspecies chimeras.

**Figure 4**

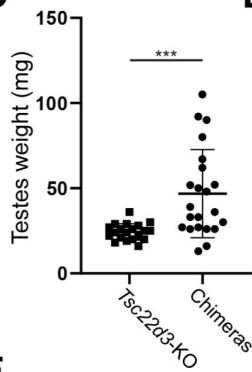
**A**



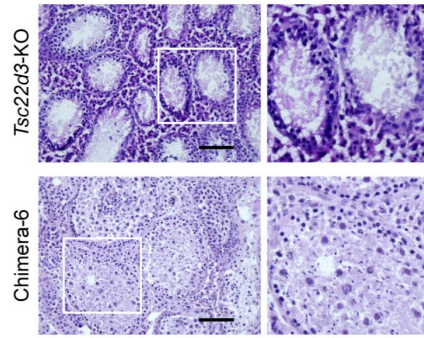
**B**



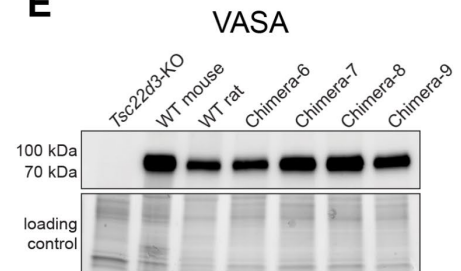
**C**



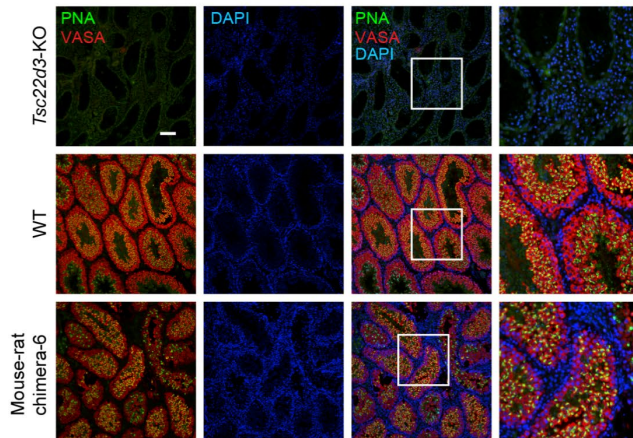
**D**



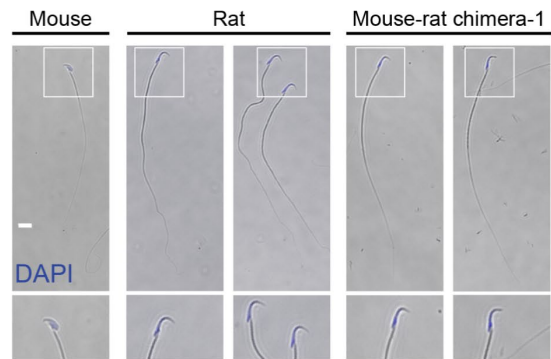
**E**



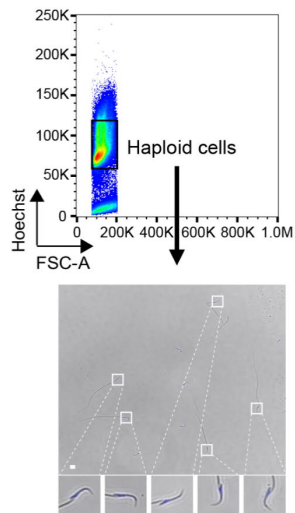
**F**



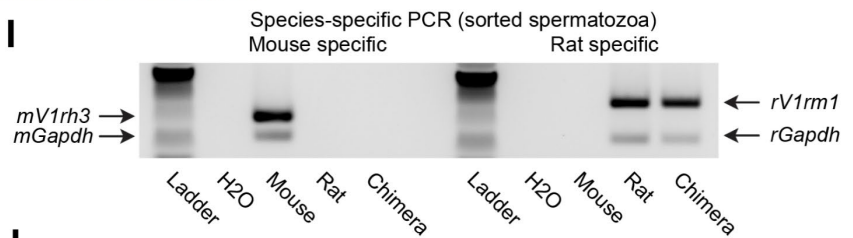
**G**



**H**



**I**



**J**

Gapdh (R+M primers)

Rat	1	AGCCCAA	ACTAACCG	TGTCTCA	ATCTGTT	CTAGGT	ATG	-	-	-	ACAAT	44
Chimera	1	AGCCCAA	ACTAACCG	TGTCTCA	ATCTGTT	CTAGGT	ATG	-	-	-	ACAAT	44
Mouse	1	-	-	-	-	-	-	-	-	-	-	-
Rat	45	GAATAT	TGGCTA	CAGCAAC	AGGGT	TGGAC	CTCAT	GGCCT	ACAT	GGCC	-	92
Chimera	45	GAATAT	TGGCTA	CAGCAAC	AGGGT	TGGAC	CTCAT	GGCCT	ACAT	GGCC	-	92
Mouse	23	AAATAT	GAACA	CTCACT	CAAGAT	TGT	CAGCA	ATGCAT	CCT	GCA	-	67
Rat	93	TCCAAG	GAGTA	AAGAA	ACCCT	TGGAC	-	-	-	-	-	135
Chimera	93	TCCAAG	GAGTA	AAGAA	ACCCT	TGGAC	-	-	-	-	-	135
Mouse	68	ACCAAC	CTGCT	TAG	CCCC	CTGG	CAAG	GT	CAT	TCCA	TGAC	115
Rat	136	ACTGAG	AGCA	AGAG	AGGG	CCCT	CAGTT	GCTG	AGG	AGTC	-	178
Chimera	136	ACTGAG	AGCA	AGAG	AGGG	CCCT	CAGTT	GCTG	AGG	AGTC	-	178
Mouse	116	ATTG	TGGA	AGG	GCTCAT	GGTAT	TGT	AG	GCAG	TGG	GAG	160

**Fig 4: Exclusive generation of rat spermatozoa in mouse-rat chimeras**



(A) A schematic illustrating experimental design. (B) A representative photo of isolated testes from the indicated animals. (C) Quantification of testes weight in the indicated animals (n= 20-22 biological replicates; each dot represents a single testis, unpaired two tailed t-test was used, error bars denote SD, \*\*\*p<0.001). (D) H&E staining of testes cross-sections from the indicated samples. Scale bar, 100µm. (E) Western blot analysis for VASA protein expression in the indicated testes samples. (F) Immunostaining for VASA and PNA in testes of the indicated animals. Scale bar, 100µm. (G) Representative images of spermatozoa extracted from the cauda epididymis of the indicated animals and counterstained with DAPI. Scale bar, 10µm. (H) FACS-sorting strategy for purification of haploid cells from the cauda epididymis of RFP<sup>+</sup>DAC8rESCs/*Tsc22d3*-KO mouse-rat chimera-1. Shown is a representative image of sorted spermatozoa embodying rat sperm head-morphology. Scale bar, 10µm. (I) A gel showing species-specific PCR for the indicated genes in haploid spermatozoa sorted from the cauda epididymis of the indicated animals. (J) DNA sequencing of the mouse and rat *Gapdh* PCR products shown in Fig. 4I. Misalignments are highlighted in yellow.

### Characterization of cell types and differentiation trajectory in a mouse-rat chimera testis by scRNA-seq

Our observation that rat germ cells can be produced in the testes of mouse-rat chimeras prompted us to investigate to what extent rat cells undergo spermatogenesis in a xenogeneic environment lacking a TSC22D3 protein. To this end, we performed scRNA-seq of dissociated testes from a *Tsc22d3*-KO mouse and a mouse-rat chimera. Expectedly, the *Tsc22d3*-KO testis was devoid of germ cells yet consisted of white blood, endothelial and Leydig cells (Figure 5A). Further, as we expected to find cells of both rat and mouse origin in a chimera testis, we created a custom mouse-rat chimeric reference genome and mapped both samples against it to ensure species specificity. Mapping results demonstrated that the *Tsc22d3*-KO testis was only composed of mouse cells, whilst the chimera testis contained cells expressing either mouse or rat genes, albeit predominantly the latter (Figures 5B and S5A). Mouse cell populations in a chimera testis consisted of white blood, stromal and Leydig cells in addition to a very small population of pre-meiotic germ cells, which presumably indicate an early cell population preceding the differentiation blockage inflicted by the *Tsc22d3* mutation (Figure 5C). In stark contrast, rat cells in the chimera testis were annotated as spermatogonial cells (*Crabp1*<sup>+</sup>, *Uchl1*<sup>+</sup>), spermatocytes (*Sycp3*<sup>+</sup>, *Piwil1*<sup>+</sup>), round spermatids (*Acrv1*<sup>+</sup>, *Spaca1*<sup>+</sup>) and elongated spermatids (*Tnp1*<sup>+</sup>, *Prm2*<sup>+</sup>), thus representing multiple differentiation stages of spermatogenesis (Figures 5C and 5D). Interestingly, only germ cells yet no other somatic cell type was of rat origin, suggesting a preferential contribution of rat PSCs towards the germline in the chimera testis (Figure 5C). Further, a cell cycle analysis demonstrated that rat spermatogonia and spermatocytes are predominantly in an S and G2/M

proliferation state, whereas downstream cell types gradually exited the cell cycle as they transitioned through meiosis and underwent terminal differentiation into elongated spermatids (Figure S5B). Examination of various markers for spermatogenesis revealed that none of the inspected genes were expressed in a *Tsc22d3*-KO mouse testis and only rat germ cell transcripts were expressed in a chimera testis (Figures 5D, 5E and S5C). Additionally, we documented a similar pattern of rat germ cells in a chimera testis and a WT rat testis, confirming high expression of genes such as *Prm1*, *Tnp2* and *Tssk6* that are indicative of late elongated spermatids in both samples (Figure S5C).

Next, we performed a pseudotime lineage trajectory analysis for rat cells and confirmed the progression from spermatocytes to round and elongated spermatids in a chimera testis (Figure 5F). Of note, we also detected spermatogonia, spermatocytes and spermatid cell populations that did not participate in the lineage trajectory (Figure 5F). Based on the trajectory analysis we observed a pseudotime difference within round and elongated spermatid populations indicating that these populations are composed of cells representing different stages of spermatogenesis (Figure 5G). We annotated the stages into early and late based on the high expression of well-established markers (Figures 5G and S5D). To conclude, the scRNA-seq unequivocally determined that only rat cells participate in active spermatogenesis in a mouse-rat chimera testis harboring a *Tsc22d3* mutation. This analysis helped to dissect the various rat cell types undergoing germline differentiation in a xenogeneic mouse host environment, and further highlighted several rat germ cell populations that did not participate in the differentiation trajectory.

**Figure 5**

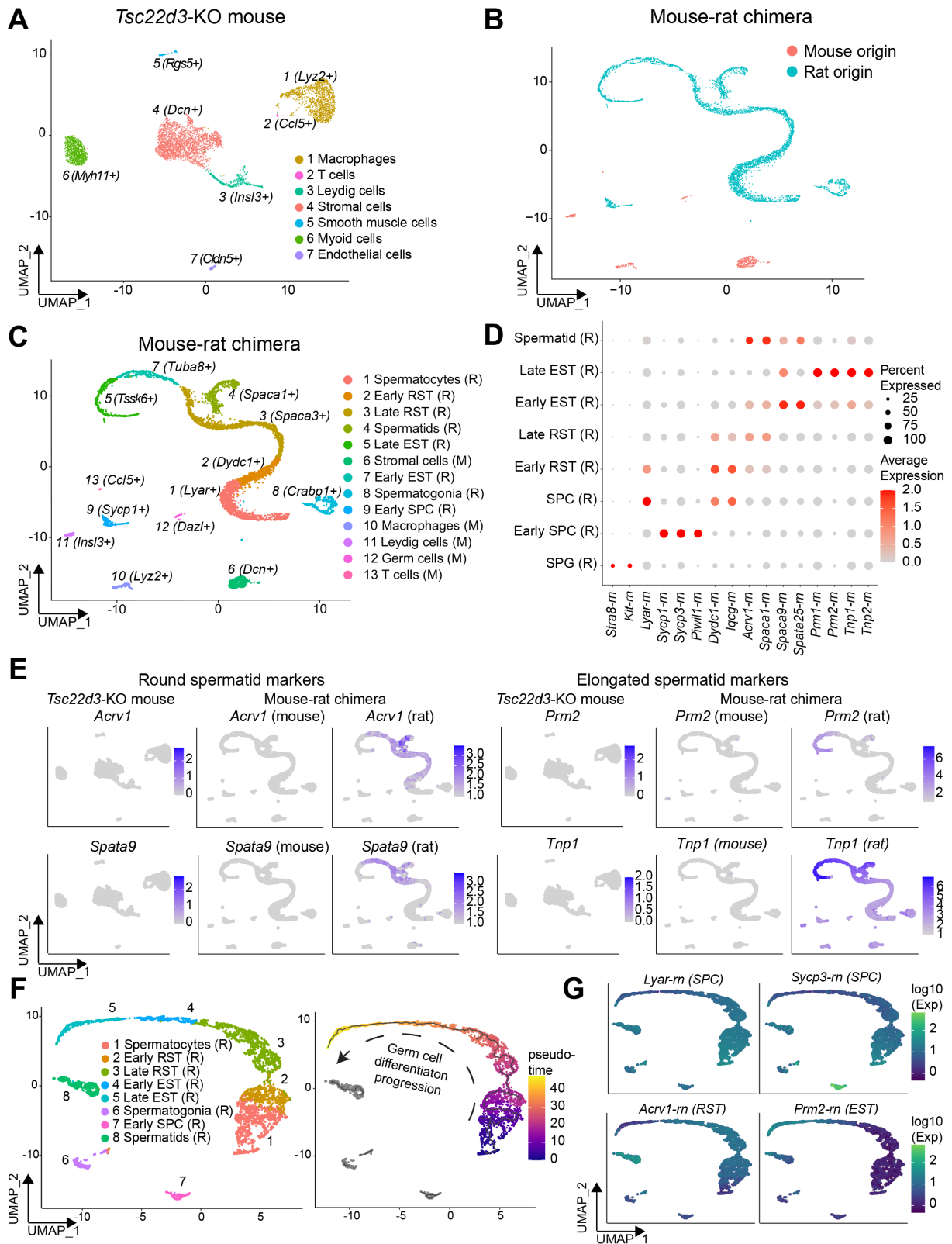


**Fig 5: scRNA-seq of testicular cells derived from a germline-complemented mouse-rat chimera**

**(A)** UMAP projection of *Tsc22d3*-KO testis representing 6,382 cells and colored by different cell types. Note absence of germ cells. **(B)** UMAP projection of mouse-rat chimera testis representing



5,060 cells colored by species. **(C)** UMAP projection based on scRNA-seq data of a mouse-rat chimera testis representing 5,060 cells colored by different cell types. R, Rat. M, Mouse. RST, round spermatids. EST, elongated spermatids. SPC, spermatocytes. **(D)** Dot plot for individual gene expression in various germ cell populations as shown in Fig. 3C. rn, *Rattus norvegicus*. SPG, spermatogonia. **(E)** UMAP projection of *Tsc22d3*-KO and mouse-rat chimera testes showing all cells colored by the expression level of the indicated spermatid markers. **(F)** Monocle3 UMAP projection showing all rat cells (n=4,491) from a mouse-rat chimera colored by different cell types (left) and calculated pseudotime values (right). **(G)** Monocle3 UMAP projection showing all rat cells from a mouse-rat chimera colored by the expression level of the indicated germ cell markers.

### **Fertilization of rat oocytes with interspecies rat spermatozoa**

The exclusive production of rat germ cells in interspecies chimeras raised the question whether these cells can fertilize rat oocytes. As mouse-rat chimeras are of mouse size and might be preyed by rats, we opted to use Intracytoplasmic Sperm Injection (ICSI), an assisted reproductive technology, to attempt fertilization of rat oocytes<sup>223</sup>. We first trialed generation of rats using frozen-thawed cauda-derived spermatozoa produced in rats (Figure 6A). We were successful in generating live and healthy rat progeny via ICSI and in addition could grow fertilized zygotes to the blastocyst stage *in vitro* (Figure 6B). As the next step, we trialed injection of frozen-thawed cauda epididymis-derived spermatozoa from an interspecies chimera into Sprague-Dawley (SD) rat oocytes (Figure 6C). To this end, we injected spermatozoa that were produced in mouse-rat chimera-1. We first attempted production of embryos *in vitro* to determine if interspecies rat spermatozoa can support early-stage embryonic development. We performed ICSI with 312 SD oocytes, out of which 213 embryos survived, resulting in several rat embryos that developed until 4-8 cell stage, in addition to morula and blastocyst stage embryos (Figures 6D and 6E). Of note, the rate of embryo production was substantially lower in comparison to similar *in vitro* trials conducted with rat spermatozoa produced in rats (Figure 6B). Next, to attempt generation of adult rats, 239 SD oocytes were injected with interspecies spermatozoa from chimera-1 and 180 embryos were transferred into the oviducts of foster SD rats, however, did not produce live rats.

Due to the inability to produce live rats from cauda epididymis-derived spermatozoa of a mouse-rat chimera, we reasoned that germ cells at an earlier developmental stage might produce rats via Testicular Sperm Extraction (TESE)-ICSI<sup>139</sup> (Figure 6C). To investigate this hypothesis, we generated new interspecies chimeras by injection of *Tsc22d3*-KO blastocysts with *F344-Tg.EC4011/Rrrc* rESCs, which are

heterozygous for a ubiquitin C promoter-EGFP (*UBC-EGFP*) transgene and were previously shown to contribute to germline transmission in rats<sup>224,225</sup>. Similar to DAC8-rESCs, *UBC-EGFP* rESCs could contribute to chimerism in mice and produce interspecies chimeras of normal mouse bodyweight (Figure S6A). Notably, two *UBC-EGFP*-rESC/*Tsc22d3*-KO mouse-rat chimeras exhibited significantly larger testes in comparison to *Tsc22d3*-KO mice and expressed the EGFP transgene (Figures S6B-SE). We dissociated the EGFP<sup>+</sup> testes posthumously and detected multiple spermatozoa showing typical rat sperm head-morphology in the testes of one chimera (Figure S6F). We then performed TESE-ICSI with 208 oocytes, out of which 136 survived, with frozen-thawed interspecies testicular germ cells derived from an EGFP<sup>+</sup> mouse-rat chimera. This trial gave rise to an EGFP<sup>+</sup> blastocyst upon *in vitro* embryo culture (Figures 6G and S6G). Notably, transfer of 113 embryos (194 injected) into foster mothers did not produce live rats. Last, as we did not document rat births, we decided to investigate whether blastocysts can be produced *in vivo* and implant into the uterus (Figure 6C). To this end, we performed a C-section of foster mothers which were subjected to embryo transfer with 1 or 2 cell-stage embryos (206 embryos in total). Surprisingly, we detected several implantation sites containing resorbed embryos, and one expressing the EGFP reporter (Figures 6H and S6H). In summary, frozen-thawed germ cells from the two examined interspecies chimeras contained cells that carry potential to fertilize rat oocytes and give rise to blastocysts *in vitro*, or implanted embryos that resorbed; however not to live rats.

**Figure 6**

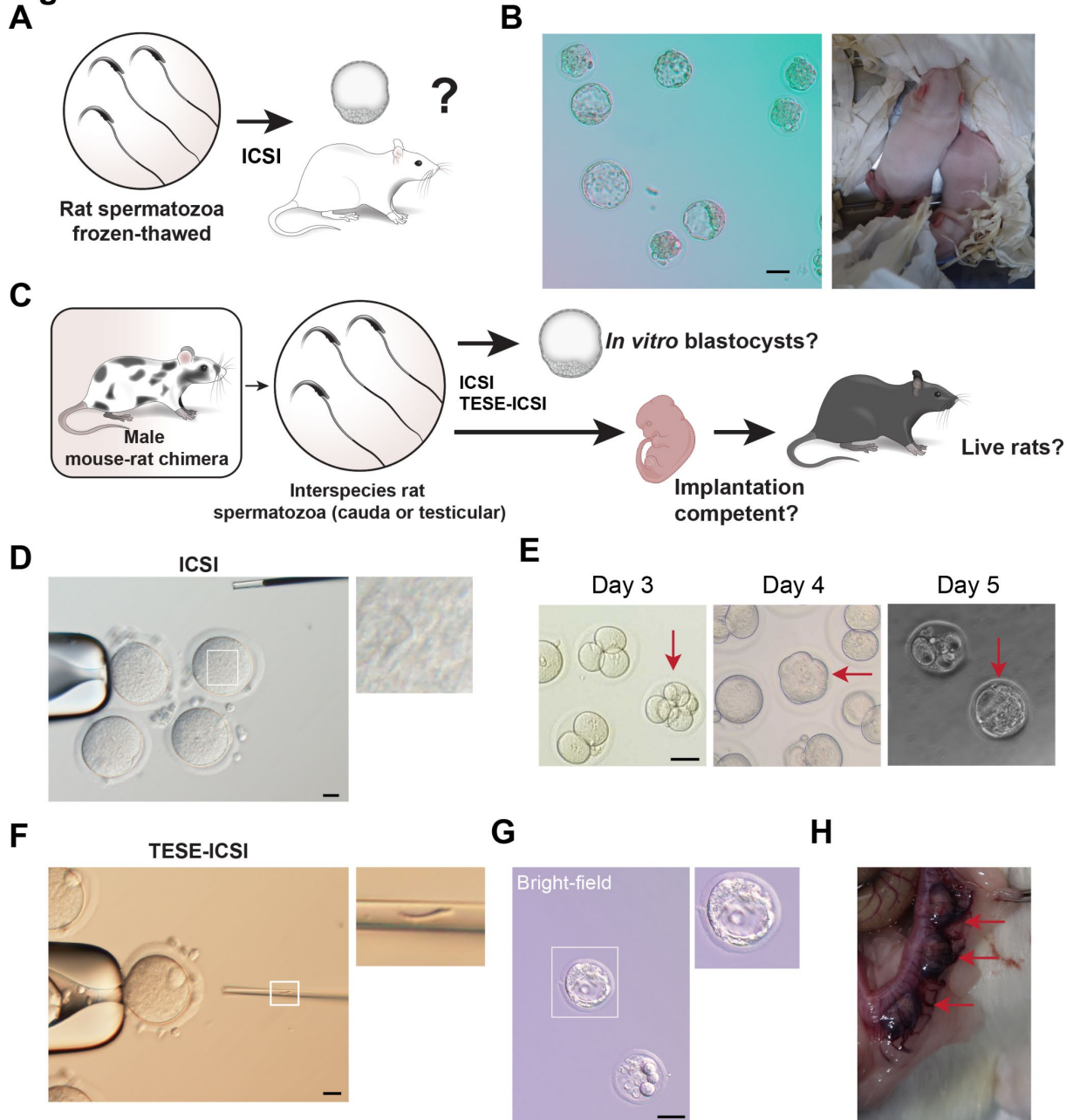


**Fig 6: Fertilization of rat oocytes with rat spermatozoa exclusively produced in interspecies chimeras**

**(A)** A schematic illustrating experimental design. **(B)** Blastocysts generated via ICSI from cauda epididymis-derived spermatozoa produced in rats (left) and derivative pups (right). Scale bar, 50µm. ICSI, Intracytoplasmic Sperm Injection. **(C)** A schematic illustrating experimental design. TESE-ICSI, Testicular Sperm Extraction ICSI. **(D)** Rat oocytes injected with cauda epididymis-derived spermatozoa produced in mouse-rat chimera-1 via ICSI. Scale bar, 20µm. **(E)** Images showing rat embryos produced from interspecies rat spermatozoa of mouse-rat chimera-1. Frozen-thawed cells were injected into rat Sprague-Dawley (SD) oocytes via ICSI and cultured *in vitro*. Shown are 4-8 cell stage, morula-stage and blastocysts-stage rat embryos at the indicated days, as pointed by arrows. Scale bar, 50µm. **(F)** Image depicting an interspecies testicular rat germ cell prior to injection into an SD oocyte. Scale bar, 20µm. **(G)** An image showing a blastocyst

that was generated using an interspecies rat germ cell from the testes of a GFP<sup>+</sup> mouse-rat chimera. Frozen-thawed cells were injected into SD oocytes via TESE-ICSI and cultured *in vitro*. Scale bar, 50µm. **(H)** A photo showing three embryonic implantation sites in a foster female after embryo transfer of SD oocytes injected with mouse-rat chimera germ cells. Arrows point to implantation sites.

## Discussion

In this study we report on a method to exclusively produce germ cells of one species in another utilizing blastocyst complementation with PSCs. Capitalizing on the sterility-associated mutation in *Tsc22d3*-KO mouse blastocysts, we documented production of intraspecies and interspecies chimeras that embody mouse or rat spermatozoa solely from injected ESCs or iPSCs. Notably, mouse intraspecies chimeras harboring PSC-derived spermatozoa solely gave rise to PSC-derived adult mice, whereas interspecies rat spermatozoa could fertilize oocytes and produce blastocysts and implantation-competent embryos. However, for the two examined mouse-rat chimeras, embryos fertilized with frozen-thawed interspecies germ cells did not develop normally, and live births were not recorded.

In general, the capacity to produce interspecies chimeras with somatic and germline contribution is expected to be dependent on species similarity and a physiologically receptive environment that is permissive for two distinct genotypes to coalesce in the same organism, as demonstrated in recent years for adult or fetal mouse-rat, human-monkey and human-pig chimeras<sup>50,52,53,226</sup>. Furthermore, contribution to interspecies chimerism is highly dependent on cell competition and the capacity of PSCs to overcome evolutionary barriers<sup>227</sup>. Recent efforts to overcome such barriers have been reported and include injection of *TP53*, *Myd88*- or *P65*-null PSCs, overexpression of the anti-apoptotic gene *Bcl2* in PSCs or harnessing mouse *Igf1r*-null blastocysts to increase contribution of PSCs to chimerism<sup>53,228-230</sup>. In respect to germline complementation, given that we documented a relatively low number of interspecies chimera production, we postulate that utilizing such methods may augment the capacity of PSCs to contribute to chimerism and in particular to the germline. However, such methods also warrant caution, as production of chimeras with extensive contribution from xenogeneic PSCs could be detrimental to survival during embryonic development<sup>58,59</sup>.

To date, interspecies blastocyst complementation between a mouse and a rat has been documented for various organs and tissues including pancreas, thymus, kidney and blood vasculature<sup>39,48,49,57,138,216,226</sup>. In respect to contribution of rat PSCs to the germline in mice, two studies previously reported on the production of functional rat spermatozoa

in mouse-rat chimeras from injected rESCs or iPSCs<sup>139,140</sup>. However, chimera testes contained both mouse and rat spermatozoa, necessitating a genetic reporter or morphological examination to distinguish between the two cell types<sup>139,140</sup>. The capacity to solely generate rat spermatozoa in sterile mice renders use of such methods potentially dispensable. Moreover, in agreement with our findings, a recent study by Kobayashi and colleagues documented germline blastocyst complementation in rats utilizing embryos that carry a mutation in *Prdm14*, an essential gene for germ cell production<sup>47,66,141</sup>. The authors further demonstrated interspecies blastocyst complementation via injection of mouse PSCs into *Prdm14*-KO rat embryos, solely generating functional mouse spermatids in rats that could give rise to live mice via Round Spermatid Injection (ROSI)<sup>141</sup>. The findings reported in that study, and the results reported herein, synergize to suggest that both mouse and rat PSCs can complement the male germline in interspecies chimeras by injection into blastocysts that carry mutations that preclude spermatogenesis. Furthermore, these and other observations suggest that mutations in different essential genes for germ cell production provides a vacant niche receptive for reconstitution with PSCs<sup>132,134,141,217</sup>.

Our efforts to produce live rats from frozen-thawed interspecies spermatozoa produced in two mouse-rat chimeras were unsuccessful. We hypothesize two reasons which may account for this result: (i) Effect of cell freezing: the ICSI and TESE-ICSI trials reported in this study were performed using frozen-thawed cauda epididymis or testicular germ cells. We speculate that use of non-frozen germ cells may carry increased chances of fertilization by mitigating potential impairment due to freeze-thaw cycles. (ii) Impaired interspecies germ cells: rat spermatogonia subjected to differentiation in mouse testes encounters a xenogeneic environment that is receptive towards differentiation of mouse and not rat cells, potentially impairing the functionality of interspecies rat germ cells. In support of this hypothesis, we documented via scRNA-seq several rat germ cell populations in a chimera testis that did not participate in the lineage differentiation progression towards an elongated spermatid cell population, potentially indicating an impaired process. To address this limitation, using immature germ cells via ROSI may lend a more favorable technique for production of animals from interspecies germ cells. Indeed, generation of live mice from mouse round spermatids produced in *Prdm14*-KO rats via ROSI was recently reported<sup>141</sup>. Nonetheless, further work is certainly required to explore the molecular and functional nature of rat germ cells produced in a xenogeneic mouse host in comparison to rat germ cells produced in rats. In particular, it will be of

interest to assess whether contribution of rat PSCs to spermatogenesis support cells in the form of Sertoli or Leydig cells will increase the portion of functional interspecies spermatozoa.

Given future experimental success, two additional implications may emanate from our study. The first involves production of rat transgenic models via sterile mice. Rats are commonly used as an animal model for human diseases in biomedical research, however production of transgenic rats from genetically modified PSCs are oftentimes challenged by low germline transmission rates. As such, the capacity to utilize sterile mice as hosts for genetically modified rat PSCs may assist in generation of transgenic rats via a one-step and faster solution<sup>139</sup>. This approach is particularly attractive for models that cannot rely on genome engineering tools such as CRISPR-Cas9 to produce transgenic rats, namely insertion of large DNA fragments or an artificial chromosome<sup>141</sup>. Last, an additional potential implication of this study may extend to animal conservation efforts, as the technique reported herein can be adapted to produce xenogeneic germ cells of endangered animal species. Notably however, blastocyst complementation of the germline has mostly been trialed thus far for mouse and rat PSCs, whose culture conditions and propensity to contribute to chimerism and the germline are well-established. To assess whether this technique can be adapted to other animal species, generation of additional mammalian PSCs with germline transmission competency is warranted. With success, we envision that germline blastocyst complementation may provide a useful tool to generate germ cells *in vivo* for production of transgenic animal models, or potentially assisting in the preservation efforts of endangered species.

## Experimental procedures

Details on methods, reagents, multiomics analyses, reprogramming and transgenic techniques can be found in the supplemental information.

## Animal strains and cell lines used in this study

The following mouse and rat strains were used in this study: KH2-ESCs, a subclone of V6.5 ESCs derived from a cross between C57BL/6 X 129/sv mice (a kind gift from Dr. Konrad Hochedlinger)<sup>218</sup>. *Pax7-nGFP* MEFs were derived from *Tg:Pax7-nGFP/C57BL6;DBA2* mice (a kind gift from Dr. Shahragim Tajbakhsh)<sup>219</sup>. *Tsc22D3-KO* male embryos, also known as “GoGermline” were purchased from Ozgene (Ozgene,

Perth, Australia). Rat DAC8-ESCs were derived from a *DA/OlaHsd-ES8/Qly* rat strain<sup>12</sup> and UBC-GFP ESCs were derived from a *F344-Tg(UBC-EGFP)F455Rrrc* rat strain<sup>224</sup>, and both were purchased from the Rat Resource and Research Center (RRRC) (<https://www.rrrc.us>). Animals were housed in Allentown cages in standard laboratory conditions, room temperature 23°C; relative humidity 50 to 60%; 12:12-h light-dark cycle. Photos of chimeras were taken with Canon PowerShot G7 X Mark II camera. The present study was approved by the Federal Food Safety and Veterinary Office, Cantonal veterinary office (Zurich) and granted animal experiment license numbers ZH124/19 and FormG-135.

### Data and code availability

The bulk and scRNA-seq datasets generated in this study are available in Gene Expression Omnibus (GEO) repository under accession number GSE167435.

### Author contributions

J. Zvick and O. Bar-Nur conceptualized the experiments, interpreted the results and wrote the manuscript. J. Zvick performed most experiments and analysis of results. O. Bar-Nur supervised the study. M. Tarnowska-Sengül helped with experiments involving chimera production and performed the PESA, blastocyst injection, embryo transfer, ICSI and TESE-ICSI procedures. A. Ghosh oversaw the generation of bulk mRNA-seq and scRNA-seq data in addition to analysis and interpretation of results and manuscript writing. N. Bundschuh assisted with FACS, H&E staining, PCR analysis, karyotype preparation and lentiviral production. F. Noé created the mouse-rat chimeric reference genome, P. Gjonlleshaj helped to produce interspecies chimeras, X. Qabrati performed Western blots, S. Domenig helped with isolation of myoblasts and performed the *in vitro* differentiation of myoblasts and I. Kim helped to perform immunofluorescence of testes cross-sections. T. Hennek oversaw the IVF and injection of PSCs in the ETH Phenomics Center at ETH Zurich and helped with interpretation of results. F. von Meyenn, L. Hinte and C. Trautmann, helped to conceptualize the single cell sequencing experiment, assisted in its execution and helped in result interpretation and manuscript writing.

### Conflict of interests

The authors declare no competing interest.

## Acknowledgments

We wish to thank Dr. Konrad Hochedlinger, Dr. Bruno Di Stefano, Dr Justin Brumbaugh as well as members of the Regenerative and Movement Biology Laboratory for their constructive comments and feedback. We are grateful to Dr. Shahragim Tajbakhsh for providing the *Pax7-nGFP* mouse strain and Dr. Konrad Hochedlinger for providing the KH2-ESCs, *M2rtTA* and *STEMCCA* lentiviral cassettes. We further wish to thank Dr. Hongsheng Men and Dr. Elizabeth Bryda from the Rat Resource and Research Center (RRRC) at the University of Missouri for their valuable suggestions in respect to rat embryo culture, DNA sequencing and ICSI. We are also grateful to the staff members at the EPIC transgenic core in the ETH Phenomics center of ETH Zurich for their help with a portion of the injections. We acknowledge the use of the Functional Genomics Center Zurich (FGCZ) and are grateful to their staff members for their assistance with next generation library preparation and Illumina sequencing of mRNA and scRNA samples. We also wish to thank SciArtWork for their help with preparation of graphical images, whereas a few other graphical schematics were also created with BioRender.com. This work was supported by startup funds from ETH Zurich to O. Bar-Nur. Other support to the Bar-Nur group includes an Eccellenza Grant from the Swiss National Science Foundation (grant no. PCEGP3\_187009) as well as grants from The Good Food Institute Foundation, The Novartis Foundation for Medical-Biological Research, The Helmut Horten Foundation and NCCR Robotics (grant number 51NF40\_185543). Work in the von Meyenn group is supported by the European Research Council (ERC) under the European Union's Horizon 2020 research and innovation program (Grant agreement No. 803491).



**Fig. S1**

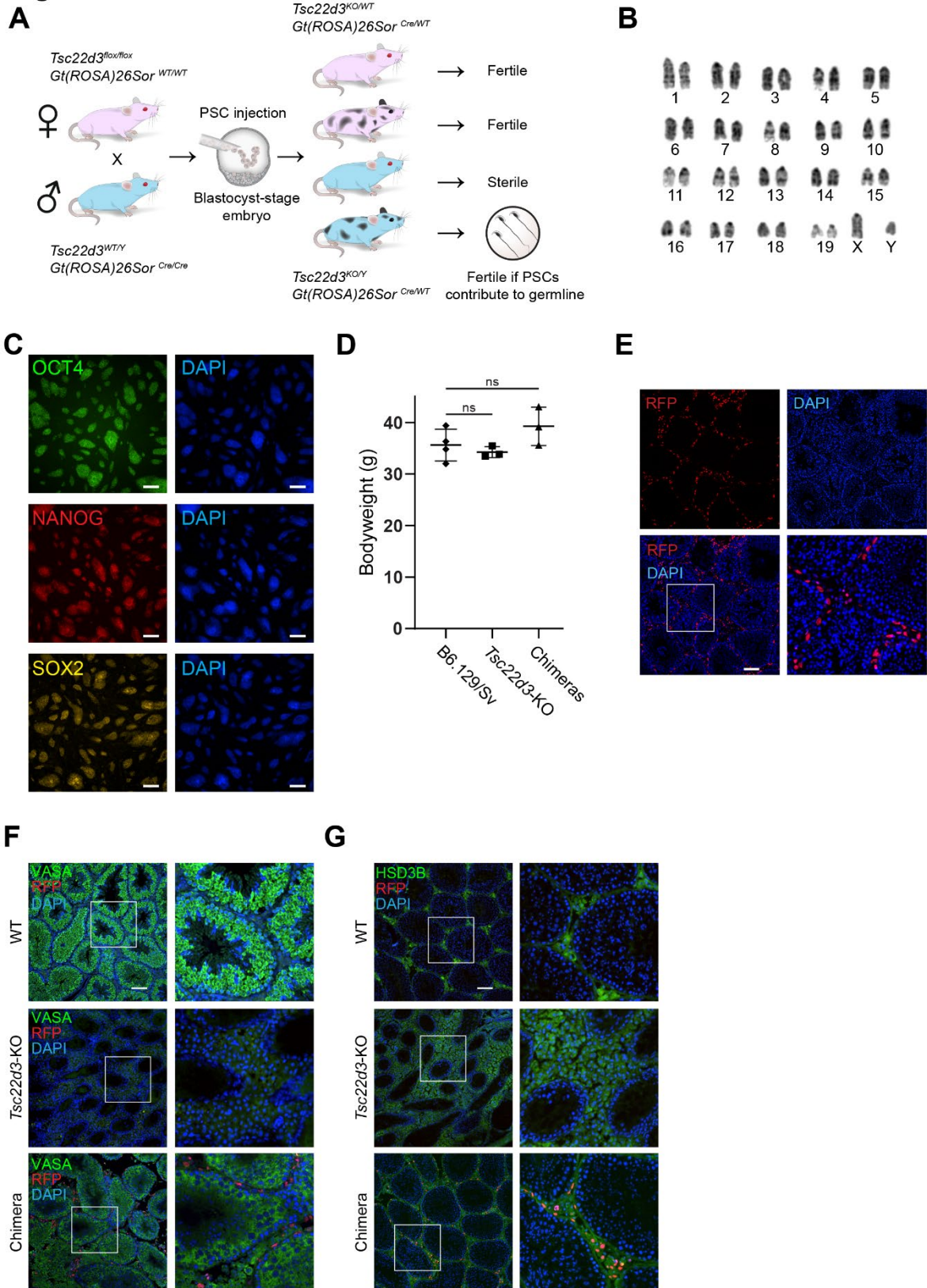


**Figure S1 related to Figure 1: Molecular characterization of KH2-mESCs and analysis of chimeras**

**(A)** A schematic depicting the breeding strategy used to produce *Tsc22d3-KO* blastocysts and chimeras. **(B)** A karyogram of KH2-mESCs showing 40 mouse chromosomes. **(C)** Representative

immunofluorescence images for OCT4, NANOG and SOX2 expression in KH2-mESCs. Scale bar, 200 $\mu$ m. **(D)** A graph showing bodyweight quantification of the indicated mouse strains, (n = 3-4 biological replicates, each dot represents a single animal, one-way ANOVA test with Tukey Post-Hoc analysis was used, ns; non-significant, error bars denote SD). **(E)** A representative image of a testis cross-section of an RFP<sup>+</sup>KH2-mESCs/*Tsc22d3*-KO chimera, demonstrating transgenic RFP expression. Note that RFP<sup>+</sup> cells were not detected in the center of the tubules. Scale bar, 100 $\mu$ m. **(F)** Immunostaining for VASA expression in testes of the indicated animals. Note that VASA positive germ cells do not express the transgenic lentiviral RFP reporter most likely due to transgene silencing. Scale bar, 100 $\mu$ m. **(G)** Immunostaining for the Leydig cell marker HSD3B in the testis cross-section of the indicated animals, demonstrating that lentiviral RFP<sup>+</sup> testicular cells in a chimera are predominantly Leydig cells. Note that in a *Tsc22d3*-KO testis HSD3B is widely expressed, cautiously suggesting that in the absence of mouse spermatogenesis more Leydig cells are present. Scale bar, 100 $\mu$ m.

**Fig. S2**

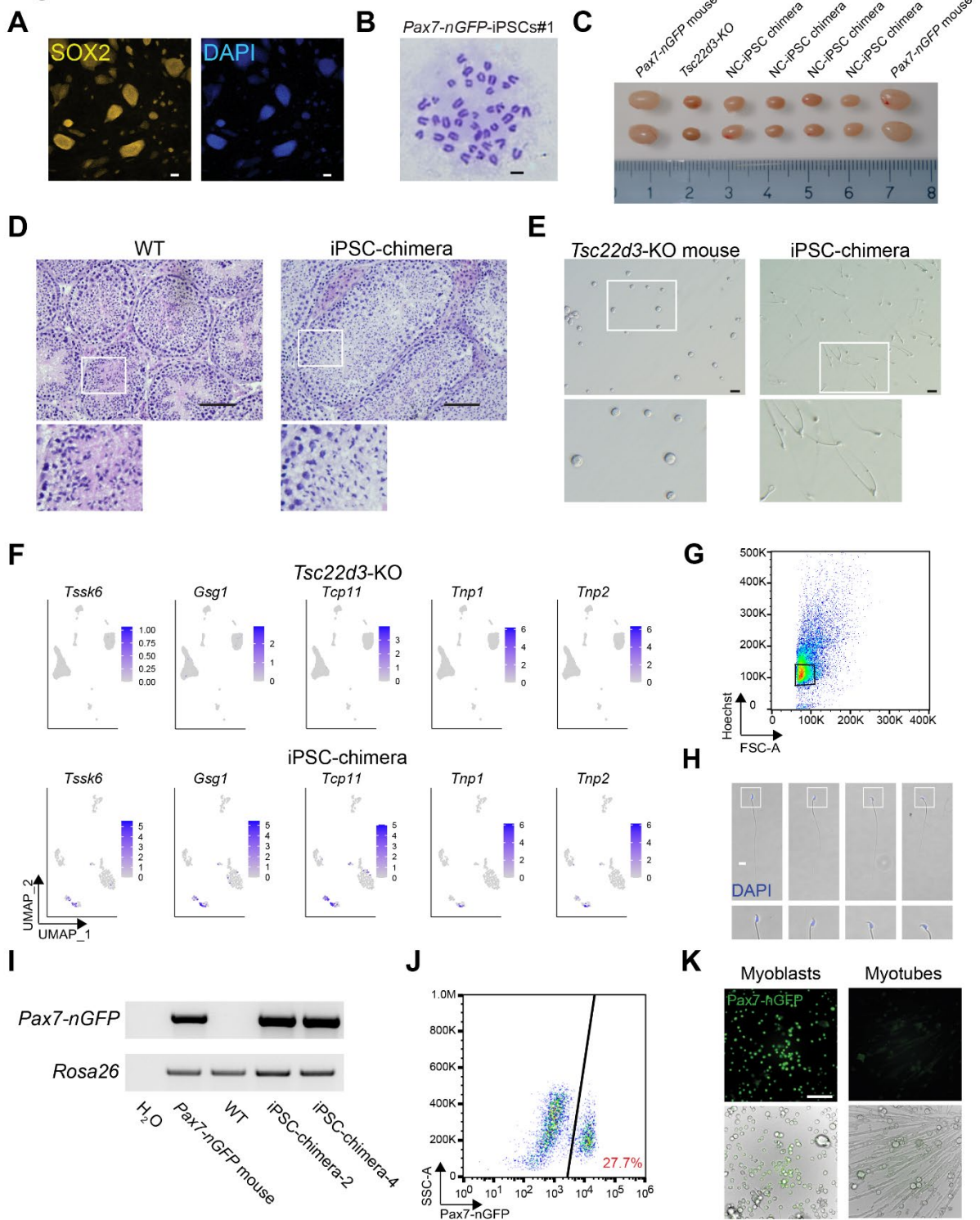


**Figure S2 related to Figure 2: Characterization of intraspecies miPSC-derived germ cells**  
**(A)** A representative immunofluorescence image for SOX2 expression in *Pax7-nGFP* iPSCs. Scale bar, 100µm. **(B)** A karyogram of *Pax7-nGFP*-iPSCs showing 40 mouse chromosomes. Scale bar, 5µm. **(C)** A representative photo of testes isolated from the indicated mouse strains. NC-iPSC-chimera, non-complemented iPSC chimera. **(D)** Hematoxylin and Eosin staining of testes cross-sections of the indicated animals. Scale bar, 100µm. **(E)** Bright-field images showing PESA biopsies extracted from the indicated animals. Note complete lack of spermatozoa in the biopsy taken from the *Tsc22d3*-KO mouse and the abundance of spermatozoa in the biopsy taken

from the complemented *Pax7-nGFP*-iPSC/*Tsc22d3*-KO chimera. PESA, percutaneous epididymal sperm aspiration. Scale bar, 20 $\mu$ m. **(F)** UMAP plots showing all cells colored by spermatid and spermatozoa-associated markers in a cauda epididymis biopsy of a *Tsc22d3*-KO mouse or a *Pax7-nGFP*-iPSC/*Tsc22d3*-KO chimera. Note expression of germ cell-associated markers only in the cauda epididymis of the chimera. **(G)** A FACS plot showing the sorting strategy used to purify haploid spermatozoa from the cauda epididymis of a *Pax7-nGFP*-iPSC/*Tsc22d3*-KO chimera. Spermatozoa were stained with Hoechst 33342. **(H)** A bright-field image showing FACS-purified *Pax7-nGFP*-iPSC/*Tsc22d3*-KO chimera-derived spermatozoa. Scale bar, 10 $\mu$ m. **(I)** PCR genotyping analysis for the transgenic *Pax7-nGFP* allele in FACS-purified spermatozoa from *Pax7-nGFP*-iPSC/*Tsc22d3*-KO chimeras. Spermatozoa from a *Pax7-nGFP* mouse and a WT mouse were used as positive and negative control, respectively. **(J)** Flow cytometric analysis for *Pax7-nGFP* expression in cells that were extracted from skeletal muscles of a 5-week-old F1 pup; a progeny of a *Pax7-nGFP*-iPSC/*Tsc22d3*-KO male chimera. **(K)** Representative bright-field and GFP images of *Pax7-nGFP*<sup>+</sup> myoblasts extracted from skeletal muscles of a progeny of a *Pax7-nGFP*-iPSC/*Tsc22d3*-KO male chimera (left) and derivative myotubes (right). Note lack of *Pax7-nGFP* expression in multinucleated myotubes due to the downregulation of the *Pax7* reporter expression. Scale bar, 100 $\mu$ m

**Fig. S3**

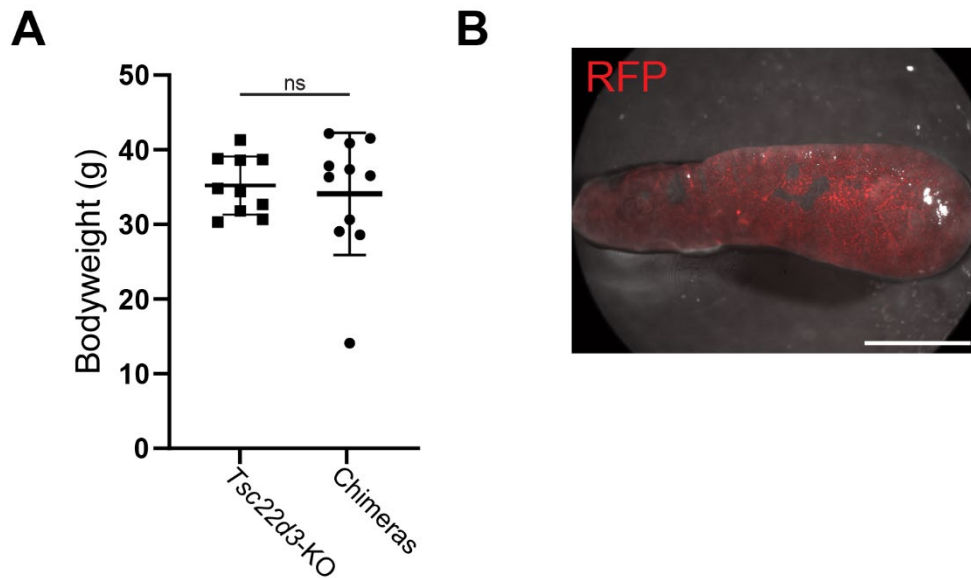
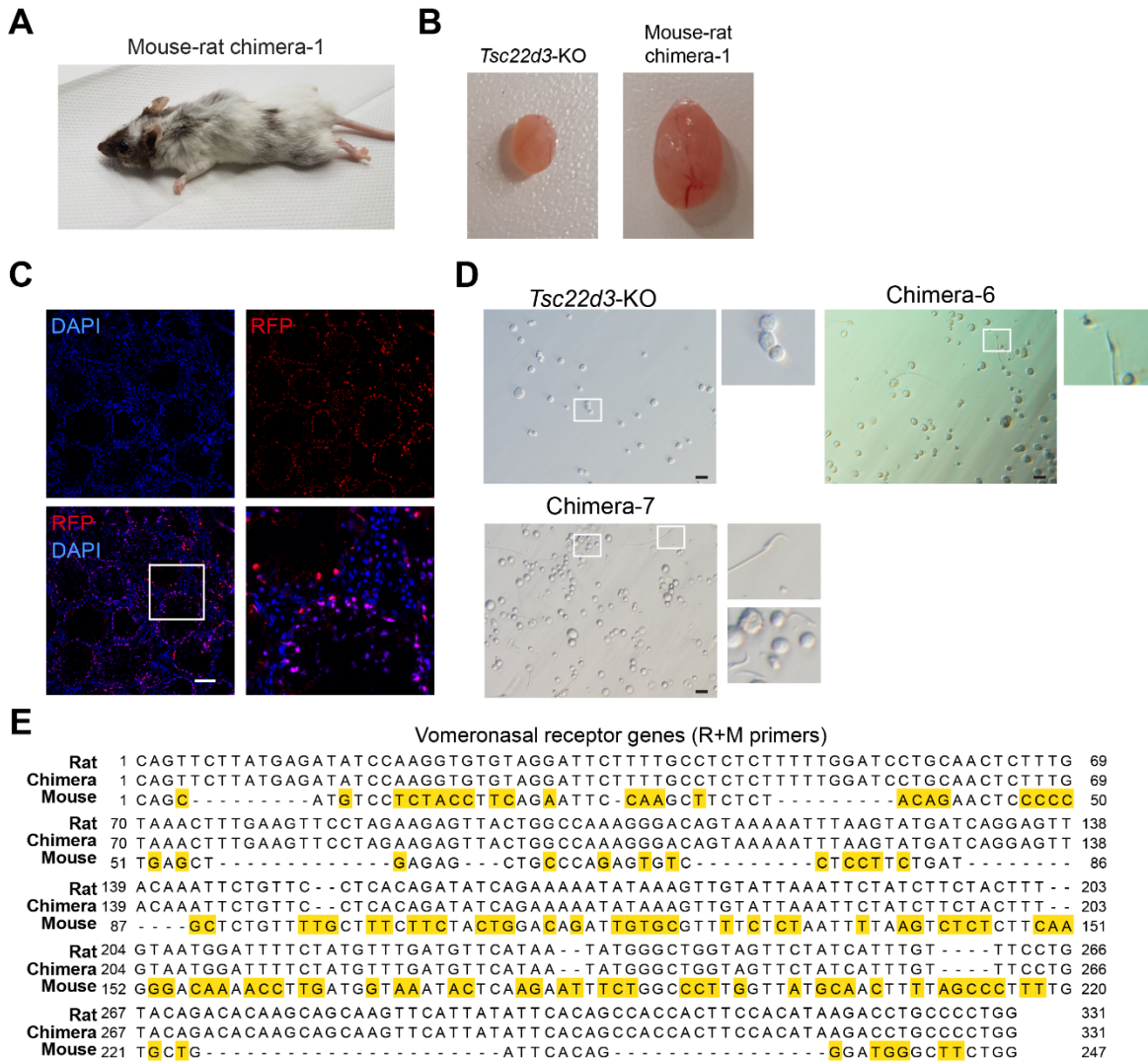


**Figure S3 related to Figure 3: Analysis of mouse-rat chimeras**

**(A)** A graph showing total bodyweight measurement of mouse-rat chimeras in comparison to *Tsc22d3*-KO mice (n = 10-11 biological replicates; each dot represents a single male animal, unpaired two tailed t-test was used, ns; non-significant, error bars denote SD). **(B)** A representative bright-field and RFP overlay image of a spleen that was harvested from a mouse-rat chimera. Note nuclear RFP expression emanating from the lentiviral *EF1 $\alpha$ -H2B-RFP* transgenic reporter present in rESCs. Scale bar, 2mm.

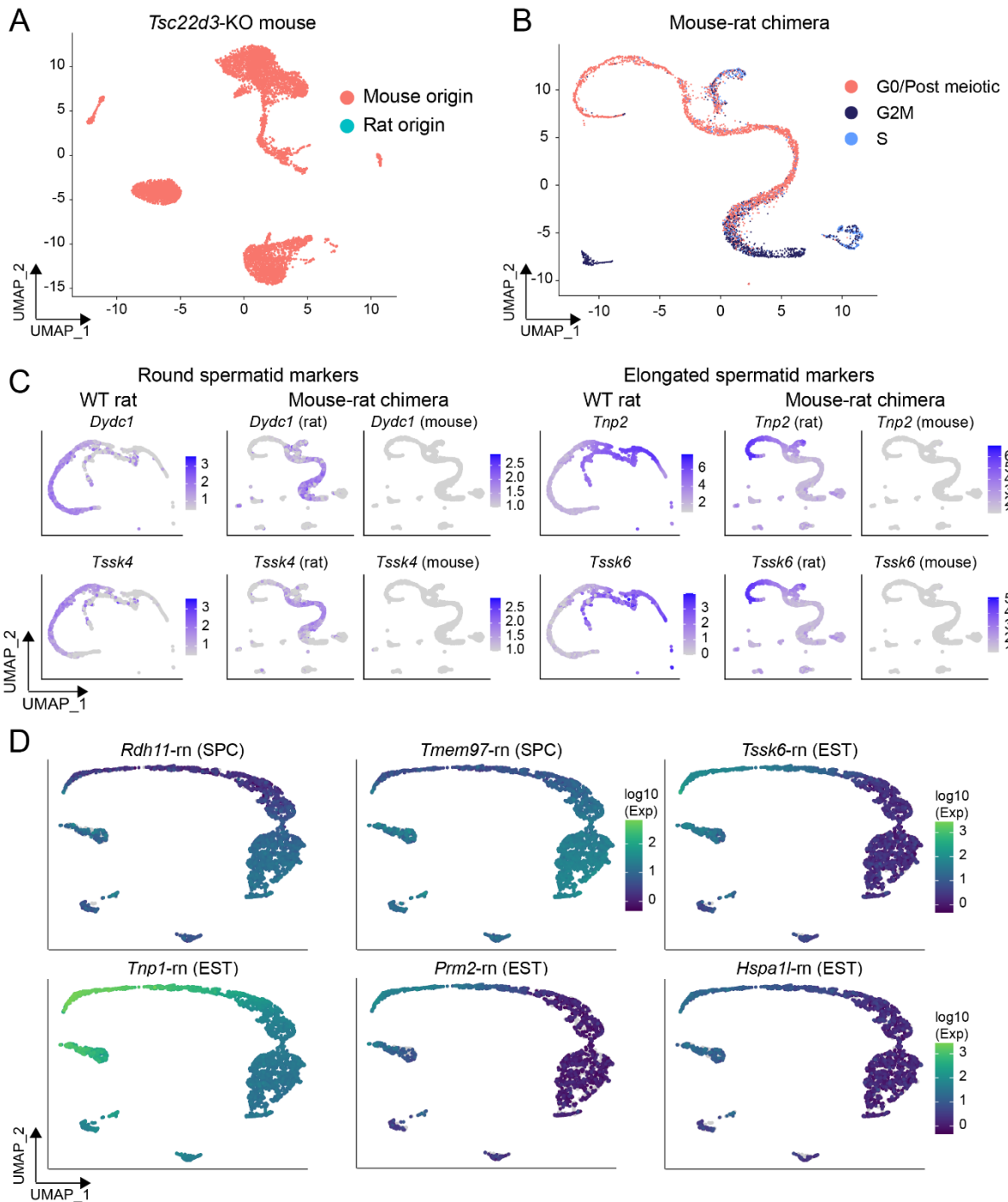


**Fig. S4**



**Figure S4 related to Figure 4: Characterization of rat spermatozoa exclusively produced in interspecies chimeras**

(A) A photo of a deceased RFP<sup>+</sup>DAC8-rESC/*Tsc22d3*-KO mouse-rat chimera-1 showing prominent contribution of RFP<sup>+</sup>DAC8-rESCs to dark coat color chimerism. (B) Camera photos of testes harvested from a *Tsc22d3*-KO mouse or a mouse-rat RFP<sup>+</sup>DAC8-rESC/*Tsc22d3*-KO chimera-1. (C) A representative cross-section image of a testis that was harvested from an RFP<sup>+</sup>DAC8-rESC/*Tsc22d3*-KO chimera-1. Note extensive *EF1 $\alpha$ -H2B-RFP* nuclear reporter expression. Scale bar, 100 $\mu$ m. (D) Representative bright-field images of PESA biopsies extracted from the cauda epididymis of the indicated animals. PESA, percutaneous epididymal sperm aspiration. Scale bar, 20 $\mu$ m. (E) DNA sequences of the mouse *V1rh3* and rat *V1rm1* genes using the PCR products shown in Fig. 4I. The DNA was isolated from the sorted spermatozoa of the indicated animals. Sequence misalignment is indicated in yellow.

**Fig. S5****Figure S5 related to Figure 5: scRNA-seq analysis of a mouse-rat chimera testis**

**(A)** UMAP projection of a *Tsc22d3*-KO mouse testis based on mapping against the mouse-rat chimeric reference genome. **(B)** UMAP projection of a mouse-rat chimera testis showing 4,491 rat cells colored by different cell cycle states. **(C)** UMAP projection of a WT rat or mouse-rat chimera testis showing the expression level of the indicated rat and mouse spermatid markers. Note the absence of the indicated mouse spermatid markers in the mouse-rat chimera testis. **(D)** Monocle3 UMAP projection showing all rat cells from a mouse-rat chimera colored by the expression level of the indicated germ cell markers. EST, elongating spermatids. SPC, spermatocytes.

**Fig. S6**

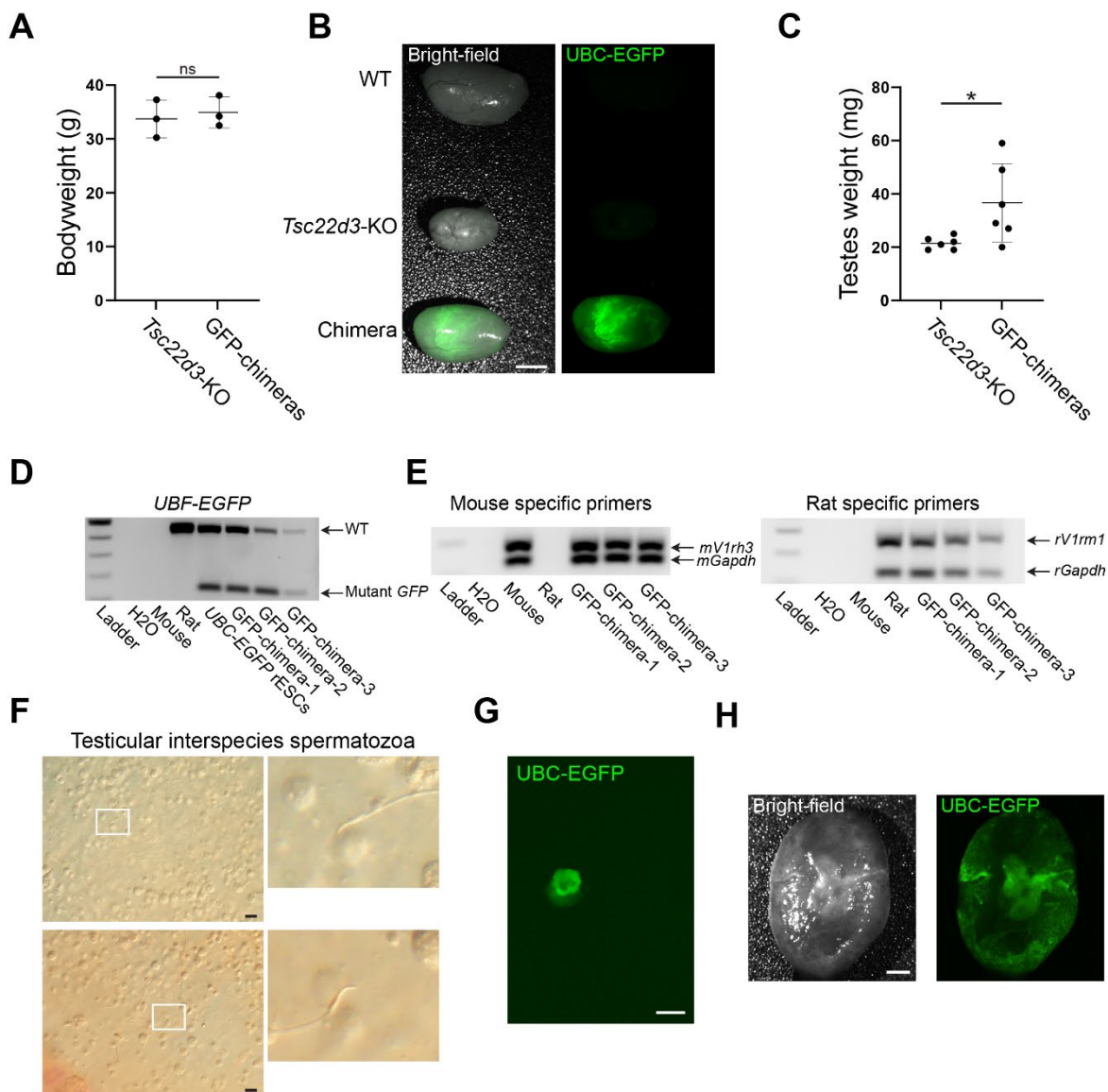


**Figure S6 related to Figure 6: Characterization of UBC-EGFP mouse-rat chimeras**

**(A)** A graph showing quantification of the total bodyweight of the indicated animals, (n=3 biological replicates; each dot represents a single animal. Unpaired two tailed t-test was used, ns; non-significant, error bars denote SD). **(B)** Representative bright-field and GFP images of testes isolated from the indicated animals. Scale bar, 2mm. **(C)** A graph showing quantification of the testes weight of the indicated animals, (n = 6 biological replicates; each dot represents a single testis, unpaired two tailed t-test was used, \*p<0.05, error bars denote SD). **(D)** A gel showing PCR for the UBC-EGFP transgene in the indicated samples. **(E)** A gel showing species-specific PCR for mouse and rat genes in the indicated animals. **(F)** Representative images of testicular germ cells extracted from a UBC-EGFP mouse-rat chimera. Scale bar, 20µm. **(G)** An image showing a hatched UBC-EGFP blastocyst that was generated using interspecies rat germ cells isolated from the testes of a GFP<sup>+</sup> mouse-rat chimera. Scale bar, 50µm. **(H)** Resorbed UBC-EGFP positive rat embryo or placenta generated via TESE-ICSI from UBC-EGFP interspecies spermatozoa. Scale bar, 2mm.



**Table S1: Summary of mESC-intraspecies chimera production and germline transmission**

Cell type	Culture condition	Embryos injected	Embryos transferred	Animals born	Chimeras	Germ cells detected (M)
mESCs	Regular	30	30	8M	8M (100%)	7 (87.5%)

Summary of blastocyst injections using RFP<sup>+</sup>KH2-mESCs. F, female, M, male.

**Table S2: Summary of Pax7-nGFP-miPSC chimera production and germline transmission**

Cell type	Culture condition	Embryos injected	Embryos transferred	Animals born	Chimeras	Germ cells Detected (M)
miPSCs	Regular	34	32	24 (8M, 26F)	11 (8M, 3F) (46%)	1 (12.5%)
miPSCs	Enhanced <sup>20</sup>	27	26	4M	4M (100%)	2 (50%)

Summary of blastocyst injections using Pax7-nGFP miPSCs. F, female, M, male

**Table S3: Summary of mouse-rat chimera production and germline transmission**

Cell type	Culture condition	Embryos injected	Embryos transferred	Animals born	Chimeras	Germ cells detected (M)
DAC8-rESCs	Regular	588	588	123	14 (5F, 9M) (11%)	6 (66.6%)
DAC8-rESCs	Enhanced <sup>20</sup>	203	198	29	2M (7%)	1 (50%)
GFP-rESCs	Regular	328	311	41	4 (1F, 3M) (10%)	1 (33.3%)

Summary of blastocyst injections using DAC8-rESCs or UBC-EGFP-rESCs. F, female, M, male.

**Data S1: Cell-specific markers for Tsc22d3-KO and mouse-rat chimera testes**

Mouse and rat markers used to annotate scRNA-seq cell populations in a mouse-rat chimera testis. Related to Figure 5, S5.

**Video S1: Motile spermatozoa of an RFP+KH2-mESC/Tsc22d3-KO chimera.**

**Video S2: Motile spermatozoa of a Pax7-nGFP iPSC/Tsc22d3-KO chimera.**

**Supplemental experimental procedures****Cell culture**

Mouse embryonic fibroblasts (MEFs) and tail tip fibroblasts (TTFs) were cultured in “MEF medium” consisting of DMEM (Thermo Fisher Scientific, 41966029), supplemented with 10% Fetal Bovine Serum (FBS) (Thermo Fisher Scientific, 10270106), 1% non-essential amino acids (Thermo Fisher Scientific, 11140035), 1% penicillin-streptomycin (Thermo Fisher Scientific, 15140122), 0.05% β-mercaptoethanol (Thermo Fisher Scientific, 21985-023). Mouse ESCs and iPSCs were maintained on γ-irradiated CF-1 fibroblasts (Thermo Fisher, A34181) and cultured in “conventional” mESC medium containing KnockOut DMEM (Thermo Fisher Scientific, 10829018) supplemented with 15% Fetal Bovine Serum (FBS) (Thermo Fisher Scientific, 10270106), 1%

GlutaMAX (Thermo Fisher Scientific, 35050038), 1% non-essential amino acids (Thermo Fisher Scientific, 11140035), 1% penicillin-streptomycin, 0.05%  $\beta$ -mercaptoethanol and 10ng/ml mouse LIF (ESLIF) (PolyGene Transgenics, PG-A1140-0010). Alternatively, mouse iPSCs were also cultured for 5d before blastocyst injections in “enhanced” culture conditions consisting of: mESC medium supplemented with 1.5 $\mu$ M of CGP77675 (Merck, SML0314-5mg), 0.5mM of valproic acid (VPA, Merck, P4543-10G) and 3 $\mu$ M of CHIR99021 (R&D Systems, 4423) as previously reported<sup>20</sup>. Rat ESCs were maintained on  $\gamma$ -irradiated CF-1 fibroblasts and cultured in rat ESC medium consisting of advanced DMEM-F12 (Thermo Fisher scientific, 12634010) mixed 1:1 with Neurobasal medium (Thermo Fisher scientific, 21103049), 0.5x N2 and 0.5x B27 supplements (Thermo Fisher Scientific, 17502048 and 17504044), 1% penicillin-streptomycin and in the presence of the small molecules GSK3- $\beta$  inhibitor CHIR99021 (1 $\mu$ M) (R&D Systems,4423), the MEK inhibitor PD0325901 (1 $\mu$ M) (Tocris, 4192) and rat LIF (10ng/ml, Prospec, CYT-731) as previously described<sup>231</sup>. Alternatively, rat ESCs were also cultured for 5d before blastocyst injection using “enhanced” culture conditions consisting of rat ESC medium supplemented with 1.5 $\mu$ M of CGP77675 (Merck, SML0314-5mg) and 0.5mM of valproic acid (VPA, Merck, P4543-10G). All PSC were maintained in a humidified incubator at 37°C in 5% CO<sub>2</sub>. Mouse ESCs and iPSCs were passaged with 0.05% trypsin-EDTA (Thermo Fisher Scientific, 25300054) whereas rat ESCs were passaged with TrypLE Express (Thermo Fisher Scientific, 12605010).

### **Blastocyst injections, embryo transfer and assessment of chimerism**

Blastocyst injections and embryo transfer were performed in the ETH Phenomics Center (EPIC) at ETH Zurich and in house, abiding to all legal rules of the Federal Food Safety and Veterinary Office, Cantonal veterinary office (Zurich) and an animal experimental license (FormG-135). *Tsc22d3*-KO embryos (also known as “goGermline”) were purchased from Ozgene, Australia, and handled according to the manufacture’s guidelines. Morula-stage embryos were thawed 24 hours before injections according to standard Ozgene embryo thawing protocol guidelines. Prior to commencing injections, ESCs and iPSCs were dissociated and pre-plated on gelatin coated plastic dishes to remove irradiated mouse feeder cells. Injections were carried out in droplets of M2 Media (Merck, M7167, HEPES-buffered embryo handling media) covered with Paraffin Oil (Merck, 76235). Typically, 12–15 ES cells were injected per blastocyst. Successfully injected blastocysts were transferred to a 60ml IVF culture dish containing CO<sub>2</sub>-buffered culture medium (e.g. KSOM+AA) and kept in an incubator at 37°C and 5% CO<sub>2</sub>. The injected blastocysts were transferred to the uteri of pseudo-pregnant females on the same day. The injections were performed with an Eppendorf TransferMan 4r (Eppendorf, Hamburg, Germany), combined with a CellTram Air holding capillary and a CellTram Vario, with support of an Eppendorf Piezo Device (PiezoXpert). Presence of chimerism in intraspecies or interspecies chimeras was first assessed using visual examination of fur coat color or expression of GFP or RFP. Presence of chimerism was also assessed by genotyping for the GFP or RFP transgenes, or via species specific PCR for presence of mouse and rat genes in interspecies chimeras. Of note, we solely analyzed male and not female chimeras as the latter were heterozygotes for the *Tsc22d3* mutation and as such are not sterile.

### **Percutaneous epididymal sperm aspiration (PESA)**

This method entails sperm cell extraction from the cauda epididymis of live animals under isoflurane-induced anesthesia. Prior to commencing the PESA procedure, the animals were pre-emptively treated with the analgesic drug carprofen (5 mg/kg; Rimadyl, Zoetis Schweiz GmbH, Switzerland) which was injected subcutaneously. Anesthesia was initiated in a chamber with the vaporizer set at 3% isoflurane with 0.6L/min oxygen flow. Once anesthesia was induced, the mouse was laid on its back on a heating pad and connected to the isoflurane nose cone with a setting of 2% isoflurane in 0.5L/min oxygen flow. The eyes were covered with a vitamin A eye ointment (Vitamin A Blache, Bausch+Lomb). In order to facilitate visual identification of the epididymis through the skin, the caudal abdomen was massaged in such a way, that the testes were gently pushed towards the scrotum. The skin was then disinfected with 70% ethanol. The cauda epididymis was fixed with a curved forceps (F.S.T., 11051-10), holding the cauda in place with gentle pressure. A 30-gauge needle on an insulin syringe (B. Braun, 4656300), prefilled with

0.05 mL PBS was used to puncture the tissue. After penetration of the cauda epididymis, sperm was gently aspirated for further analysis. For postoperative analgesia, carprofen (5 mg/kg) was injected subcutaneously every 24h until 2 days post treatment.

### **In Vitro Fertilization (IVF)**

Sperm of RFP<sup>+</sup>KH2-mESC/*Tsc22d3*-KO chimeras was frozen and stored in liquid nitrogen<sup>232</sup>. Swiss webster recipient females (4-5 weeks old) were superovulated according to a standard scheme (Pregnant mare serum gonadotropin PMSG 5:00 pm, human chorionic gonadotropin hCG 4:00 pm) and sacrificed 15 hours after hCG administration. Sperm from the chimeras was added to the cumulus complexes and incubated for 4 hours. The oocytes were washed with 5 drops of equilibrated HTF media, covered with Paraffin Oil (Merck, 76235-500ML) and incubated in the same media overnight. Embryo transfer was performed the following day.

### **Intracytoplasmic Sperm Injection (ICSI) and Testicular Sperm Extraction (TESE)-ICSI**

Female rats (Sprague–Dawley, 4–6 weeks old, purchased from Janvier, France) were superovulated by intraperitoneal injections of 300IU/kg PMSG (Prospec) followed by intraperitoneal injections of 300IU/kg hCG (Prospec) 48 hours later. At 14–17h post hCG injection, the cumulus-oocyte complexes were collected and treated with 0.1% hyaluronidase. The oocytes were then washed three times with KSOM (Cosmo Bio LTD, CSR-R-R149) and incubated at 37°C, 5% CO<sub>2</sub> until injection. The sperm suspension was sonicated using an ultrasonic bath at lowest power for 10 seconds, or the tails were cut off with the PiezoXpert drill (Eppendorf, Germany). The sperm heads were then injected into the oocytes using a piezo-actuated micromanipulation, according to the method described previously<sup>113</sup>. After drilling the zona pellucida, the sperm head was hung with the hook over the edge of the injection capillary (inner diameter 3–5µm), or the entire sperm head was inserted into the capillary, especially in the absence of a well-formed hook. The pipette tip was pressed against the oolemma to stretch it, and the oolemma was punctured via a piezo pulse at the lowest setting and the sperm head was ejected into the oocyte. The injection pipette was then gently withdrawn. After sperm injection, the oocytes were washed three times with rat KSOM and cultured in 500µl of rat KSOM under mineral oil in a low oxygen incubator for 5 days without medium changing or transferred into a 0.5dpc foster mother<sup>233</sup>. For TESE-ICSI, an established protocol for spermatogenic cell isolation was followed<sup>234</sup>. In brief, testes were placed in ACK lysing buffer (Thermo Fisher Scientific, A1049201) and the tunica albuginea removed. After gentle loosening of the seminiferous tubules with a blunt-end forceps, the seminiferous tubules, were washed in cold GL-PBS, consisting of 5.6mM glucose (Carl Roth, HN06.2), 5.4mM sodium lactate (Merck, L7022) and 0.01% PVP (Merck, P8136) in PBS. The seminiferous tubules were cut several times with sharp scissors, and gently triturated to release spermatogenic cells. Cells were dispersed in 5ml GL-PBS and spun down at 5°C, 200g for 5min. The cell pellet was resuspended in Cellbanker-1 (Zenoaq, 11888), while the supernatant containing spermatozoa was then collected, washed and spun down twice with GL-PBS at 5°C, 800g for 15mins. The cells were then diluted in TE buffer (Thermo Fisher Scientific, AM9849) and frozen at -80°C followed by transfer to LN<sub>2</sub>. TESE-ICSI was performed in the same way as described for ICSI.

### **Isolation and differentiation of myoblasts into myotubes**

Skeletal muscles of 5-week-old *Pax7-nGFP* mice (offspring of *Pax7-nGFP*-iPSC/*Tsc22d3*-KO male) were harvested and subjected to mechanical and enzymatic dissociation. In brief, muscles were mechanically minced, suspended in PBS and the supernatant was removed via short centrifugation step. Muscle tissue pellets were incubated in a digestion solution containing 0.2% Collagenase Type II (Thermo Fisher Scientific, 17101015) in DMEM for 90min using a shaking 37°C water bath. The cells were then washed with F-10 medium (Thermo Fisher Scientific, 22390025) supplemented with 10% horse serum (Thermo Fisher Scientific, 16050122), and muscle tissue pellets were incubated in a digestion solution consisting of 14ml F-10 (Thermo Fisher Scientific, 22390025) supplemented with 10% horse serum (Thermo Fisher Scientific, 16050122), 1ml of 0.2% Collagenase Type II (Thermo Fisher Scientific, 17101015) and 2.5ml of 0.4% Dispase (Thermo Fisher Scientific, 17105041) for 30min in a shaking 37°C water bath.

Following the second digestion step, cells were further dislodged from the muscle fibers using an 18-gauge needle (Henke-Sass, Wolf GmbH, 613-2029). Cells were filtered through 100 $\mu$ m (Corning, 734-0004), 70 $\mu$ m (Corning, 734-0003) and 30 $\mu$ m (Miltenyi Biotec, 130-041-407) cell strainers before they were resuspended in FACS buffer consisting of 2% FBS in PBS. Freshly isolated *Pax7-nGFP* satellite cells and derivative myoblasts were sorted using an SH800S cell sorter. Myoblasts were cultured in a 1:1 ratio of DMEM and F-10, supplemented with 10% horse serum, 20% FBS, 1% Penicillin-Streptomycin (10,000 U/mL) and 10ng/ml basic FGF (R&D Systems, 233-FB-500). Myoblasts were cultured on plates coated with Matrigel Basement Membrane Matrix (Corning, FAL354234) and passaged using Trypsin (0.05%). Differentiation was induced in DMEM medium containing 2% horse serum and 1% Penicillin-Streptomycin.

### **Lentiviral vector transduction**

Lentiviruses generation commenced with transfection of 60-70% confluent HEK293T cells in 15cm culture dishes (Corning, 430599). To this end, 16.5 $\mu$ g pLV- $\Delta$ 8.9, 11 $\mu$ g of pLV-VSVG envelope and 22 $\mu$ g of one of the target plasmids were mixed and incubated for 10 minutes with Polyethylenimine 4-8 $\mu$ g/ml (Polysciences, POL23966-1) and 150mM Sodium chloride (Merck, 1.06404.1000). The plasmids used in this study include: *LV-mSTEMCCA*, *LV-FUW-M2rtTA*, *LV-EF1 $\alpha$ -H2B-RFP* and *LV-EF1 $\alpha$ -TurboRFP-T2A-H2B-RFP*. Cells were transfected using regular MEF medium. Twenty-four hours post transfection, the medium was replaced, and 48 or 72hrs after transfection the supernatant was collected, filtered through a 0.45 $\mu$ m filter (Corning, 431220) and incubated over night at 4 $^{\circ}$ C using PEG-it Virus Precipitation Solution (System Biosciences, LV825A-1). The Virus/Peg-it solution was centrifuged at 1500xg for 30 minutes at 4 $^{\circ}$ C. The supernatant was removed and the virus pellet was resuspended in 1/100 of the initial volume with PBS 25mM Hepes (Thermo Fisher Scientific, 15630056). Virus aliquots were stored at -80 $^{\circ}$ C until used. Approximately 20uL was added to a confluent well and supplemented with 4-8 $\mu$ g/ml polybrene transfection reagent (Merck, TR-1003-G).

For the preparation of “fresh” lentiviral supernatant, 60-70% confluent HEK293T cells in a 10cm dish were transfected in “MEF medium” without Penicillin-Streptomycin. A solution containing 770 $\mu$ l Opti-MEM (Thermo Fisher Scientific, 21985047), 50 $\mu$ l TransIT-LT1 (Labforce, MIR2300), 8.5 $\mu$ g pLV- $\Delta$ 8.9, 5.5 $\mu$ g pLV-VSVG envelope and 22 $\mu$ g of the target plasmid (*LV-mSTEMCCA*, *LV-FUW-M2rtTA*, *LV-EF1 $\alpha$ -TurboRFP-T2A-H2B-RFP*). Around 24h after transfection, the medium was changed to “MEF medium” and around 48h and 72h after transfection, the supernatant was collected and filtered through a 0.45 $\mu$ m syringe filter and supplemented with 4-8 $\mu$ g/ml polybrene transfection reagent. ESCs were transduced for two consecutive days. A few thousand RFP-transduced mouse or rat ESCs were sorted directly onto plates containing  $\gamma$ -irradiated CF-1 fibroblasts and cultured until confluency.

### **Production of iPSCs**

Reprogramming of *Pax7-nGFP* MEFs into iPSCs was done in “reprogramming medium” consisting of mESC media supplemented with 2 $\mu$ g/ml doxycycline (Merck, D9891), 50 $\mu$ g/ml ascorbic acid (Merck, A92902) and 3 $\mu$ M of the GSK3- $\beta$  inhibitor CHIR99021 (R&D Systems, 4423). In brief, *Pax7-nGFP* MEFs at P1 were transduced with a polycistronic *LV-mSTEMCCA*<sup>221</sup> and an *LV-FUW-M2rtTA* lentiviral vector cassettes (Addgene plasmid #20342). Reprogramming media was changed daily until the appearance of iPSCs. Dox-independent iPSC colonies were picked and replated onto  $\gamma$ -irradiated CF-1 fibroblasts and propagated in the absence of dox, ascorbic acid and CHIR99021.

### **Immunofluorescence**

ESCs or iPSCs were washed with PBS and fixed with 4% paraformaldehyde (PFA, Fisher Scientific, 11400580, diluted to 4% with PBS) for 10min at room temperature (RT). Afterwards, cells were washed twice with PBS and blocked using a solution consisting of PBS, 0.1% Triton X-100 (Merck, 9002-93-1) and 2% bovine serum albumin (BSA, AppliChem, A1391) for 30min at RT. Primary and secondary antibodies were diluted in a solution consisting of PBS, 0.1%BSA and 0.1% Tween (Merck, P9416). Samples were incubated with primary antibodies for 3hrs at RT or at 4 $^{\circ}$ C overnight. Following two washes with PBS, the secondary antibodies were applied for

1h at RT with 1µg/ml DAPI (Thermo Fisher Scientific, 62248). Cells were then washed twice with PBS and mounted with anti-fade reagent to prevent photobleaching (ProLong Gold antifade mountant, Thermo Fisher Scientific, P36930). The following primary antibodies were used in this study: mouse anti-OCT4 (1:200, Invitrogen, MA1-104), rabbit anti-SOX2 (2.5µg/ml, Invitrogen, 48-100), rat anti-NANOG (10µg/ml, Invitrogen, 50-5761-82). Secondary antibodies used were donkey anti-mouse IgG Alexa Fluor 488 (1:400, Invitrogen, A21202), goat anti-mouse IgG1 AF546 (1:400, Invitrogen, A21123), and donkey anti-rabbit IgG AF546 (1:400, Invitrogen, A10040).

### **Immunofluorescence staining of testes sections**

Testes were either embedded directly in optimal cutting temperature (OCT) reagent (CellPath, KMA-0100-00A) after isolation or fixed with 4% PFA overnight at 4°C and embedded in OCT and frozen in isopentane cooled in liquid nitrogen and stored at -80°C. Unfixed testis sections were washed with PBS, followed by 5min fixation in Bouin's fixative (Carl Roth, 6482). Fixed sections were washed with PBS three times and incubated for 1h using blocking solution containing 2% BSA and 0.1% Triton-X100. After removal of the blocking solution, primary antibody diluted in blocking solution was applied to the section for 2hrs at room temperature or overnight at 4°C. After two PBS washes for 5 mins, sections were incubated with secondary antibodies and DAPI diluted in blocking solution for 30mins. About 2-3 drops of ProLong™ Glass Antifade Mountant (Merck, P36980) were applied to immunostained sections and covered with a coverslip. The following antibodies were used: rabbit anti-GILZ (1:100, Thermo Fisher Scientific, PA5-93215), rabbit anti-VASA/DDX4 (1:200, Abcam, AB13840), mouse anti-HSD3B (1:200, Santa Cruz Biotechnology, sc-5151520) and Lectin PNA (1:400, Thermo Fisher Scientific, L21409). Secondary antibodies used were: goat anti-rabbit IgG Alexa Fluor 488 (1:400, Thermo Fisher Scientific, A11008), donkey anti-rabbit IgG Alexa Fluor 647 (1:400, Thermo Fisher Scientific, A31573) and goat anti-mouse IgG3 Alexa Fluor 488 (1:400, Thermo Fisher Scientific, A21151).

### **Spermatozoa DAPI staining**

Isolated spermatozoa were washed in PBS and spun down at 1000g for 10min. The supernatant was discarded and the cell pellet was resuspended in PBS. Spermatozoa in suspension were spread on Superfrost plus slides (Thermo Fisher Scientific, J1800BMNT) and left to dry for 1h, followed by fixation in 4% PFA at room temperature. After rinsing the slides twice with PBS, spermatozoa were blocked and stained using a solution consisting of PBS, 2% Triton X-100, 0.1% BSA and 1µg/ml DAPI for 1h before washing twice with PBS and mounting with ProLong Glass antifade reagent (Thermo Fisher Scientific, P36980).

### **Hematoxylin and Eosin staining**

Slides were fixed for 5 mins using 4% Paraformaldehyde. Next, the sections were incubated for 5 mins with Hematoxylin (Merck, MHS16) followed by a 5min wash with water. The sections were then incubated for 10 seconds in Eosin (Carl Roth, X883.1) followed by a 90 second washing step. Slides were next incubated for 5 seconds in 70% Ethanol and 5 seconds in 100% Ethanol, dried and mounted with Entellan (Merck Millipore, 107960). Hematoxylin and Eosin pictures were imaged using a Nikon Eclipse Ti2-E microscope.

### **Karyotype analysis**

PSCs used for the karyotype analysis were first pre-treated for 4 hours with KaryoMAX Colcemid Solution (Thermo Fisher Scientific, 15212012) at a concentration of 100ng/ml. Cells were then harvested and incubated for 30mins with a hypotonic solution containing 0.56g KCl + 0.5g Sodium Citrate (Carl Roth, 3580.4 and Sigma, W302600) in 200ml H<sub>2</sub>O. As the next step, the cells were fixed with Methanol (VWR, 20847.295) and Acetic acid (Carl Roth, 7332.1) at a 3:1 ratio. Metaphase spreads were prepared by dripping fixed cells from 1-2 meters onto microscope slides, which were further stained with Giemsa (Carl Roth, T862.1) and imaged using a Nikon Eclipse Ti2-E microscope. The pluripotent cell lines KH2-ESCs and DAC8-rESCs were sent to Cell Guidance Systems Ltd in Cambridge for reconstructing karyogram images. At least 10 metaphases were analyzed from each respective cell line.

### DNA extraction and PCR genotyping and sequencing

Skin biopsies were lysed with DirectPCR Lysis Reagent (Viagen Biotech, 102-T) containing Proteinase K at a 50µg/ml concentration (AppliChem, 10027587). The samples were incubated for 1h at 55°C and 45min at 85°C using a thermo block. 1µl of the lysed sample was then used for the PCR reaction. For spermatozoa DNA extraction, cells were washed twice in wash buffer, consisting of 150mM NaCl (Merck, 1.06404.1000) and 10mM EDTA (pH 8.0) in sterile water and spun down at 1000g for 10min<sup>235</sup>. Then, the cells were resuspended in sperm lysis buffer consisting of 20mM TrisHCl (Carl Roth, 9090.2), 20mM EDTA (Merck, EDS), 200mM NaCl (4%), 80mM DTT (Merck, D0632) and 200µg/ml Proteinase K (AppliChem, A3830), according to a Qiagen-supplied protocol (Qiagen QA04 Jul-10). The sperm was then lysed at 56°C for 3-3.5 hours. Following lysis, DNA was extracted using a DNeasy Blood & Tissue kit (Qiagen, 69506). The PCR reaction products for rat and mouse *Gapdh*, *rV1rm1* and *mV1rh3* were purified using the QIAquick PCR Purification Kit (Qiagen, 28104) prior to sequencing. PCR products were subjected to Sanger sequencing (Microsynth AG, Balgach, Switzerland). Sequence alignment was performed using Jalview (Version 2.11.1.0).

**Table illustrating primer sequences used in this study:**

Primer name	Primer sequence
<i>Pax7 nGFP F (sv40pA F3)</i>	5'-CCA CAC CTC CCC CTG AAC CTG AAA CAT AAA-3'
<i>Pax7 nGFP R (Pax7 R10)</i>	5'-GAA TTC CCC GGG GAG TCG CAT CCT GCG G-3'
<i>mRFP1 F</i>	5'-CCC CGT AAT GCA GAA GAA GA-3'
<i>mRFP1 R</i>	5'-CTT GGC CAT GTA GGT GGT CT-3'
<i>mouse V1rh3 F</i>	5'-GGG AGG GGC CAG TGG CTA CAT-3'
<i>mouse V1rh3 R</i>	5'-TGC CAC CAA TCA ACC AGA AGC CCA-3'
<i>V1rm1 rat F</i>	5'-TGG CTT TCA GGC CAC CAG GC-3'
<i>V1rm1 rat R</i>	5'-GCT CTG TCC TCA GGG GCA GGT-3'
<i>Mouse Gapdh F</i>	5'-GCC AAA AGG GTC ATC ATC TCC G-3'
<i>Mouse Gapdh R</i>	5'-GTC CAC TCA TGG CAG GGT AAG ATA AG-3'
<i>Rat Gapdh F</i>	5'-CTG GCT CTT GAG AGT AAC TGA AGG-3'
<i>Rat Gapdh R</i>	5'-TGG GGA CTC CTC AGC AAC TG-3'
<i>Rat UBC-EGFP F</i>	5'-AAC CTC CCA GTG CTT TGA ACG CTA-3'
<i>Rat UBC-EGFP R</i>	5'-GGT GCC AAG CCT CAA CTT CTT TGT-3'
<i>Rat UBC-EGFP Mutant</i>	5'-ATC AGG GAA GTA GCC TTG TGT GTG-3'
<i>Rosa 26 F</i>	5'- AAA GTC GCT CTG AGT TGT TAT-3'
<i>Rosa 26 R</i>	5'- GGA GCG GGA GAA ATG GAT ATG-3'

### Organ, testes and embryo harvest and visualization

All organs were harvested from freshly euthanized animals. After imaging, the organs were frozen in optimal cutting temperature compound (OCT, CellPath, KMA-0100-00A) in isopentane cooled in liquid nitrogen and stored at -80°C. Kidney and heart sections were made at 12µm section thickness. Brains were harvested from freshly euthanized animals and fixed in 4% PFA overnight, followed by two rinses in PBS and sucrose protection in 30% sucrose (Merck, S7903) for 24-48h before freezing in an isopentane-dry ice mixture and stored at -80°C. Sections were taken at 100µm section thickness. All sections were made with a Leica CM1950 cryostat. Testes were frozen in OCT and isopentane cooled in liquid nitrogen and stored at -80°C. Sections were made at 7µm section thickness. Images of testes were taken with a Canon PowerShot G7 X Mark II camera. Embryos were harvested at E13.5. The uterus was removed from a euthanized female and rinsed in diluted iodine solution, followed by rinsing in 70% ethanol solution. The embryos were removed from the uterus and rinsed in PBS before imaging. Fluorescence images of organs and embryos were taken with a Nikon SMZ-1270 stereomicroscope with a Qimaging Retiga R1 camera. Sections were imaged with a Nikon Eclipse Ti2-E microscope with a DS-Qi2 camera.

### **Flowcytometry and Fluorescent-Activated Cell Sorting (FACS)**

For cell sorting of RFP<sup>+</sup> PSCs, cells were detached from the cell culture plate and spun down for 5min at 300g. The cell pellet was then resuspended in 500µl of PBS solution supplemented with 2% BSA, filtered through a cell strainer to remove aggregates and supplemented with 1µg/ml DAPI (Thermo Fisher Scientific, 62248). For spermatozoa sorting, cells were washed twice in wash buffer consisting of 150mM NaCl, 10mM EDTA (pH 8.0) in sterile water and spun down at 1000g for 10min<sup>235</sup>. The sperm pellet was resuspended in 500µl of PBS and supplemented with 2% BSA and 5µg/ml Hoechst 33342 (Thermo Fisher Scientific, H3570) at 37°C for 30min. The tubes containing the spermatozoa were placed immediately on ice. Prior to FACS-purification, 1µg/ml of Propidium iodide (PI, Merck, 81845) was added and the cell suspension was filtered through a cell strainer to remove aggregates. After exclusion of debris and cell doublets, cells were sorted for haploidy based on DNA content. All cell sorting was performed on a Sony SH800S Cell Sorter (Sony Biotechnology).

### **Western blot analysis**

Total protein was isolated from the testes of WT mice, *Tsc22d3*-KO mice and chimeras. About 10-15 mg of frozen testis tissue was placed in 200µl RIPA buffer (50 mM Tris, 150 mM NaCl (Merck, 1.06404), 2mM EDTA (Merck, EDS-100g), 1% Triton (Merck, X100-100ML), 0.1% SDS (Carl Roth, 2326.1), supplemented with 1x Halt protease inhibitor cocktail (Thermo Fisher Scientific, 87785) and lysed using a rotor-stator tissue homogenizer (Omni THQ). After centrifugation at 10'000xg for 20 minutes at 4°C, the supernatant was collected and protein content was quantified with DC protein assay kit (Bio-Rad, 5000111) using BSA for standardization. Electrophoresis was performed using 4-20% pre-cast gels (Bio-Rad, 4568094). About 25µg of protein was loaded per lane. Stain-free gel images were taken after electrophoresis (UV trans-illumination, 45s activation time, optimal auto-exposure) and served as loading control (Figure 4e). Protein transfer was conducted using the Trans-Blot Turbo Transfer System (Bio-Rad) on the mixed molecular weight setting to transfer onto PVDF membranes (Bio-Rad, 1704156). Following protein transfer, membranes were blocked for 1h at RT in 1xTBS-T with 5% non-fat dry milk (Carl Roth, T145.1). Next, membranes were incubated overnight at 4°C in the presence of primary antibodies against GILZ (TSC22D3) (1:1000, Rabbit IgG, Thermo Fisher Scientific, PA5-93215) and VASA (1:1000, Rabbit IgG, Abcam, AB13840). On the next day, membranes were washed three times for 10 minutes in TBS-T and incubated for 1h at RT with anti-Rabbit IgG HRP-linked secondary antibody (1:5000, Cell Signaling, 7074S). Then, membranes were washed again three times for 10 minutes in TBS-T. For detection of chemiluminescence, membranes were then developed in ECL substrate according to the manufacturer's instructions (Bio-Rad, 1705060). For detection of GAPDH protein expression, membranes were stripped for 20 minutes at room temperature in stripping buffer (200 mM Glycine (AppliChem, A1067), 0.1% SDS, 1% Tween, pH 2.2) and washed three times in TBS-T for 5 minutes. Then, membranes were re-blocked for 1h at room temperature in TBS-T and 5% non-fat dry milk followed by a 1h incubation at room temperature with anti-GAPDH HRP-conjugated antibody (1:5000, Cell Signaling, 3683). Last, membranes were washed three times in TBS-T for 10 minutes before proceeding to imaging as described above. TBS-T consisted of 50mM Tris, 154mM NaCl and 0.1% Tween-20. All washing and incubation steps were performed on a shaker. All imaging was performed using the Chemidoc MP imaging system (Bio-Rad).

### **Bulk RNA sequencing analysis**

Total RNA was extracted using the RNeasy mini kit (Qiagen, 74106). Prior to RNA extraction, PSCs were pre-plated on gelatin coated culture dishes for 90min to remove CF1 "feeder" fibroblasts. RNA sequencing was performed on an Illumina NovaSeq instrument at the Functional Genomics Center Zurich (FGCZ). Approximately 30-40 million reads were produced per sample and analyzed using the SUSHI framework developed at the FGCZ<sup>236,237</sup>. The initial quality control (adapter and low-quality base trimming) was performed with fastp v0.20<sup>238</sup>. Next, raw reads were mapped against the reference rat genome (the Ensembl genome assembly Rnor\_6.0: [https://www.ensembl.org/Rattus\\_norvegicus/Info/Index](https://www.ensembl.org/Rattus_norvegicus/Info/Index)) using STAR v2.7.a<sup>239</sup>. The R package

Rsubread v2.2.4 was used to determine the gene expression values<sup>240</sup>. Genes were considered to be detected if they had at least 10 counts in 50% of the replicates in one of the groups. Differential gene expression analysis was performed using the negative binomial generalized linear model approach of the R package edgeR v3.30.3<sup>241</sup>. The quasi-likelihood F-test was used to determine the significance of differential expression. Correction for multiple testing was done by applying the Benjamini-Hochberg algorithm. A threshold of  $|\log_2FC| > 0.5$  and  $p < 0.05$  was selected to identify the differentially expressed genes between the various conditions.

### **scRNA-seq sequencing of mouse cauda epididymis**

Isolated cells from the cauda epididymis were resuspended in 1% BSA/PBS solution and subjected to sodium azide treatment (3mM) to reduce sperm mobility. The cells were then counted and checked for viability. Samples with fewer than 95% viable cells were not processed. Post quality examination, around 6000–8000 cells were loaded onto the 10x Chromium System (10x Genomics) for single-cell encapsulation with barcoded gel beads as per the manufacturer's instructions in Chromium Single Cell 3' Reagents kits v3.1 user guide RevD. Libraries were prepared using Single Cell 3' v3.1 chemistry. Briefly, reverse transcription was performed in the gel bead emulsion, cDNA amplified while adding three additional PCR cycles to compensate for low RNA content of spermatids and spermatozoa. Final libraries were quantified and assessed for fragments size using the Agilent 4200 TapeStation System. Libraries were pooled and sequenced on a NovaSeq 6000 (Illumina).

### **scRNA-seq data analysis of mouse cauda epididymis**

The 10x Genomics Cell Ranger v6.1.2 pipeline<sup>242</sup> was used for demultiplexing, aligning the reads, processing the barcodes and counting the unique molecular identifiers (UMIs). During read alignment, the mouse genome assembly GRCm38.p6 was used as the reference. The resulting filtered gene–cell barcode matrices were imported into R v4.1.2 and analyzed using the Seurat v4.1.0 pipeline<sup>243,244</sup>. Since the majority of droplets in *Pax7-nGFP-iPSC/Tsc22d3-KO* chimera were empty partly due to the low RNA content of spermatids and spermatozoa, cells with at least > 100 UMIs were considered for downstream analysis based on the raw count matrix. As a quality control step, cells with unique feature counts < 250 or > 5,000 and mitochondrial gene counts > 10% were excluded from both samples. The filtered data were log-normalized and scaled. Principal component analysis (PCA) with 2,000 variable genes was performed on the scaled data for dimensional reduction. The neighborhood graph of cells was computed based on 20 principal components (PCs) and clustered using the Louvain algorithm with a resolution of 0.4. Clustered cells were visualized in a two-dimensional space using the uniform manifold approximation and projection (UMAP) of PCs. For each sample, differential gene expression analysis (Wilcoxon rank-sum test with  $\log_2$  fold-change > 0.25 and adjusted p-value < 0.01) was performed to determine the top cluster markers. Marker genes combined with single cell reference databases (PanglaoDB<sup>245</sup> and Mouse Cell Atlas<sup>246</sup>) and published literature on mouse epididymis<sup>247</sup> were used for cell type annotation.

### **scRNA-seq of testes**

Testes were isolated, placed on ice and immediately processed as previously reported<sup>248</sup>. The tunica albuginea was removed using fine tipped forceps, and the testes were placed in 5ml of digestion buffer, consisting of 1mg/ml collagenase type IV (Thermo Fisher Scientific, 17104019) in HBSS (Thermo Fisher Scientific, 14025050). The tissue was digested for 5min at 37°C with gentle shaking, then manually shaken and incubated for additional 3min. After centrifugation at 200g for 5min at room temperature, the cells were washed with HBSS and spun down again. The cells were then digested with 4.5ml 0.25% Trypsin EDTA (Thermo Fisher Scientific, 25200056) and 4kU DNase I (Merck, D4527-20KU) in HBSS, and triturated with a 10ml serological pipette 3-5 times and incubated at 37°C for 5 mins on a shaking platform. The trituration with incubation was repeated two times, until the digestion was stopped by the addition of 10% FBS (Thermo Fisher Scientific, 10270106). The cell suspension was then filtered through a 70µm cell strainer (Bioswisstec, 10270106), followed by a 40µm cell strainer (Bioswisstec, 93040) and centrifugation at 400g for 15min in 4°C, and washed twice with PBS containing 5% FBS solution. The cells were



FACS-purified with 1µg/ml DAPI (Thermo Fisher Scientific, 62248) to exclude dead cells, and further processed similar to the cauda epididymis biopsies.

### **scRNA-seq data analysis of testes**

The mouse-rat chimeric reference genome was created by merging the rat reference genome (Rnor\_6.0 with gene model definition Ensembl release 98) and mouse reference genome (GRCm38.p6 with gene model definition GENCODE release 23) using the R package ezRun<sup>249</sup>. The 10x Genomics Cell Ranger v6.1.2 pipeline<sup>242</sup> was used for filtering the merged genome for protein-coding and rRNA gene biotypes, sample demultiplexing, read alignment against filtered chimeric genome and feature-barcode count matrix generation. Feature names were appended by “-rn” and “-mm” for rat and mouse respectively to distinguish between their reference genome origin. In addition, *Tsc22d3*-KO mouse and WT rat testis samples were mapped against their respective reference genome assemblies GRCm38.p6 and Rnor\_6.0 using the 10x Genomics Cell Ranger v6.1.2 pipeline<sup>242</sup>. Downstream analysis was performed on the feature-barcode count matrices using the R package Seurat v4.1.2<sup>243,244</sup>. Cells with unique feature counts < 250 or > 5,000, UMI counts > 60,000 and mitochondrial gene counts > 5% were discarded as a measure of quality control. Filtered data was log-normalized and scaled. Dimensional reduction was performed using PCA with 2,000 highly variable genes. Louvain algorithm was applied with a resolution of 0.4 to cluster the cells using the first 30 PCs. The clustered cells were visualized in a two-dimensional space via UMAP of the same PCs. For each cluster, the markers were identified based on the differential gene expression analysis (Wilcoxon rank-sum test with log<sub>2</sub> fold-change > 0.25 and adjusted p-value < 0.01). Marker genes combined with single cell reference database PanglaoDB<sup>245</sup> and published literature<sup>250,251</sup> on spermatogenesis were used for cell type annotation. Pseudotime trajectory analysis was performed only on the rat cells from the chimera testis using the R package Monocle3<sup>252-254</sup>.

### **Statistical analysis**

Statistical analysis of graphs was performed with GraphPad Prism (Version 9.2.0, GraphPad Software) and presented as mean ± SD. Values of p<0.05 were considered statistically significant. Differences were evaluated using Student’s t-test (two sided) or one-way ANOVA with Tukey Post-Hoc analysis.

## Chapter 4. Interspecies generation of functional muscle stem cells

Authors: Seraina A. Domenig<sup>1#</sup>, Ajda Lenardič<sup>1#</sup>, Joel Zwick<sup>1#</sup>, Monika Tarnowska-Sengül<sup>1</sup>, Nicola Bundschuh<sup>1</sup>, Adhideb Ghosh<sup>1,2</sup> & Ori Bar-Nur<sup>1\*</sup>

### Affiliations:

<sup>1</sup> Laboratory of Regenerative and Movement Biology, Department of Health Sciences and Technology, ETH Zurich, Schwerzenbach, Switzerland.

<sup>2</sup> Functional Genomics Center Zurich, ETH Zurich and University of Zurich, Zurich, Switzerland.

# These authors contributed equally

\*Correspondence: Ori.bar-nur@hest.ethz.ch

### Contribution:

Conceptualization: SD, AL, JZ, OBN

Experiments intraspecies part: SD, AL, NB

Experiments interspecies part: AL, JZ, NB

Chimera production: MTS

RNA sequencing analysis: AG

Writing – original draft: SD, AL, JZ, OBN

---

This article is currently in under revision in The Journal of Clinical Investigation. This chapter is a reprint of the submitted article.

## Abstract

Satellite cells, the stem cells of skeletal muscle tissue, hold a prodigious regeneration capacity. However, low satellite cell yield from autologous or donor-derived muscles precludes adoption of satellite cell transplantation for the treatment of muscle diseases including Duchenne muscular dystrophy (DMD). To address this limitation, here we investigated whether sufficient quantity of satellite cells can be produced in allogeneic or xenogeneic animal hosts. First, we report on exclusive satellite cell production in intraspecies mouse chimeras by injection of CRISPR/Cas9-corrected DMD-induced pluripotent stem cells (iPSCs) into blastocysts carrying an ablation system of host Pax7<sup>+</sup> satellite cells. Additionally, injection of genetically-corrected DMD-iPSCs into rat blastocysts produced interspecies rat-mouse chimeras harboring mouse muscle stem cells that efficiently restored dystrophin expression in DMD mice. This study thus provides a proof-of-principle for generation of therapeutically-competent stem cells between divergent species, raising the possibility of procuring human stem cells in large animals for regenerative medicine purposes.

## Introduction

Muscle degeneration denotes the loss of skeletal muscle mass as a consequence of pathological affliction in the form of sarcopenia, cachexia or muscular dystrophies<sup>255</sup>. Following muscle insult, quiescent satellite cells orchestrate a myogenic regeneration program by means of activation and differentiation into transit-amplifying myoblasts that further differentiate into fusion-competent myocytes that merge with damaged multinucleated muscle fibers for tissue repair<sup>255,256</sup>. This step-wise differentiation process is characterized by upregulation of specific transcription factors including paired box 7 (*Pax7*) in satellite cells and myogenic differentiation 1 (*MyoD*) in myoblasts<sup>255,256</sup>.

DMD is the most common and currently incurable muscular dystrophy, which arises due to a mutation in the dystrophin gene, a large structural protein that connects skeletal muscle fibers to the extracellular matrix<sup>257-259</sup>. In DMD patients, lack of dystrophin renders muscle fibers highly susceptible to breakage due to muscle contraction forces, resulting in increased regeneration cycles by satellite cells<sup>259</sup>. However, continuous erosion of myofibers gradually exhausts the regeneration capacity of satellite cells, precipitating muscle fiber replacement with fibrotic and adipogenic tissues over time<sup>260</sup>. As a consequence of skeletal muscle wasting, DMD patients become wheelchair-dependent during childhood and eventually succumb to untimely death due to cardiorespiratory failures in the second or third decade of life<sup>260</sup>.

A variety of therapeutic interventions are currently being explored for their capacity to restore dystrophin expression<sup>163</sup>. Such efforts include gene therapy using overexpression of micro-dystrophin or correction of the DMD mutation by CRISPR/Cas9, typically via use of adeno associated viruses (AAVs)<sup>163</sup>. While promising, these approaches still carry various concerns including AAV toxicity, genomic integration or DNA breakage as well as an unfavorable immunological response against repeated AAV treatment or Cas9<sup>261-264</sup>. Alternatively, cell-based therapies have been extensively explored for their potential to restore dystrophin expression in DMD animal models via injection of myogenic stem or progenitor cells into dystrophic muscles<sup>159,265</sup>. Such trials aim to add healthy myonuclei to dystrophic myofibers via cell fusion for dystrophin restoration<sup>266</sup>. Early endeavors performed in the 1990's utilizing healthy myoblasts to restore dystrophin expression in DMD patients were unsuccessful, albeit more recent trials reported a better outcome<sup>182,267,268</sup>. One explanation for this unfavorable result is that myoblasts lose *in vivo* engraftment capabilities following extensive *in vitro*

expansion<sup>204</sup>. As such, major efforts have been directed towards finding means to augment the engraftment potential of myoblasts, or seek additional expandable myogenic cell types that can efficiently restore dystrophin expression *in vivo* following intramuscular injection in DMD animal models<sup>159,265</sup>. Several notable examples include iPSC-derived myogenic precursor cells, teratoma-derived muscle stem cells or directly reprogrammed induced myogenic progenitor cells (iMPCs)<sup>195,197,198,202,203,269,270</sup>. However, satellite cells are still widely-accepted as the most potent source capable of restoring dystrophin expression, since low number of satellite cells can efficiently engraft and regenerate muscles *in vivo*<sup>151,156,204,271</sup>. In respect to treating DMD patients, harvesting sufficient number of satellite cells from autologous or donor-derived muscles represents a major challenge for cell-based therapy<sup>159</sup>.

Blastocyst complementation is an innovative technology that enables the creation of specific organs, tissues, or cell-types from donor-derived PSCs<sup>226</sup>. To this end, PSCs such as embryonic stem cells (ESCs) or iPSCs are injected into blastocysts that carry genetic mutations that impede the formation of specific organs or cell types in animal chimeras, thereby enabling exclusive generation from injected PSCs<sup>226</sup>. In recent years, this approach has been utilized to produce cells and organs in intraspecies mouse-mouse or pig-pig chimeras<sup>226</sup>. Most notably, this technique was also utilized in an interspecies manner, demonstrating production of organs or cell types in xenogeneic hosts such as pancreas, blood vasculature, kidneys, thymi or germ cells in mice or rats<sup>39,48,49,57,138,141,216,272</sup>. However, production of genetically-corrected interspecies adult stem cells between different animal species has not been reported to date<sup>226</sup>. Here, we set out to combine cellular reprogramming, genome engineering and *in vivo* differentiation of PSCs in mouse-mouse and rat-mouse chimeras to generate allogeneic and genetically-corrected mouse stem cells that can be exploited to restore dystrophin expression in DMD mice.

## Results

### **Substantial production of mESC-derived satellite cells in intraspecies chimeras**

We commenced our study by setting out to explore whether mESCs can solely produce satellite cells in intraspecies chimeras generated using mouse blastocysts carrying *Pax7-CreERT2* and *Rosa26-loxSTOPlox-Diphtheria toxin A (R26-LSL-DTA)* homozygous alleles<sup>273,274</sup>. As satellite cells uniquely express the *Pax7* gene in skeletal muscles<sup>153</sup>, this system ensures specific ablation of host satellite cells following tamoxifen

injection, and can potentially provide a vacant niche receptive for mESC-derived satellite cell colonization in skeletal muscles of chimeras (Figure 1A). To investigate this question, we used lentiviral-transduced Red Fluorescent Protein positive (RFP<sup>+</sup>) KH2-mESCs, which have been previously reported to contribute robustly to mouse chimerism (Figure S1A)<sup>218,272</sup>. Of note, prior to blastocyst injections, RFP<sup>+</sup>mESCs were cultured for 5 days in 'enhanced' culture medium to increase chimeric contribution<sup>20</sup>. Altogether, we performed three blastocyst injection rounds which produced 28 out of 58 (48%) chimera offspring based on genotyping for the RFP allele and presence of agouti coat color emanating from KH2-mESCs (Figure 1B, 1C and S1B). Furthermore, all mice carried the *R26-LSL-DTA* allele as expected (Figure S1B). Next, we wished to assess whether we can exploit the genetic system to ablate host satellite cells in newborn pups, aiming to create this way a vacant niche for reconstitution with mESC-derived satellite cells during postnatal growth. To this end, we performed tamoxifen injections in 3 day-old chimeric or non-chimeric pups for three consecutive days. This early developmental time point was chosen as it is characterized by rapid muscle growth associated with high proliferation rate of endogenous PAX7<sup>+</sup> satellite cells<sup>275</sup>. Over a course of three weeks after birth, we observed significant bodyweight reduction in tamoxifen injected non-chimeric *Pax7-CreERT2: R26-LSL-DTA* animals, however not in non-injected control animals (Figures 1C and 1D). Notably, intraspecies *Pax7-CreERT2: R26-LSL-DTA* / RFP<sup>+</sup>KH2-mESC chimeras showed no appreciable reduction in size or bodyweight, even when subjected to tamoxifen injection, suggesting rescue by mESCs (Figure 1C and 1D). To validate efficient satellite cell ablation, we harvested leg muscles from non-chimeric *Pax7-CreERT2: R26-LSL-DTA* mice subjected to tamoxifen injections and non-injected controls. We solely detected *Pax7* expressing satellite cells in non-injected muscle sections, however not in muscles of injected animals (Figure 1E). Next, we observed that RFP<sup>+</sup>KH2-mESCs extensively contributed to skeletal muscle tissue in chimeras as muscle sections exhibited strong RFP expression in resident muscle cells, independent of host satellite cell ablation (Figure 1F). We then assessed whether all PAX7<sup>+</sup> satellite cells expressed the RFP label in these muscle sections. Unexpectedly, we detected PAX7<sup>+</sup> satellite cells that were RFP negative, suggesting that either host satellite cells remained following tamoxifen injection, or that transgene silencing occurred in mESC-derived satellite cells (Figure 1G).

To assess which hypothesis is correct, we Fluorescence Activated Cell Sorting (FACS)-purified satellite cells using the established surface markers<sup>276</sup> CD45<sup>-</sup>/CD31<sup>-</sup>

/SCA1<sup>-</sup>/ITGA7<sup>+</sup> from muscles of chimeras subjected to host satellite cell ablation or non-injected controls (Figure S1C). Surprisingly, we detected both RFP positive and negative satellite cell populations and generated either RFP<sup>+</sup> or RFP<sup>-</sup> myoblast lines from chimeric muscles (Figures 1H and 1I). Importantly, PCR analysis for the RFP allele revealed that both the positive and negative RFP cell populations contained the RFP transgene, indicating that lentiviral vector silencing occurred in mESC-derived satellite cells (Figure 1J). Collectively, in this first trial we established a system to ablate host satellite cells in intraspecies chimeras and successfully produced satellite cells and myoblasts from donor-derived mESCs. However, lentiviral transgene silencing occurred in mESC-derived satellite cells, raising a need to find a genetic system that will allow to distinguish between host and donor-derived satellite cells.

**Figure 1**

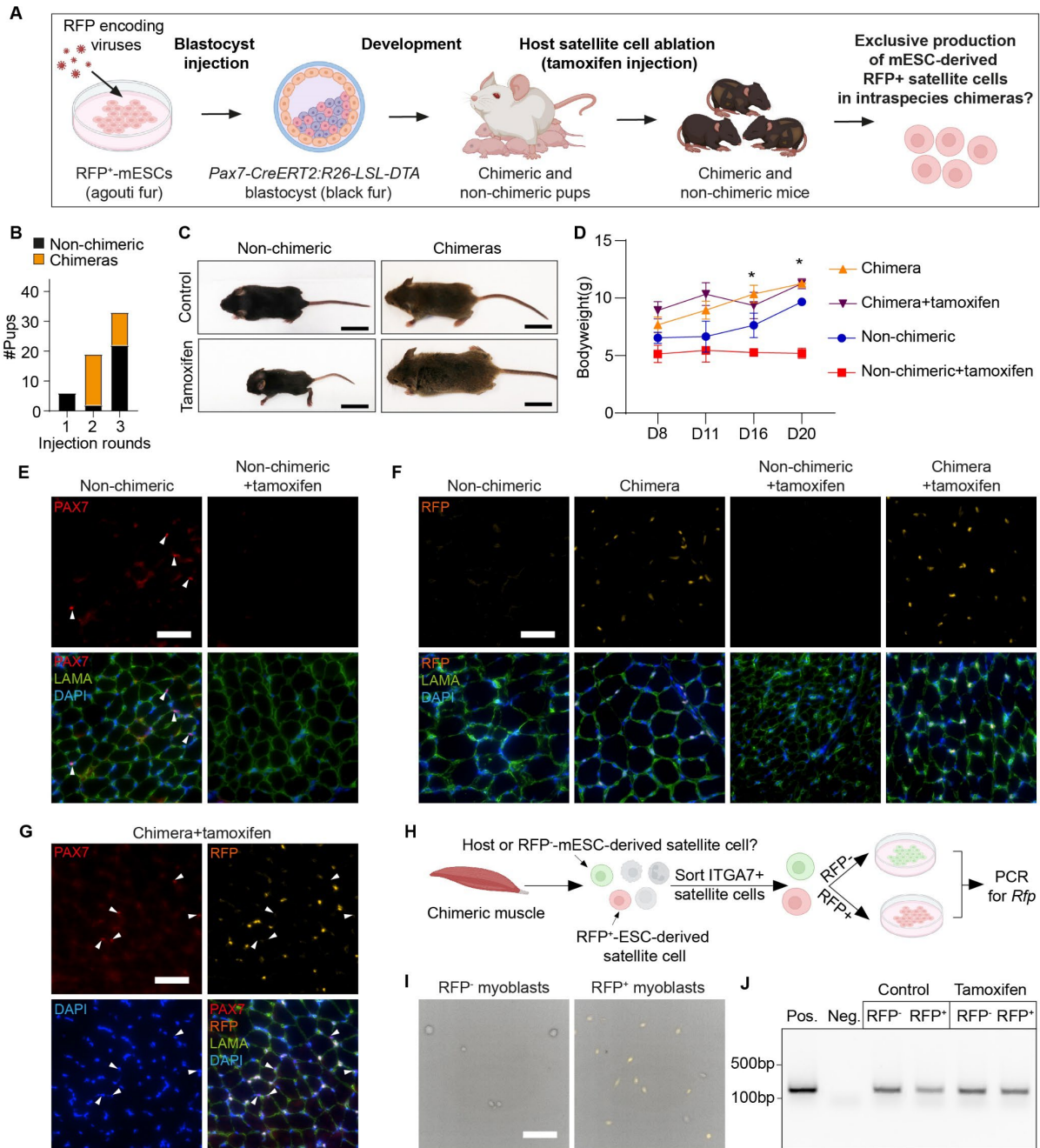


**Fig. 1. Satellite cells generated in intraspecies chimeras solely from mESCs. (A)** A schematic of experimental design. RFP, red fluorescent protein; mESCs, mouse embryonic stem cells. **(B)** A graph showing chimera numbers. **(C)** Photos depicting the indicated mouse strains at day 17. Chimerism is represented by agouti coat color. Scale bar, 1cm. **(D)** Graph showing weight during postnatal growth of the indicated strains. Only the non-chimeric+tamoxifen group showed a significant difference in bodyweight compared to the other groups.  $N \geq 3$ , error bars denote SD. Statistical analysis was performed using 2-way ANOVA.  $*p \leq 0.05$ . **(E)** Immunofluorescence images of the indicated markers and strains in skeletal muscle cross-sections at day 17. Scale bar, 50 $\mu$ m. **(F)** Immunofluorescence staining for the indicated markers and strains in skeletal muscle cross-sections at day 17. Note presence of RFP positive cells only in chimeras. Scale bar, 50 $\mu$ m. **(G)** Immunofluorescence staining for PAX7 in muscle cross-sections of a chimera at day 17, that has been subjected to host satellite cell ablation. White arrowheads point to PAX7<sup>+</sup>/RFP<sup>+</sup> satellite cells. Scale bar 50 $\mu$ m. **(H)** A schematic illustrating strategy to assess if the RFP reporter



is silenced in PAX7 expressing satellite cells. **(I)** Bright-field and fluorescence images of ITGA7<sup>+</sup> satellite cell-derived myoblasts isolated from chimera muscles subjected to host satellite cell ablation. Scale bar, 100µm. **(J)** PCR for RFP in the indicated myoblast lines and conditions.

## Exclusive production of gene-edited DMD iPSC-derived functional satellite cells in intraspecies chimeras

Given the encouraging results involving production of mESC-derived satellite cells in intraspecies chimeras, we next wished to test whether a similar approach may enable exclusive and allogeneic production of therapeutically-competent and gene-edited satellite cells from the well-established *Dmd*<sup>mdx</sup> mouse model<sup>277</sup>. Specifically, we set out to explore whether we can produce and genetically correct *Dmd*<sup>mdx</sup>-iPSCs that carry a *Pax7-nuclear(n)GFP* satellite cell-specific genetic reporter, and then utilize *Dmd*<sup>mdx</sup>; *Pax7-nGFP* iPSCs to exclusively generate functional satellite cells in intraspecies chimeras following host satellite cell ablation (Figure 2A)<sup>219</sup>.

As the first step, we crossed homozygous *Dmd*<sup>mdx</sup> female mice with homozygous *Pax7-nGFP* males and generated mouse embryonic fibroblast (MEF) lines. As the dystrophin gene is located on the X chromosome, all male MEF lines inherit the *Dmd*<sup>mdx</sup> mutation and are heterozygous for the *Pax7-nGFP* allele. Reprogramming to pluripotency was performed using a polycistronic *STEMCCA* cassette together with small molecule treatment (Figure S2A)<sup>220,221</sup>. Following manual picking and propagation of clones, we were able to establish *Dmd*<sup>mdx</sup>; *Pax7-nGFP* iPSCs that expressed well-known pluripotency markers (Figures S2B-E).

Next, we set out to correct the dystrophin mutation in exon 23 of *Dmd*<sup>mdx</sup>; *Pax7-nGFP* iPSC clones and employed a previously described CRISPR/Cas9 exon-skipping-based strategy that results in a restored reading frame (Figures S2F and S2G)<sup>192</sup>. To this end, we utilized a previously reported single plasmid which encodes for Cas9, guide RNAs and a puromycin selection cassette (Figures S2F and S2G)<sup>203</sup>. Transfection and antibiotic selection led to the generation of 24 DMD-iPSC sub-clones, of which two were correctly edited, and appeared indistinguishable from parental iPSCs (Figure 2B). We confirmed successful editing in these sub-clones at the DNA level by PCR and Sanger sequencing (Figures 2C and 2D). To unequivocally validate whether *Dmd*<sup>mdx</sup>; *Pax7-nGFP* iPSC sub-clones were successfully edited, we employed an established directed differentiation protocol of PSCs into muscle fibers *in vitro*<sup>195,278</sup>. This effort led to the generation of contractile muscle fibers from edited *Dmd*<sup>mdx</sup>; *Pax7-nGFP* iPSC sub-clones,

which showed successful reframing of dystrophin at the mRNA level (Figures 2E-G). Furthermore, immunostaining revealed dystrophin<sup>+</sup> myofibers solely in ESCs and edited *Dmd<sup>mdx</sup>; Pax7-nGFP* iPSCs subjected to the differentiation protocol, however not in unedited *Dmd<sup>mdx</sup>; Pax7-nGFP* iPSC-derived myogenic cultures subjected to this protocol (Figure S2H).

Based on these results, we proceeded to inject karyotypically normal and gene-edited *Dmd<sup>mdx</sup>; Pax7-nGFP* iPSCs into *Pax7-CreERT2: R26-LSL-DTA* blastocysts and produced 36 pups (Figures 2H and S2I). As both iPSCs and host blastocysts carry genes which encode for black fur coat color, we employed genotyping for the *Pax7-nGFP* allele to assess for chimerism, revealing this way that 21 out of 36 (58%) of the offspring were chimeric (Figures 2H and 2I). We then injected chimeras with tamoxifen between days 3-5 postnatally and harvested skeletal muscles from injected and non-injected chimeras at 5 weeks of age, aiming to assess the number of *Pax7-nGFP*<sup>+</sup> satellite cells with and without host satellite cell ablation (Figure 2A). Remarkably, we detected presence of *Pax7-nGFP*<sup>+</sup> satellite cells in chimeras following host satellite cell ablation (Figures 2J and S2J). Unexpectedly, we also detected approximately the same number of *Pax7-nGFP*<sup>+</sup> satellite cells in non-injected chimeras, suggesting that cell ablation is not critical for substantial production of donor-derived satellite cells in chimeras (Figures 2J, 2K). FACS-purified satellite cells were then extracted from both injected and non-injected chimeras, giving rise to *Pax7-nGFP*<sup>+</sup> myoblast lines (Figures S2J and S2K). Importantly, we confirmed that all of the *Pax7-nGFP*<sup>+</sup> myoblast lines solely carried a correctly edited dystrophin gene (Figure S2L).

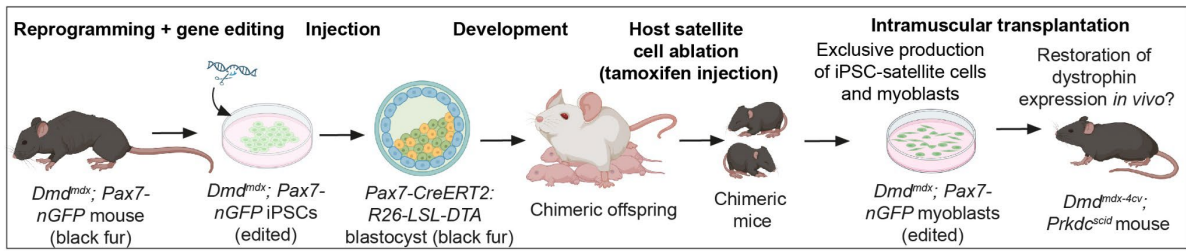
The observation that a comparable number of edited *Dmd<sup>mdx</sup>; Pax7-nGFP* satellite cells were generated in injected and non-injected chimeras promoted us to explore to what extent PAX7<sup>+</sup> cell ablation may promote enhanced iPSC contribution to the satellite cell niche. To this end, we analyzed additional chimeras that have been treated with and without tamoxifen injections and FACS-purified satellite cells from their skeletal muscles using established satellite cell surface markers (CD45<sup>-</sup>/CD31<sup>-</sup>/SCA1<sup>-</sup>/ITGA7<sup>+</sup>)<sup>276</sup>. We determined this way that most ITGA7<sup>+</sup> satellite cells were GFP positive with and without tamoxifen administration (Figures 2L, 2M and S2M). We further plated CD45<sup>-</sup>/CD31<sup>-</sup>/SCA1<sup>-</sup>/ITGA7<sup>+</sup> satellite cells and observed that nearly all myoblasts were GFP positive (Figures S2M and S2N). Most importantly, all ITGA7<sup>+</sup> satellite cell-derived myoblast lines contained only the gene-edited dystrophin allele, suggesting that indeed all satellite cells were derived from edited *Dmd<sup>mdx</sup>; Pax7-nGFP* iPSCs (Figure 2N).

Next, we embarked on molecular and functional characterization of edited *Dmd<sup>mdx</sup>; Pax7-nGFP* myoblasts, confirming strong GFP expression in multiple myoblast lines (Figures S3A and S3B). Bulk RNA-seq analysis of FACS-purified edited *Dmd<sup>mdx</sup>; Pax7-nGFP*<sup>+</sup> myoblasts revealed high expression of myoblast-related myogenic markers, and these cells were highly similar to FACS-purified PAX7<sup>+</sup> myoblasts harvested from *Pax7-nGFP* mice<sup>279</sup> (Figures 2O and S3C). We then differentiated *Dmd<sup>mdx</sup>; Pax7-nGFP* myoblasts into myotubes by serum withdrawal and observed formation of elongated, multinucleated fibers that downregulated the *Pax7-nGFP* reporter (Figure S3D). PCR and cDNA sequencing analyses of differentiated myotubes revealed faithful correction of the mutation in dystrophin (Figures S3E and S3F). Notably, we detected dystrophin<sup>+</sup> myotubes only in WT and edited *Dmd<sup>mdx</sup>; Pax7-nGFP* myotubes but not in unedited control (Figures 2P and S3G).

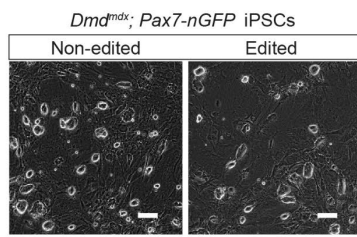
Finally, we explored whether edited *Dmd<sup>mdx</sup>; Pax7-nGFP* myoblasts can efficiently restore dystrophin expression *in vivo* in dystrophic muscles of immunodeficient *Prkdc<sup>scid</sup>; Dmd<sup>mdx-4Cv</sup>* mice, which were chosen due to the low rate of naturally-occurring revertant myofibers<sup>280,281</sup>. We transplanted 1 million edited *Dmd<sup>mdx</sup>; Pax7-nGFP* myoblasts into *tibialis anterior* (TA) muscles that have been pre-injured with cardiotoxin (CTX) injection to facilitate myoblast engraftment (Figures S3H and S3I). At 4 weeks post cell transplantation, we harvested the TA muscles and analyzed cross-muscle sections for presence of dystrophin expression. We observed a significant increase in dystrophin<sup>+</sup> myofibers in dystrophic muscles transplanted with edited *Dmd<sup>mdx</sup>; Pax7-nGFP* myoblasts compared to PBS-injected controls (Figures 2Q and 2R). Altogether, we conclude that genetically-corrected *Dmd<sup>mdx</sup>; Pax7-nGFP* iPSCs can exclusively give rise to *bona fide* satellite cells in intraspecies chimeras, even without host satellite cell ablation. Myoblasts derived from these satellite cells can efficiently contribute to dystrophin restoration *in vivo*.

**Figure 2**

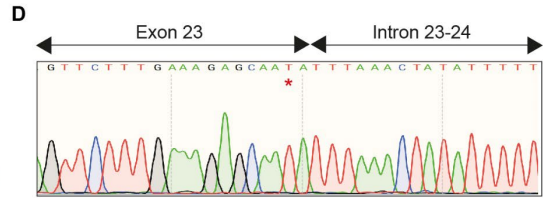
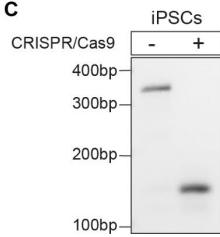
**A**



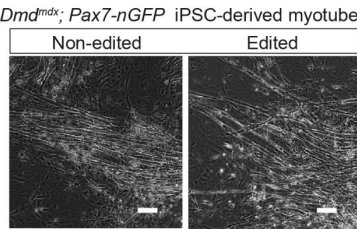
**B**



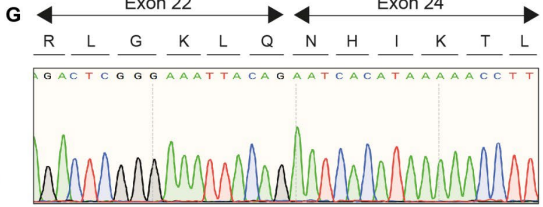
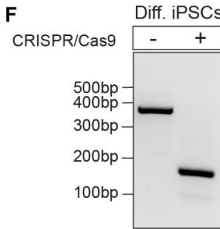
**C**



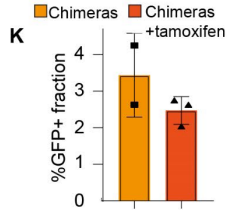
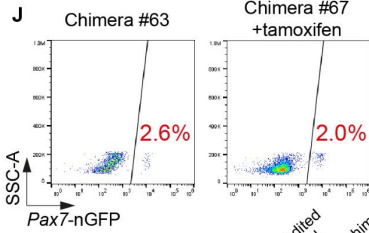
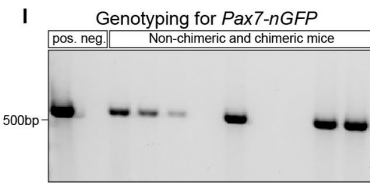
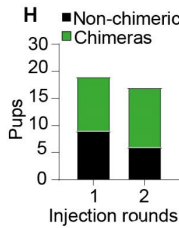
**E**



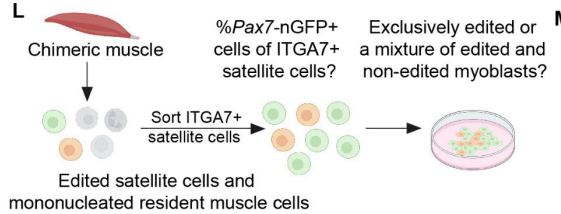
**F**



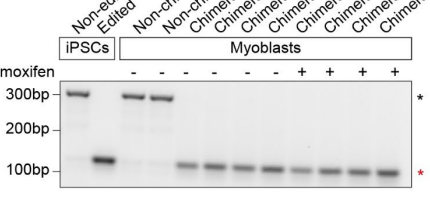
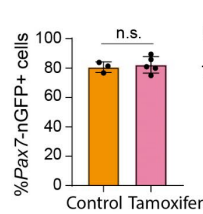
**H**



**L**



**M**



**O**

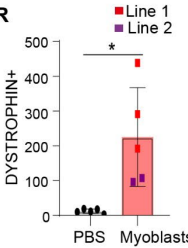
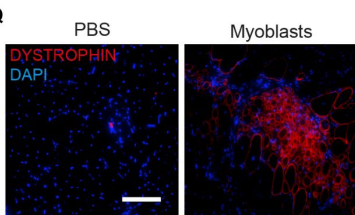
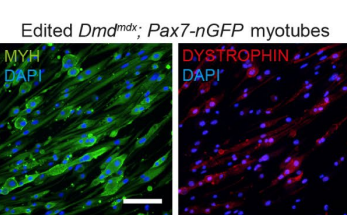
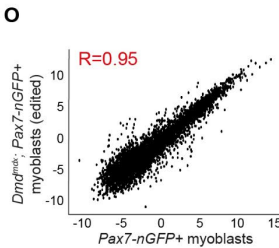


**Fig. 2. Functional muscle stem cells derived solely from edited *Dmd<sup>mdx</sup>; Pax7-nGFP* iPSCs in chimeras.** (A) A schematic overview of experimental plan. (B) Representative bright-field images on the indicated cells. Scale bar, 500µm. (C) PCR products for *Dystrophin* amplified from DNA of non-edited (-) and edited (+) *Dmd<sup>mdx</sup>; Pax7-nGFP* iPSCs. Non-edited DNA formed a PCR fragment of 340bp, whereas gene editing leads to a shorter PCR product of 146bp (red asterisk). (D) DNA sequencing of the edited *Dystrophin* PCR product lacking a splice site. Red asterisk indicates the *mdx* mutation. (E) Myogenic differentiation of non-edited and edited *Dmd<sup>mdx</sup>; Pax7-nGFP* iPSCs into myotubes. Scale bar, 500µm. (F) PCR on cDNA of non-edited (396bp) and

edited (183bp) *Dmd<sup>mdx</sup>; Pax7-nGFP* iPSC-derived myogenic cultures. The edited dystrophin band is marked by a red asterisk. **(G)** DNA sequencing of an edited dystrophin band, revealing successful exon skipping and reframing. **(H)** A graph showing chimera numbers. **(I)** Representative DNA genotyping for the *Pax7-nGFP* allele in non-chimeric and chimeric offspring. **(J)** Flow cytometry analysis of *Pax7-nGFP* in the indicated animals and conditions. **(K)** Quantification showing the percentage of *Pax7-nGFP*<sup>+</sup> cells in muscles derived from chimeras upon satellite ablation or control. N=2-3. **(L)** Strategy to investigate the proportion of *Pax7-nGFP*<sup>+</sup> cells within the ITGA7<sup>+</sup> satellite cell population. **(M)** Quantification of the percentage of *Pax7-nGFP*<sup>+</sup> cells within the ITGA7<sup>+</sup> satellite cell population derived from chimeras with or without tamoxifen treatment. N=3 for control, N=5 for the tamoxifen treated group. Statistical analysis was performed with percentage of GFP cells using ordinary one-way ANOVA, n.s., not significant. **(N)** PCR for dystrophin in ITGA7<sup>+</sup>-derived myoblasts from the indicated animals and conditions. Note that all myoblasts show only an edited band. **(O)** Scatterplot based on log<sub>2</sub>-normalized gene counts from bulk RNA-seq of the indicated samples. N=3 cell lines per group, p<2.2e-16. **(P)** Immunofluorescence staining for the indicated cells. Scale bar, 100µm. **(Q)** Immunofluorescence staining of cross-muscle sections of *tibialis anterior* (TA) muscles of the indicated conditions. Scale bar, 100µm. **(R)** Quantification of transplantation trials. Statistical analysis using paired t-test, N=5, \*p ≤ 0.05, each dot represents an individual muscle.

## Functional mouse satellite cells produced in interspecies rat-mouse chimeras

The capacity to generate genetically corrected satellite cells in intraspecies chimeras even without host satellite cell ablation prompted us to assess whether mouse satellite cells can be generated in another animal host. To address this objective, we chose rats as recipients, as xenogeneic cells and organs were previously produced in rat-mouse chimeras<sup>216</sup>. We chose to inject edited *Dmd<sup>mdx</sup>; Pax7-nGFP* iPSCs into WT Sprague-Dawley (SD) rat blastocysts and assess production of satellite cells in rat-mouse adult chimeras (Figure 3A). We injected 8-12 edited *Dmd<sup>mdx</sup>; Pax7-nGFP* iPSCs into SD rat blastocysts, and embryos were transferred into the oviducts of foster rats. Collectively, this trial resulted in production of 4 rat-mouse chimeras out of 7 born pups (57.1%), as judged by patches of black fur. The extent of chimerism was varied, ranging between small fur patches to prominent contribution to fur black color (Figures 3B and S4A). Of note, most of these chimeras appeared healthy although one chimera, which showed the highest chimerism, was smaller in size and demonstrated body asymmetry and malocclusion (Figure S4A, top), in line with previous reports that documented abnormalities in interspecies chimeras with extensive xenogeneic contribution<sup>58,59,282</sup>. We then opted to isolate and digest skeletal muscles from rat-mouse chimeras #2 and #4 and confirmed presence of the rat dystrophin allele and the mouse gene-edited dystrophin (Figures 3B, 3C and S4B). Flow cytometry analysis revealed presence of *Pax7-nGFP*<sup>+</sup> satellite cells in the chimeras' muscles, however less than in skeletal muscles harvested

from young *Pax7-nGFP* mice (Figure 3D). Collectively, out of the four rat-mouse chimeras, we detected presence of *Pax7-nGFP*<sup>+</sup> satellite cells in 3 chimeras (75%) (Figures 3D and S4C). We next decided to produce and characterize myoblast lines from rat-mouse chimeras #2 and #4, which showed robust *Pax7-nGFP* reporter expression *in vitro* (Figures 3D and 3E). DNA analysis confirmed the presence of only the corrected dystrophin gene and lack of rat DNA, as well as presence of the *Pax7-nGFP* transgene (Figures 3F, S4D and S4E). Additionally, myoblast mRNA showed reframing of dystrophin and Sanger sequencing validated this result (Figures 3G and 3H). Of note, differentiation of myoblasts downregulated the *Pax7-nGFP* reporter and gave rise to dystrophin<sup>+</sup> myotubes, unlike unedited control (Figures 3I and S4F).

Last, we set out to explore whether xenogeneic satellite cells or derivative myoblasts produced in rat-mouse chimeras can restore dystrophin expression in DMD mice in an allogeneic manner following intramuscular transplantation (Figure 3J). To this end, we FACS-purified *Pax7-nGFP*<sup>+</sup> satellite cells from rat-mouse chimera #2 and injected about 10'000 cells into CTX pre-injured TA muscles of *Prkdc<sup>scid</sup>; Dmd<sup>mdx</sup>* mice. Alternatively, we injected 1 million myoblasts at passage 7 that have been isolated from rat-mouse chimera #2 into CTX pre-injured TA muscles of *Prkdc<sup>scid</sup>; Dmd<sup>mdx-4Cv</sup>* mice (Figures 3J and 3K). At 1-month post transplantation, TA muscles were harvested, sectioned, and analyzed. Remarkably, we could detect areas of dystrophin<sup>+</sup> myofibers in dystrophic muscles subjected to satellite or myoblast cell transplantation (Figures 3L and 3M). Quantification of these muscle cross-sections in comparison to a PBS-injected control revealed around 40 times more dystrophin<sup>+</sup> myofibers following myoblast engraftment (Figure 3N). Together, these results demonstrate that mouse *Dmd<sup>mdx</sup>; Pax7-nGFP* iPSC-derived satellite cells or myoblasts produced in rat-mouse chimeras can efficiently restore dystrophin expression in muscles of DMD mice.



**Figure 3**

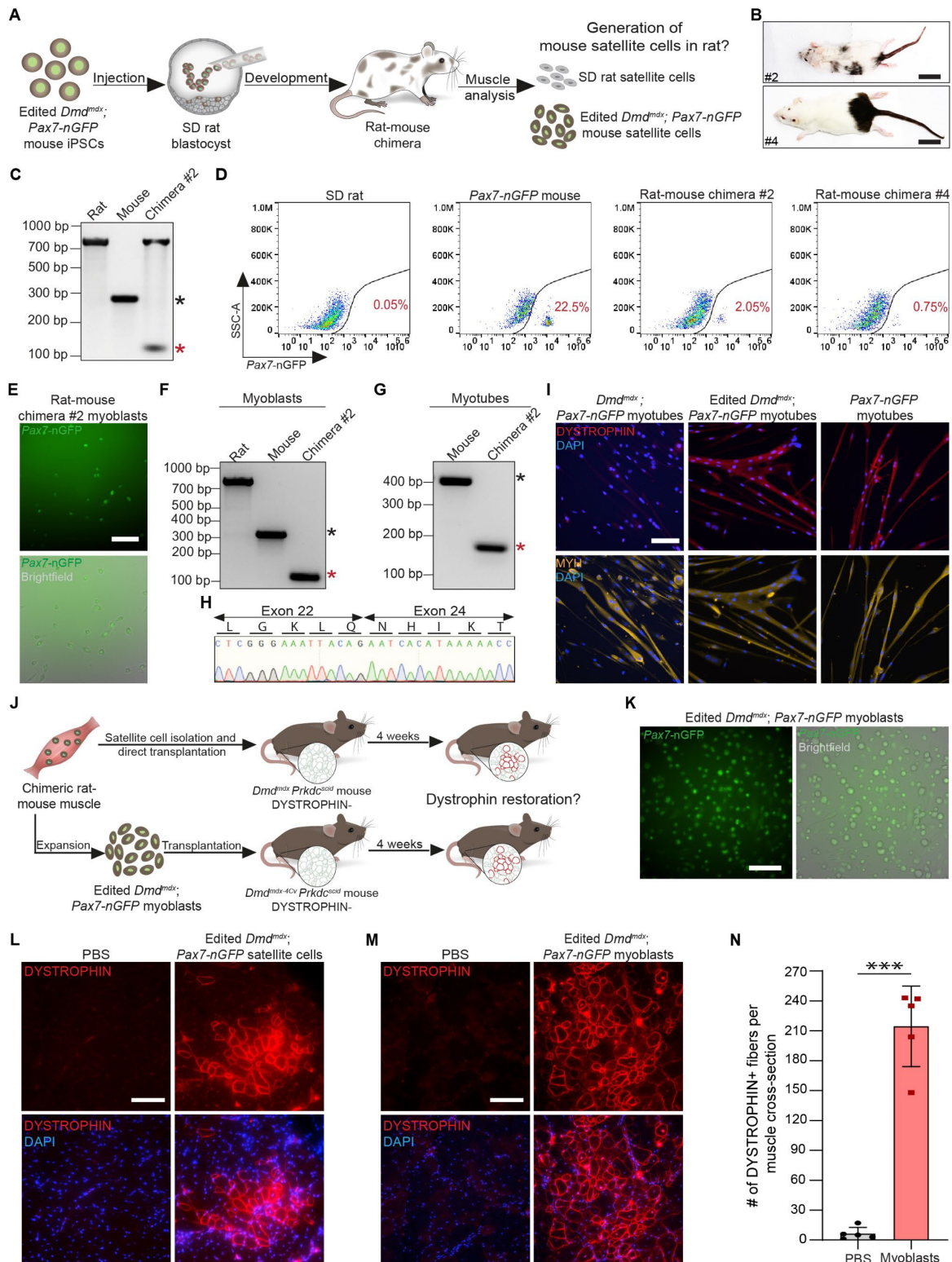


**Fig. 3. Production of edited *Dmd<sup>mdx</sup>*; *Pax7-nGFP* iPSC-derived functional mouse satellite in rat-mouse chimeras. (A) A schematic overview of experimental design. (B) Photos of rat-mouse chimeras at 7 weeks of age. Scale bar, 3.5cm. (C) PCR for rat and mouse dystrophin from muscle lysates of the indicated animals. Black and red asterisks denote unedited (340bp) and edited (146bp) murine dystrophin, respectively. (D) Flow cytometry analysis of *Pax7-nGFP* expression in muscle lysates of the indicated animal strains. (E) Representative images of *Dmd<sup>mdx</sup>*; *Pax7-nGFP* mouse myoblasts isolated from rat-mouse chimera #2 at P0. Scale bar, 100µm. (F) PCR**

for rat and mouse dystrophin of myoblasts isolated from the indicated animals. Black and red asterisks denote unedited and edited murine dystrophin, respectively. **(G)** PCR for mouse *Dystrophin* using cDNA of myotubes derived from edited *Dmd<sup>mdx</sup>; Pax7-nGFP* myoblasts produced in rat-mouse chimera vs. control. **(H)** Sanger sequencing reveals reframing of the dystrophin gene at the cDNA level of the myotubes analyzed in (G). **(I)** Immunofluorescence for dystrophin in edited *Dmd<sup>mdx</sup>; Pax7-nGFP* myotubes differentiated from rat-mouse chimera myoblasts vs. controls. Scale bar, 100 $\mu$ m. **(J)** A schematic overview of transplantation experiments. **(K)** Edited *Dmd<sup>mdx</sup>; Pax7-nGFP* myoblasts before transplantation. Scale bar, 100 $\mu$ m. **(L)** TA muscle cross-section of *Dmd<sup>mdx</sup>; Prkdc<sup>scid</sup>* mice stained for dystrophin at 4 weeks after transplantation with satellite cells. Scale bar, 100 $\mu$ m. **(M)** *Dmd<sup>mdx-4Cv</sup>; Prkdc<sup>scid</sup>* TA muscle cross-sections stained for dystrophin at 4 weeks after transplantation with myoblasts. Scale bar, 100 $\mu$ m. **(N)** Quantification of dystrophin<sup>+</sup> fibers. Statistical analysis was performed using paired t-test, N=5, \*\*\*p  $\leq$  0.001, each dot represents an individual muscle.

## Discussion

In this study, we report on production of genetically corrected and functional DMD satellite cells in mouse-mouse or rat-mouse chimeras. For intraspecies chimeras, we utilized an inducible ablation system of host *Pax7*<sup>+</sup> cells to preferentially obtain ESC- or gene-edited iPSC-derived satellite cells and myoblasts capable of restoring dystrophin expression *in vivo* (Figure 4). Surprisingly, we observed efficient production of satellite cells even without an ablation system, prompting us to investigate production of gene-edited iPSC-derived mouse satellite cells in rat-mouse chimeras. Strikingly, multiple rat-mouse chimeras contained appreciable numbers of donor-derived and gene-edited mouse satellite cells and derivative myoblasts that could efficiently restore dystrophin expression in DMD mice (Figure 4).

Our work raises the possibility that a similar approach may enable production of xenogeneic lineage-specific human adult stem cells in interspecies chimeras. In recent years, several papers reported on contribution of human PSCs to chimerism in mouse, pig and monkey embryos<sup>50-53,283</sup>. However, adapting such a technique for production of human cells in animal chimeras is associated with ethical considerations and barriers, and most notably will require means to exclude production of undesired human cell types such as brain cells or gametes in human-animal chimeras<sup>284-286</sup>. To this end, use of PSCs that carry a genetic mutation that precludes their differentiation into these cell types may provide a plausible solution as recently shown in mice<sup>285</sup>.

Utilizing blastocyst complementation, a recent study reported on pig and human skeletal muscle formation by injection of pig PSCs or P53-null human iPSCs into pig embryos carrying triple knockout in *MYOD*, *MYF5* and *MYF6*, thus enabling PSC-colonization of the skeletal muscle lineage in chimeric embryos<sup>53</sup>. However, assessing the contribution of human PSCs to the embryonic muscle stem cell compartment, or *in*



*in vitro* production of human myogenic cell lines from these interspecies embryos has not been documented<sup>53</sup>. Moreover, one notable caveat for production of xenogeneic skeletal muscle tissue or organs in interspecies chimeras is the presence of animal host-derived endothelium, mesenchyme or other cell types, which may evoke an immunological response<sup>49,284</sup>. The approach reported in our study circumvents this major limitation as autologous muscle stem cells can be FACS-purified in considerable numbers from interspecies chimera muscles and transplanted into patients, without lingering animal cells. Another advantage for the approach detailed in our study is that the PSCs were differentiated *in vivo*, thus mitigating any potential future risk for residual PSCs to form teratomas in patients as recently reported for *in vitro* PSC-derived cells<sup>287</sup>. Last, as iPSCs differentiate into satellite cells in postnatal chimeras, this approach ensures the generation of adult muscle stem cells, in comparison to myogenic cells generated from PSCs via directed differentiation *in vitro*, which carry embryonic attributes<sup>288</sup>.

To close, our study demonstrates a proof-of-principle for combining cellular reprogramming, genome engineering and *in vivo* PSC differentiation to produce therapeutically-competent muscle stem cells in a xenogeneic chimera host. In respect to implications for human therapy, further work is certainly warranted to address the hurdles associated with generating human cells in animals. However, with further success, we envision this work may pave the way for producing autologous human satellite cells in large animals for the treatment of muscle diseases.

Figure 4

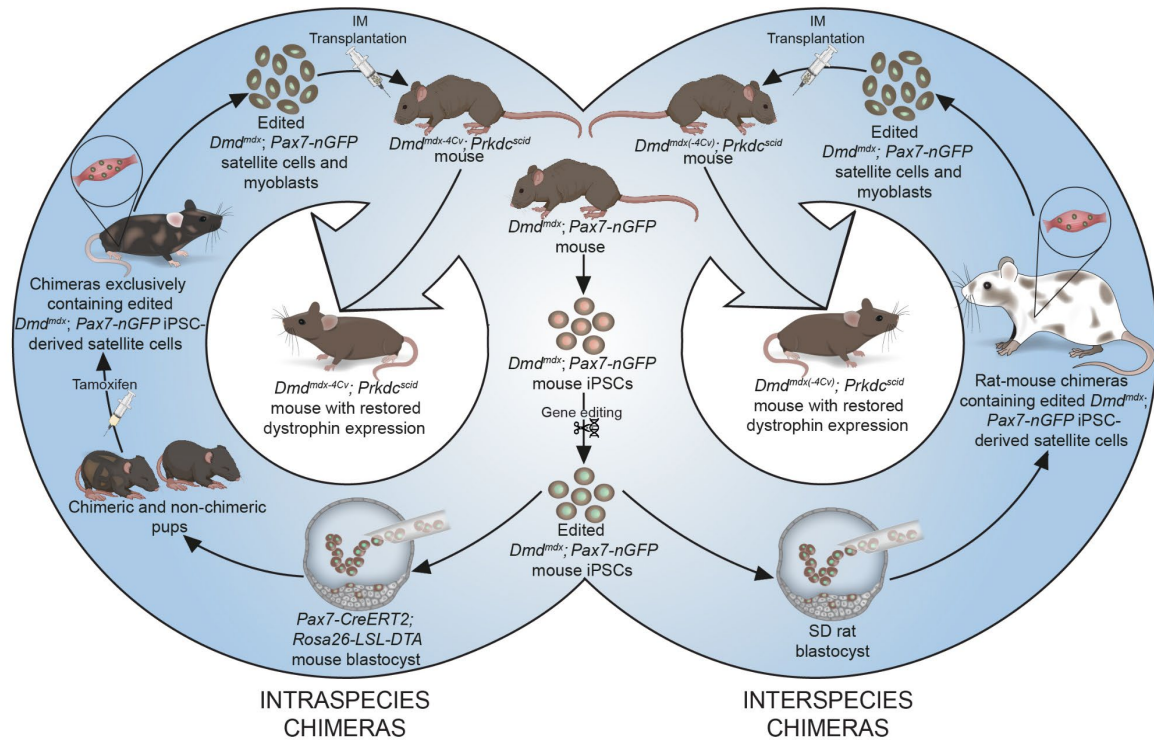


Fig. 4. Schematic overview of the study results.

#### Acknowledgments:

We are thankful to Inseon Kim and Xhem Qabrati their feedback and fruitful discussions. We further wish to thank Pjeter Gjonllshaj for his help with rat superovulation and pairing. We thank Dr. Konrad Hochedlinger for providing the M2rtTA and STEMCCA lentiviral cassettes used for iPSC reprogramming and Dr. Shhargim Tajbakhsh for providing the Pax7-nGFP mouse strain. We are also grateful to the Functional Genomics Center Zurich (FGCZ) for their assistance with bulk RNA sequencing. A few of the graphical schematics were created with BioRender.com, others with help of the graphic designer Veronique Juvin from SciArtWork.

#### Funding:

Startup fund ETH Zurich (OBN)  
 Eccellenza Grant, Swiss National Science Foundation PCEGP3\_187009 (OBN)  
 The Good Food Institute Foundation (OBN)  
 The Novartis Foundation for Medical-Biological Research (OBN)  
 The Helmut Horten Foundation (OBN)  
 NCCR Robotics 51NF40\_185543 (OBN)  
 NTN Grant Innosuisse (OBN)

#### Author contributions:

Conceptualization: SD, AL, JZ, OBN  
 Experiments intraspecies part: SD, AL, NB  
 Experiments interspecies part: AL, JZ, NB  
 Chimera production: MTS  
 RNA sequencing analysis: AG  
 Writing – original draft: SD, AL, JZ, OBN

**Competing interests:**

“Authors declare that they have no competing interests.”

**Data and materials availability:**

“All data are available in the main text or the supplementary materials.”

## Materials and Methods

**Animals**

Mice and rats used in this study were housed in Allentown cages, under standard conditions at room temperature 23°C and a relative humidity of 50-60%, with a 12-h light-dark cycle. All animals had *ad libitum* access to food and water. The following mouse strains from Jackson Laboratories were used: C57BL/10ScSn-*Dmd*<sup>mdx</sup>/J (Stock No: 001801); B10ScSn.Cg-*Prkdc*<sup>scid</sup> *Dmd*<sup>mdx</sup>/J (Stock No: 018018); B6; 129S- *Gt(ROSA)*<sup>26Sortm1.1Ksv</sup>/J (Stock No: 023139); B6.Cg-*Pax7*<sup>tm1(cre/ERT2)Gaka</sup>/J (Stock No: 017763). Additionally, the previously reported strains were used: *Tg:Pax7-nGFP/C57BL6;DBA2* mice (a kind gift from Dr. Shahragim Tajbakhsh)<sup>219</sup> for production of MEFs for iPSC reprogramming and NOD.Cg-*Prkdc*<sup>scid</sup>l2rgtm1Wjl/SzJ (005557)x B6Ros.Cg-*Dmd*<sup>mdx-4Cv</sup>/J (002378) as recipient mice for intramuscular myoblast transplantations. Swiss webster mice and Sprague-Dawley rats were purchased from Janvier, France. The present study was approved by the Federal Food Safety and Veterinary Office, Cantonal veterinary office (Zurich) and granted animal experiment license numbers ZH246/18, ZH177/18 and FormG-135.

**Cell culture**

Mouse embryonic fibroblasts (MEFs) were isolated from E13.5 mouse embryos and grown in ‘MEF medium’ containing DMEM (41966029, Thermo Fisher Scientific) supplemented with 10% FBS (10270106, Thermo Fisher Scientific), 1% MEM Non-Essential Amino Acids Solution (100X) (11140050, Thermo Fisher Scientific), 1% Penicillin-Streptomycin (10,000 U/mL) (15140122, Thermo Fisher Scientific) and 0.1% Gibco 2-Mercaptoethanol (21985023, Thermo Fisher Scientific). HEK-293T cells were grown in ‘MEF medium’. MEF reprogramming and iPSCs culture was performed in MES medium consisting of DMEM (41966029, Thermo Fisher Scientific), 1% GlutaMAX Supplement (35050061, Thermo Fisher Scientific), 1% Penicillin-Streptomycin (10,000 U/mL) (15140122, Thermo Fisher Scientific), 1% MEM Non-Essential Amino Acids Solution (100X) (11140050, Thermo Fisher Scientific), 0.1% Gibco 2-Mercaptoethanol (21985023, Thermo Fisher Scientific), 15 % FBS (10270106, Thermo Fisher Scientific) supplemented with 1000U/ml mLIF (#PG-A1140-0010, PolyGene Transgenetics). iPSCs and ESC were cultured in ‘Enhanced medium’ consisting of MES medium supplemented with 0.5µmol/l VPA (P4543-10G, Sigma-Aldrich), 1.5µmol/l CGP77675 (SML0314, Merck ) and 3µmol/l CHIR99021 (4423, Tocris Bioscience) for 5 days prior to blastocyst injections. ‘Myoblast medium’ for satellite cells and myoblast consisted of 50% DMEM (41966029, Thermo Fisher Scientific), 50% F-10 medium (22390025, Thermo Fisher Scientific), 10% Horse serum (16050122, Thermo Fisher Scientific), 20% FBS (10270106, Thermo Fisher Scientific), 1% Penicillin-Streptomycin (10,000 U/mL) (15140122, Thermo Fisher Scientific) and 10ng/ml basic FGF (233-FB-500, R&D Systems). Myoblast were differentiated in ‘Differentiation medium’ containing DMEM (41966029, Thermo Fisher Scientific) supplemented with 2% Horse serum (16050122, Thermo Fisher Scientific) and 1% Penicillin-Streptomycin (10,000 U/mL) (15140122, Thermo Fisher Scientific). All cells were passaged using Gibco Trypsin-EDTA (0.05%) (25300054, Thermo Fisher Scientific) and tested for mycoplasma (LT07-318, Lonza). All cells were maintained at 37°C in a 5% CO<sub>2</sub> incubator.

### **Generation of iPSCs**

To generate iPSCs, male MEFs were transduced with lentiviral vectors FUW-M2rtTA (Addgene plasmid #20342) and LV-mSTEMCCA-1<sup>221</sup> combined with 5ug/ml Polybrene (TR-1003-G, Sigma-Aldrich) on two consecutive days in MEF medium without Penicillin-Streptomycin. 20'000 transduced MEFs were then seeded into one well of a 6 well plate in 'MES medium' supplemented with 2ug/ml Doxycycline (D9891-5G, Sigma-Aldrich), 3µM CHIR99021 (4423/50, R&D Systems) and Ascorbic acid (A4403-100MG, Sigma-Aldrich) at the final concentration of 50 µg/ml to initiate reprogramming. Reprogramming medium was changed daily until iPSC colonies appeared. Dox-independent iPSCs colonies were picked and transferred onto γ-irradiated CF-1 fibroblasts and expanded in 'MES medium'.

### **Lentivirus preparation**

Frozen lentiviral stocks were generated by transfecting 70% confluent HEK-293T cells in 15cm cell culture dishes in 'MEF medium' together with a solution consisting of 1ml 150mM NaCl (1.06404.1000, VWR), 1ml Polyethylenimine (23966-1, Polysciences), pLV delta 8.9 (16.5µg), pLV VSVG Envelope (11µg) and the transfer vector (22µg). 24 hours after transfection, the cell medium was changed to regular 'MEF medium'. Supernatant was collected, filtered using a 0.45µm filter and stored at 4°C 48h and 72h after transfection. 0.25ml of cold PEG-it Virus Precipitation Solution (LV810A-1-SBI, System Biosciences) was added per 1ml of lentiviral-containing supernatant and kept cool at 4°C overnight. Next, the mixture was centrifuged at 1500g for 30min at 4°C, resuspended in PBS containing 25mM HEPES (15630056, Thermo Fisher Scientific) and stored at -80°C for future use.

### **Gene editing**

iPSCs were transfected as single cells using Lipofectamine CRISPRMAX Cas9 Transfection Reagent (CMAX00003, Thermo Fisher Scientific) according to the manufacturer's instructions with pRP[CRISPR]-EGFP/Puro-hCas9-U6>(long left)-U6>(long right) (Vector builder, VB190118-1126uvv). 1 day after transfection, puromycin (A1113803, Thermo Fisher Scientific) was added at a final concentration of 1 µg/ml for 3-4 days for selection. After recovery in puromycin-free medium, single iPSC colonies were picked and expanded. 24 colonies were picked and characterized. 2 out of these showed the expected editing with an additional 6 bp intronic deletion that didn't impact the final outcome.

### **iPSC differentiation**

iPSC differentiation towards myogenic cells was performed as described by Chal et al<sup>195,278</sup>.

### **Karyotyping**

KaryoMAX Colcemid Solution (15212012, Thermo Fisher Scientific) was added to the iPSCs at a final concentration of 100 ng/ml. After a 5-hour incubation at 37°C, cells were harvested, centrifuged, and supernatant was removed to 1 ml. Cells were re-suspended by vortexing at low setting and 5ml of pre-warmed hypotonic solution (0.56g KCl+0.5g sodium citrate in 200ml H<sub>2</sub>O) were added dropwise while mixing. The cell suspension was then incubated at 37°C and after 30min, 2.5ml of fixative (Methanol:Acetic acid = 3:1) were added. The mixture was centrifuged, supernatant removed, and the cell pellet was re-suspended in 2ml of fixative while vortexing and incubated at room temperature for 5 min. This step was repeated 3 times. Next, the cell pellet was re-suspended in 1ml fixative and 400µl of this cell suspension was dripped on a polarized microscope slide from a height of 150cm. After the slides dried, they were immersed in Giemsa solution for 7 min, put into Gurr's buffer (0.469 g NaH<sub>2</sub>PO<sub>4</sub> + 0.937 g Na<sub>2</sub>HPO<sub>4</sub> in 1 l of H<sub>2</sub>O) for 2 min and then washed with water. Slides were let to dry and examined. For analysis, 30 cell spreads were randomly selected and chromosomes were counted.

### **Blastocyst injection**

Blastocyst injections and embryo transfer were performed in house, abiding to all legal rules of the Federal Food Safety and Veterinary Office, Cantonal veterinary office (Zurich) and an animal experimental license (FormG-135 and ZH246/18). On the injection day, cells were pre-plated and then kept on ice until injection. For mouse intraspecies blastocyst injections, mice aged 3-4w were superovulated via intraperitoneal injection of 5IU PMSG (ProSpec). About 46-48h later, the mice were injected again with 5IU hCG (ProSpec), to induce ovulation, and were paired with stud males. The following morning the females were separated, euthanized after 48 hours, the morulae flushed from the oviduct using M2 Medium (M7167, Sigma-Aldrich) and incubated overnight at 37°C and 5% CO<sub>2</sub>. For mouse to rat interspecies blastocyst injections, SD rats (aged 8-15w) were synchronized via injection of 40µg of LHRHa (L4513, Sigma-Aldrich). About 94-96h later, the rats were paired with stud males. After 116-120h, the blastocysts were flushed in M2 medium. Injections were carried out in droplets of M2 medium covered with Mineral Oil (Sigma-Aldrich, M8410-1L). Typically, 8-12 iPSCs or ESCs cells were injected per blastocyst. Successfully injected blastocysts were transferred to a 60ml center well organ culture dish containing CO<sub>2</sub>-buffered culture medium (EmbryoMax KSOM medium (MR-106-D, Sigma-Aldrich) for mouse blastocysts, rat KSOM (CSR-R-R148, Cosmo Bio) for rat blastocysts) and kept in an incubator at 37°C and 5% CO<sub>2</sub>. The injected mouse blastocysts were transferred to the uteri of 2.5dpc pseudo-pregnant female mice on the same day, or into uteri of 3.5dpc pseudo-pregnant female SD rats in case of rat blastocysts. Injections were performed with a Narishige MTK-1 hydraulic micromanipulator (Narishige), combined with a CellTram oil and a PiezoXpert (both Eppendorf). Presence of chimerism in intraspecies or interspecies chimeras was first assessed using visual examination of fur coat color. Further, chimerism was also assessed by genotyping for the RFP transgene or the *Pax7-nGFP* reporter.

### **Satellite cell ablation**

A tamoxifen inducible '*Pax7-CreERT2: R26-LSL-DTA*' system was used to ablate host satellite cells. Mice received an intraperitoneal injection of 50µl of 1mg/ml tamoxifen (T5648-1G, Sigma-Aldrich) in corn oil (C8267, Sigma-Aldrich) every day at P3-P5 followed by bi-weekly injections /75 mg tamoxifen/kg body weight).

### **Intramuscular transplantation of myoblasts and satellite cells**

Either *B10ScSn.Cg-Prkdc<sup>scid</sup> Dmd<sup>mdx</sup>/J* mice or *NOD.Cg-Prkdc<sup>scid</sup> /SzJ; B6Ros.Cg-Dmd<sup>mdx-4Cv</sup>/J* received an injection of 50µl of 10µM Cardiotoxin (L8102, Latoxan) into the hindleg *tibialis anterior* (TA) muscles to enhance engraftment of the cells to be injected the day after. For myoblast transplantation, myoblasts were harvested, and 1'000'000 cells were resuspended in 20µl PBS. For satellite cell transplantation, 10'000 satellite cells were centrifuged at 650g for 5 min immediately after FACS and resuspended in 20µl PBS. This cell mixture was then injected craniocaudally into the pre-injured TA muscle (left leg) using an insulin syringe (324824, BD) and the cell suspension was slowly released upon retraction of the cannula. As a control, PBS was injected into the right hindleg pre-injured TA muscle. Mice were euthanized and TAs harvested 27-28 days after cell transplantation. Fifteen *NOD.Cg-Prkdc<sup>scid</sup> /SzJ; B6Ros.Cg-Dmd<sup>mdx-4Cv</sup>/J* recipient mice were used for the transplantation experiment using three different myoblast lines (two from intraspecies chimeras and one from interspecies chimera), but only ten of these mice showed engraftment. Two *B10ScSn.Cg-Prkdc<sup>scid</sup> Dmd<sup>mdx</sup>/J* mice were used for direct transplantation of satellite cells, which engrafted in only one of them.

### **Muscle embedding and processing**

Harvested TAs were placed onto a cork covered with 10% Tragacanth (G1128, Sigma-Aldrich), and frozen for 30-60s in 2-Methylbutane (3927.1, Carl Roth) pre-cooled in LN<sub>2</sub>. The samples were

added to liquid nitrogen for 1min and then stored at -80°C. Frozen muscles were cryo-sectioned into 10µm thick cross-sectional muscle sections and stored at -80°C.

### Genomic DNA isolation and PCR

Isolation of genomic DNA from cells was performed using the DNeasy Blood & Tissue Kit (69504, Qiagen) according to the manufacturer's instruction. DNA for PCR from muscle lysates was obtained by direct lysis of muscle slurry generated by muscle mincing followed by 90 min incubation in digestion solution containing 2mg/ml Collagenase Type 2 (17101015, Thermo Fisher Scientific) in DMEM (41966029, Thermo Fisher Scientific) at 37°C using DirectPCR Lysis Reagent (mouse tail) (VIG102-T, Viagen Biotech). PCR for *Pax7-nGFP* was performed using primer Pax7nGFP.F/ Pax7nGFP.R and GoTaq G2 Hot Start Green Master Mix (M7423, Promega) via the following program: 94°C 2min, 30x (94°C 30s, 65°C 30s, 72°C 30s), 72°C 5min. Dystrophin gene editing was verified by PCR for mouse dystrophin using primers Dmd\_i22-i23.F/ Dmd\_i22-i23.R and GoTaq G2 Hot Start Green Master Mix (M7423, Promega) via the following program: 94°C 5min, 30x (94°C 30s, 55°C 30s, 72°C 30s), 72°C 5min. PCR products were separated on a 1.5-2% agarose gel (7-01P02-R, BioConcept) dissolved in TAE buffer (3-07F03-I, BioConcept) and visualized using GelRed Nucleic Acid Stain (Cat# 41003, Biotium). Presence of rat cells in myoblast culture/muscle lysate was assessed by PCR for rat dystrophin using primers Rat Dmd i22-i23.F/ Rat Dmd i22-i23.R and GoTaq G2 Hot Start Green Master Mix (M7423, Promega) via the following program: 94°C 5min, 30x (94°C 30s, 57°C 1min, 72°C 30s), 72°C 5min.

Table 1: PCR primers

	Forward primer (5'-3')	Reverse primer (5'-3)
Pax7-nGFP	Pax7nGFP.F: CCA CAC CTC CCC CTG AAC CTG AAA CAT AAA	Pax7nGFP.R: GAA TTC CCC GGG GAG TCG CAT CCT GCG G
Mouse dystrophin	Dmd_i22-i23.F: TGA AAC TCA TCA AAT ATG CGT GT	Dmd_i22-i23.R: TCT GTT TCC CAT CAC ATT TTC CA
Rat dystrophin	Rat Dmd i22-i23.F: AGA AAA CTC CTG TGA TGT GAG G	Rat Dmd i22-i23.R: ACA TAG GAC AAA TAG GCG AGT T

### RNA Extraction and cDNA synthesis

RNA isolation was performed using Qiagen RNeasy kit, with 15min DNase digest (74104, Qiagen). The concentration was measured by a Tecan Spark 10M. cDNA was synthesized with the High-Capacity cDNA Reverse Transcription Kit (4368814, Thermo Fisher Scientific) using 1µg of RNA according to the manufacturer's instruction.

### RT-PCR and RT-qPCR on cDNA

To verify *Dystrophin* gene editing on mRNA derived cDNA, RT-PCR was performed with primers Dmd\_e22-e24.F / Dmd\_e22-e24.R using GoTaq G2 Hot Start Green Master Mix (M7423, Promega) via the following program: 94°C 5min, 35x (94°C 30s, 55°C 30s, 72°C 30s), 72°C 5min. PCR products were run on a 1.5-2% agarose gel (7-01P02-R, BioConcept) in TAE buffer (3-07F03-I, BioConcept) and imaged using GelRed Nucleic Acid Stain (41003, Biotium). For RT-qPCR, the Applied Biosystems PowerUp SYBR Green Master Mix (A25741, Thermo Fisher

Scientific) was used, with a final cDNA concentration of 5ng/μl according to the manufactures manual and primer sets mGapdh.F/mGapdh.R, mNanog.F/mNanog.R, mOct4.F/mOct4.R, mSox2.F/mSox2.R, Pkg.F/Pkg.R. RT-qPCR reactions were run on a 384-well block QuantStudio 5 System with comparative CT standard run mode and the following cycling conditions: Hold stage 50°C 2min- 95°C 10min; PCR stage: 95°C 15s-60°C 1min, 40x; Melt Curve stage: 95°C 15s-60°C 1min-95° 15s. All reactions were done in triplicate and Ct values were obtained. Data was analyzed using 2-ΔΔCt method and mouse *Pgk* and *Gapdh* served as housekeeping control genes.

Table 2: RT-qPCR primers

	Forward primer (5'-3')	Reverse primer (5'-3)
Dystrophin	Dmd_e22-e24.F CACTTTACCACCAATGCGCT	Dmd_e22-e24.R ACA TCA ACT TCA GCC ATC CA
mGapdh	mGapdh.F TCA CCA CCA TGG AGA AGG C	mGapdh.R GCT AAG CAG TTG GTG GTG CA
mNanog	mNanog.F AGG ACA GGT TTC AGA AGC AGA	mNanog.R CCA TTG CTA GTC TTC AAC CAC TG
mOct4	mOct4.F CAC CAT CTG TCG CTT CGA GG	mOct4.R AGG GTC TCC GAT TTG CAT ATC T
mSox2	mSox2.F GCG GAG TGG AAA CTT TTG TCC	mSox2.R GGG AAG CGT GTA CTT ATC CTT CT
Pgk	Pgk.F ATG TCG CTT TCC AAC AAG CTG	Pgk.R GCT CCA TTG TCC AAG CAG AAT

### Sequencing

Dystrophin DNA and cDNA PCR products were run on a 1.5-2% agarose gel (7-01P02-R, BioConcept) in TAE buffer (3-07F03-I, BioConcept) and products were extracted using the QIAquick Gel Extraction Kit (28706, Qiagen) and Sanger sequenced by Microsynth (Balgach, Switzerland) and evaluated with Benchling (retrieved from <https://benchling.com> in 2020) or SnapGene Viewer 3. The following primers were used for sequencing: Dmd\_e22-e24.F (for sequencing of PCR products obtained from myoblast cDNA), Dmd\_i22-i23.F (for sequencing of PCR products obtained from iPSC genomic DNA).

### Alkaline phosphatase test

Alkaline phosphatase test was performed using the Leukocyte Alkaline Phosphatase Kit (86R-1KT, Sigma-Aldrich). First, alkaline dye mixture was prepared as described in manufacturer's protocol. Next, the fixing step was adopted for cells in a culture dish: 0.5ml of fixative solution prepared as described by manufacturer was added to each well of the 6-well plate with the cells.

After 1min incubation at room temperature, cells were washed with PBS twice. Finally, 1ml of alkaline dye mixture per well of 6-well plate was added and plates were incubated for 15 min at room temperature in the dark. Alkaline dye mixture was aspirated, cells were washed twice with PBS, covered with 0.5 ml of PBS and imaged.

### **Immunofluorescent staining**

Cells cultured in 6 well plates were washed with PBS and fixed with 4% Paraformaldehyde (11400580, Fisher Scientific) in PBS for 5min at room temperature (RT). After two PBS washing steps, 'blocking solution' made up of PBS supplemented with 2% BSA (A1391, AppliChem) and 1% Triton X-100 (9002-93-1, Sigma-Aldrich) was added to the fixed cells for 30min at RT. Primary antibodies diluted in 'blocking solution' containing 0.2-1% Triton-X-100 were then added for 1 h at RT. Cells were washed twice with PBS and incubated with secondary antibodies and DAPI (62248, Thermo Fisher Scientific) in 'blocking solution' for 1h at RT. Cells were again washed twice with PBS and covered with ProLong Gold Antifade Mountant (P36934, Thermo Fisher Scientific) to prevent photobleaching before storage at 4°C.

TA muscle sections on microscope slides (J1800AMNZ, EpreDia) were fixed with 4% Paraformaldehyde (11400580, Fisher Scientific) in PBS for 5min at RT and washed twice with PBS. 'Blocking solution' consisting of PBS supplemented with BSA (Cat. # A1391, AppliChem) and 0.2% Triton X-100 (Cat. #9002-93-1, Sigma-Aldrich) was added for 15min at RT. Primary antibodies diluted in 'blocking solution' were added for 1h at RT, after which the sections were washed twice with PBS and incubated for 30min with a secondary antibody and DAPI (62248, Thermo Fisher Scientific) diluted in 'blocking solution. Sections were washed twice with PBS and covered with a few drops of ProLong Glass Antifade Mountant (P36980, Thermo Fisher Scientific) and a coverslip and stored at 4°C.

The following primary antibodies were used in this study: SOX2 Polyclonal Antibody (48-1400, Thermo Fisher Scientific), rat anti-mouse NANOG conjugated eFluor 660 (50576182, Thermo Fisher Scientific), OCT4 monoclonal antibody (9B7) (MA1-104, Thermo Fisher Scientific) and anti-Dystrophin antibody (Cat.#ab15277, Abcam), all diluted 1:200, Myosin Heavy Chain antibody (MAB4470, R&D Systems) diluted 1:500, anti-Laminin antibody (ab11575) (Cat.#ab11575, Abcam) and Human/Mouse/Rat/Chicken anti-PAX7 antibody (MAB1675, R&D Systems, 5µg/ml), both diluted 1:100. Secondary antibodies used were: goat anti-rabbit IgG 488 (A11008, Thermo Fisher Scientific), goat anti-mouse IgG1 488 488 (A21121, Thermo Fisher Scientific), goat anti-mouse IgG2b 647 (A21242, Thermo Fisher Scientific), goat anti-Mouse IgG1 647 (A-21240, Thermo Fisher Scientific), anti-rabbit IgG 647 (A31573, Thermo Fisher Scientific), anti-mouse 488 (A-21141, Thermo Fisher Scientific). All secondary antibodies were diluted 1:400.

### **Satellite cell isolation and FACS**

A Sony SH800S Cell Sorter was utilized for flow cytometry analysis and cell sorting for satellite cell isolation using Pax7-nGFP reporter, cell surface markers and for the purification of GFP positive myoblasts. For satellite cell isolation, skeletal muscles were harvested, minced and centrifuged in PBS at 350g for 3 min. The tissue pellet was then resuspended in digestion solution containing 2mg/ml Collagenase Type 2 (17101015, Thermo Fisher Scientific) in DMEM (41966029, Thermo Fisher Scientific) and incubated for 90min. This was followed by a 30min incubation step in a digestion solution consisting of 14ml F-10 (Thermo Fisher Scientific, 22390025) supplemented with 10% horse serum (Thermo Fisher Scientific, 16050122), 1ml of 0.2% Collagenase Type II (Thermo Fisher Scientific, 17101015) and 2.5ml of 0.4% Dispase II (Thermo Fisher Scientific, 17105041). Both incubation steps were performed in a shaking 37°C water bath. An 18 gauge needle syringe was then used to dislodge the cells from the fibers, followed by filtering the cells with a 100µm, 70µm and either 30µm or 40µm cell strainers. The cell pellet was resuspended in 'FACS buffer' consisting of PBS and 2% FBS (10270106, Thermo Fisher Scientific) and kept on ice until FACS. Satellite cells were FACS-purified using either Pax7-



nGFP reporter or the following combinations of cell surface markers: APC anti-mouse Ly-6A/E (Sca-1) Antibody (108111, BioLegend), mouse Integrin alpha 7 Alexa Fluor 750-conjugated Antibody (FAB3518S, R&D Systems), APC anti-mouse CD45 Antibody (103111, BioLegend), APC anti-mouse CD31 Antibody (102409, BioLegend). In each FACS experiment, DAPI (62248, Thermo Fisher Scientific) was used to exclude dead cells. For GFP based sorting, GFP positive cells were sorted using the EGFP channel. For surface marker-based sorting, all SCA1<sup>+</sup>, CD45<sup>+</sup> and/or CD31<sup>+</sup> cells were excluded using APC channel. ITGA7<sup>+</sup> were sorted from the remaining population and analyzed for GFP expression.

### **RNA sequencing**

RNA sequencing was performed at the FGCZ on an Illumina NovaSeq instrument and library was prepared according to Illumina Truseq mRNA protocol. The sequencing reads were analyzed using the SUSHI framework<sup>236,237</sup> developed at the FGCZ. After the quality control (adapter and low-quality base trimming) with fastp v0.20<sup>238</sup>, raw reads were pseudo-aligned against the reference mouse genome assembly GRCm39 and gene expression level (GENCODE release 26) was quantified using Kallisto v0.46.1<sup>289</sup>. Genes were considered to be detected if they had at least 10 counts in 50% of the samples. Pax7-nGFP MEFs and Pax7-nGFP<sup>+</sup> myoblasts samples from the GEO data set GSE169053 were re-processed in the same way<sup>279</sup>. TPM (Transcripts per Million mapped reads) was used as the unit for normalized gene expression.

Figure S1

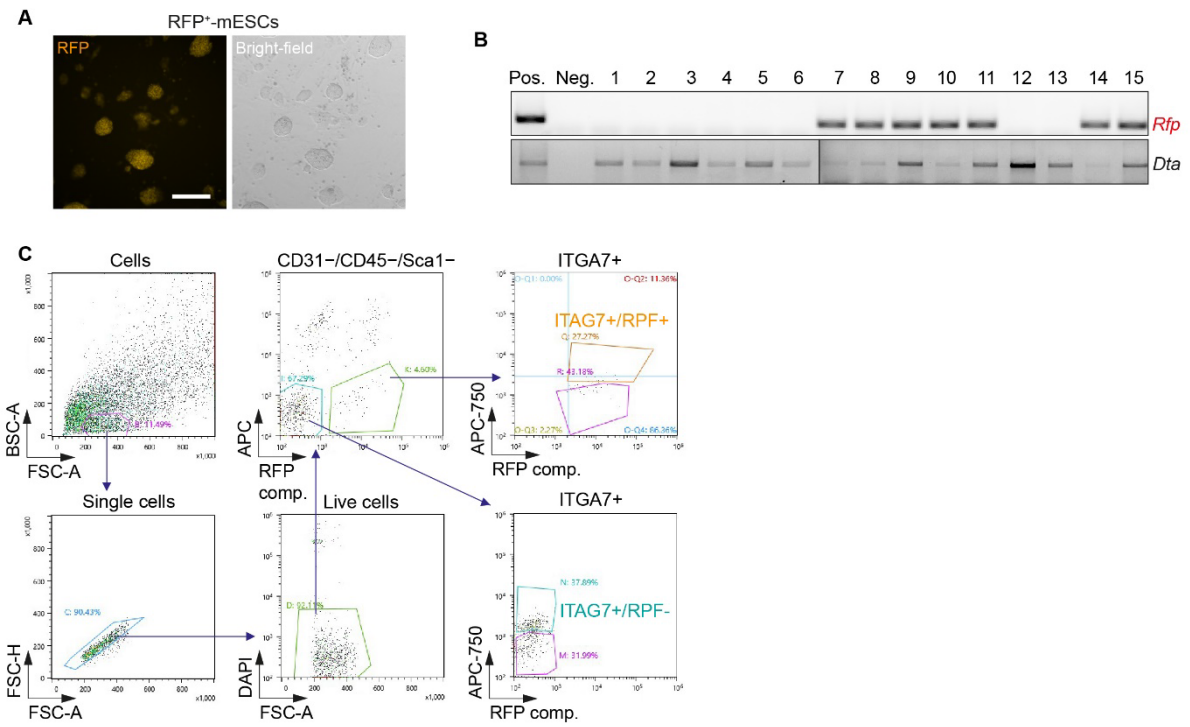


**Fig. S1.**

**(A)** Microscopy images of RFP<sup>+</sup>-mESCs. Scalebar, 100μm. **(B)** PCR of DNA extracted from ear clips of non-chimeric and chimeric mice for the *Rfp* transgene and *Rosa26-LSL-DTA* allele. **(C)** FACS plots displaying satellite cell sorting strategy.

**Figure S2**

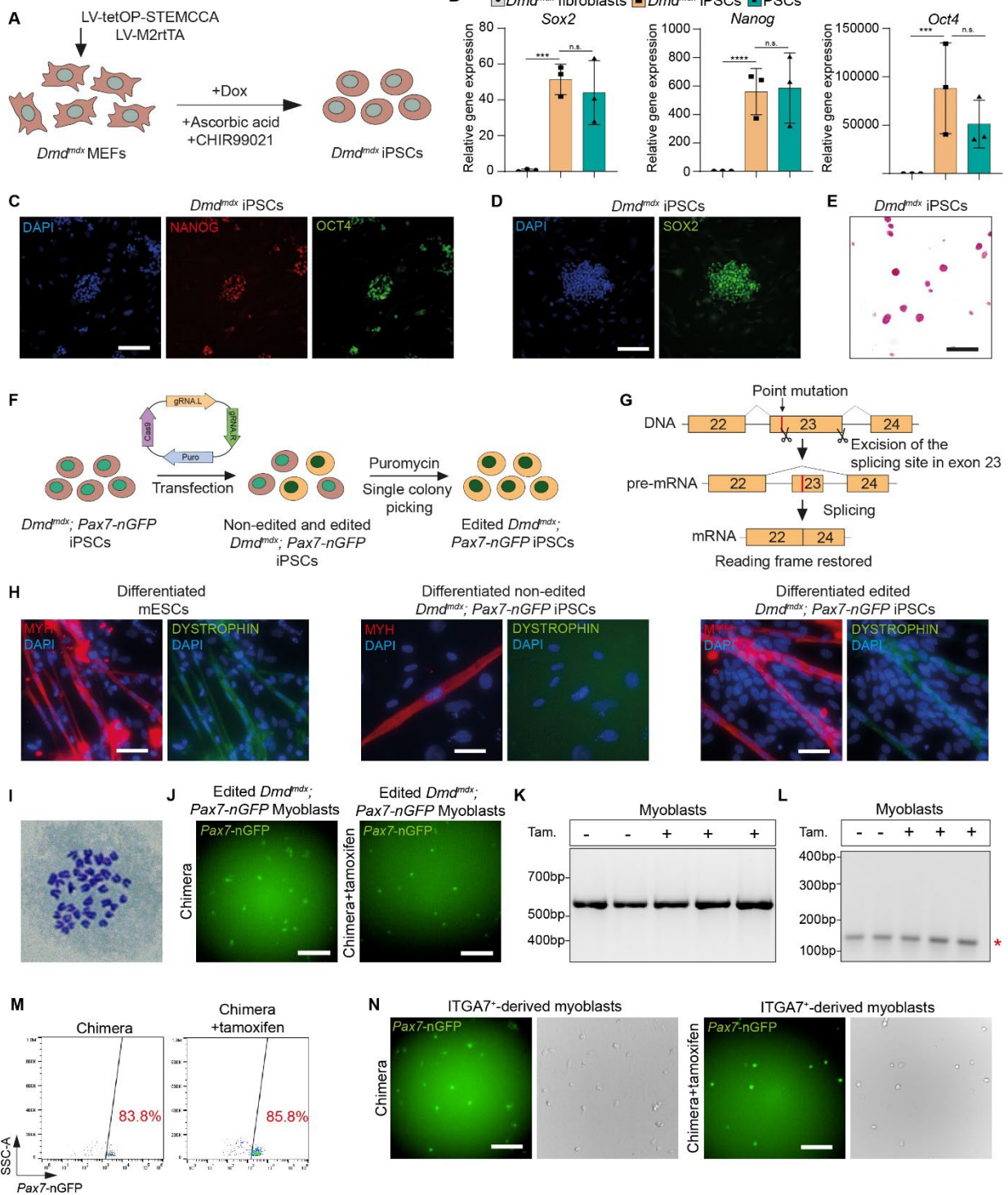


**Fig. S2.**

(A) Schematic overview. MEFs, mouse embryonic fibroblasts; dox, doxycycline. (B) Quantitative real-time PCR for the indicated genes. N=3 different lines, error bars denote SD. Statistical analysis was performed with delta Ct values using ordinary one-way ANOVA. \*\*\*p ≤ 0.001, \*\*\*\*p ≤ 0.0001, n.s., not significant. (C) Immunofluorescence images for the indicated proteins. Scalebar, 100µm. (D) *Dmd<sup>mdx</sup>* iPSCs showing expression of SOX2. Scalebar, 100µm. (E) Alkaline phosphatase staining in *Dmd<sup>mdx</sup>* iPSCs. Scalebar, 500µm. (F) Overview of gene editing of *Dmd<sup>mdx</sup>; Pax7-nGFP* iPSCs. (G) Strategy showing CRISPR/Cas9 induced gene editing of exon 23 in the dystrophin gene. (H) Immunofluorescence staining for DYSTROPHIN in the indicated samples. Scalebar, 50µm. (I) Karyotype of edited *Dmd<sup>mdx</sup>; Pax7-nGFP* iPSCs. (J) Edited *Dmd<sup>mdx</sup>; Pax7-nGFP*

*nGFP* myoblasts FACS-purified from muscle tissue of the indicated chimeras. Scalebar, 100 $\mu$ m. **(K)** PCR gel showing genotyping of the *Pax7-nGFP* allele in chimera-derived myoblasts that have been treated with or without tamoxifen (tam). **(L)** PCR for *Dystrophin* using DNA of edited *Dmd<sup>mdx</sup>*; *Pax7-nGFP* myoblasts that have been FACS-purified from muscle tissue of tamoxifen-injected chimeras (+) or non-injected control (-). Only the edited shorter 146bp (red asterisk) product was detected in both groups. **(M)** Representative flow cytometry analysis showing the *Pax7-nGFP*<sup>+</sup> / ITGA<sup>+</sup> satellite cells. **(N)** *Pax7-nGFP* expression in myoblasts that have been derived from ITGA<sup>+</sup>satellite cells of the indicated animals and conditions. Scalebar, 100 $\mu$ m.

**Figure S3**

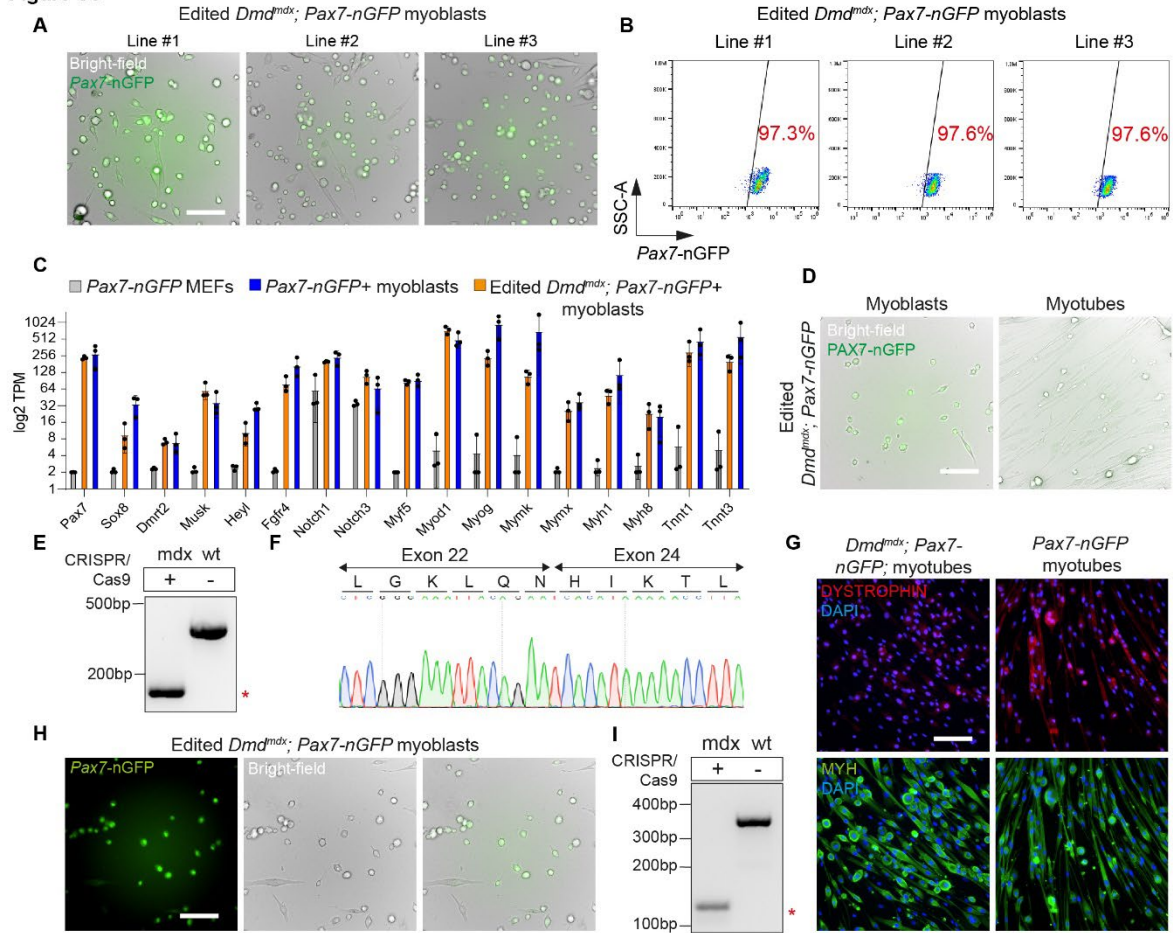


**Fig. S3.**

**(A)** Bright-field and microscopy images of myoblast lines isolated from three different intraspecies chimeras. Scalebar, 100µm. **(B)** Flow cytometry analysis for Pax7-nGFP in the indicated myoblasts lines. **(C)** Bar plots showing the log<sub>2</sub> normalized expression of the indicated genes for edited *Dmd<sup>mdx</sup>*; *Pax7-nGFP* myoblasts compared to *Pax7-nGFP* myoblasts and MEFs. N=3 cell lines per group. TPM, Transcripts per kilobase Million, MEFs, mouse embryonic fibroblasts. **(D)** Representative bright-field images showing edited *Dmd<sup>mdx</sup>*; *Pax7-nGFP* myoblasts and myotubes. Note that GFP is downregulated upon differentiation. Scalebar, 100µm. **(E)** PCR for *Dystrophin* amplified using cDNA of edited *Dmd<sup>mdx</sup>*; *Pax7-nGFP* myotubes and wt myotubes. Non-edited and edited *Dystrophin* are 396bp and 183bp (red asterisk), respectively. **(F)** DNA sequencing of (E) showing successful ligation of exon 22 and exon 24. **(G)** Immunofluorescence for dystrophin in the indicated cell lines. Scalebar, 100µm. **(H)** Bright-field and microscopy images of edited *Dmd<sup>mdx</sup>*; *Pax7-nGFP* myoblasts prior to transplantation. Scale bar, 100µm. **(I)** PCR for *Dystrophin* in *Dmd<sup>mdx</sup>*; *Pax7-nGFP* myoblasts showing only the edited shorter PCR product (red asterisk) vs. control.

**Figure S4**

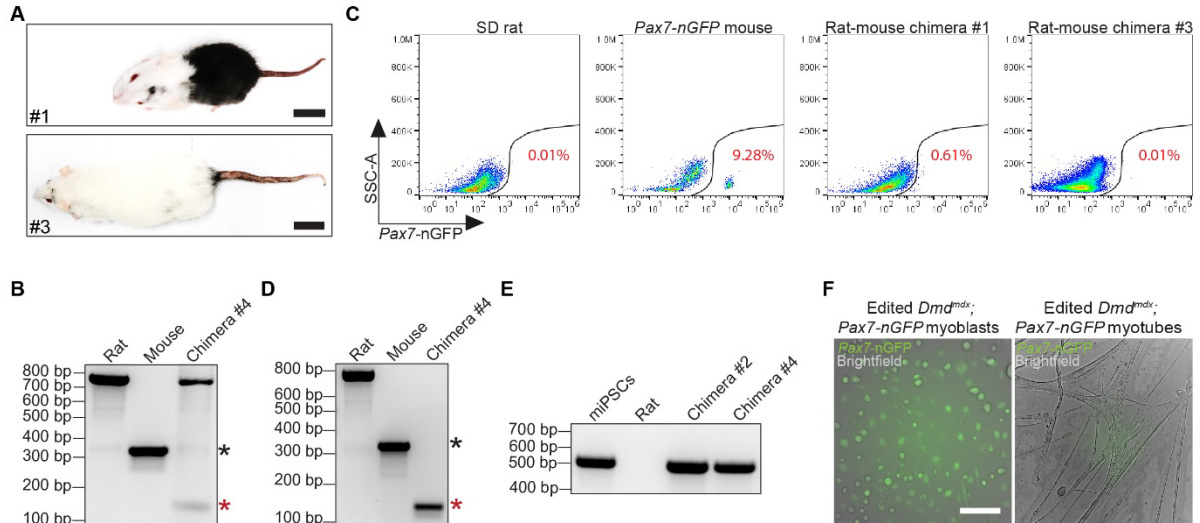


**Fig. S4.**

**(A)** Photos of rat-mouse chimeras #1 and #3 at 5 (top, chimera #1) and 17 (bottom, chimera #3) weeks of age. Scale bar, 3.5cm. **(B)** PCR for rat and mouse dystrophin from muscle lysates of the indicated animals. Black and red asterisks denote unedited (340bp) and edited (146bp) murine dystrophin, respectively. **(C)** Flow cytometry analysis of GFP expression in whole-body skeletal muscles isolated from the indicated animals. **(D)** PCR for rat and mouse dystrophin in myoblasts isolated from the indicated animals. Black and red asterisks denote unedited and edited murine dystrophin. **(E)** PCR for *Pax7-nGFP* transgene in myoblasts isolated from chimeras #2 and #4 and controls. **(F)** *Dmd<sup>mdx</sup>*; *Pax7-nGFP* myoblasts and derivative myotubes. Scale bar, 100 $\mu$ m. Bright-field and LUT settings differed between both images, GFP LUT settings are the same.

## Chapter 5. Discussion

---

Blastocyst complementation is a powerful tool to create cells, tissues and even entire organs derived exclusively from donor-derived cells via injection of PSCs into organogenesis disabled blastocysts. Recent studies have reported on the generation of kidney, forebrain, lung, thymus and pancreas, amongst others, in intra- and interspecies chimeras<sup>20,39,40,42,138</sup>. This technology holds promise not only for generation of animal gametes for species conservation efforts, but also for the generation of therapeutically competent cells or tissues.

With the studies presented here, we set out to further investigate the potential of blastocyst complementation to generate only rat gametes in rat-to-mouse chimeras as well as the generation of gene-edited mouse satellite cells in mouse-mouse or mouse-to-rat chimeras.

### 5.1 Exclusive generation of rat spermatozoa in sterile mice

Generation of gametes for production of transgenic animals or for species protection is a salient question and carries many important implications. Not only does it allow for numerous genetic alterations of PSCs for the generation of transgenic animals, but it also holds promise to generate spermatozoa of endangered species for conservation efforts<sup>145,290</sup>.

Recently, generation of rat spermatozoa in rat-to-mouse chimeras has been reported<sup>139,140</sup>. However, the chimeric testes consisted of rat and mouse germ cells, and rat germ cells had to be fluorescently labelled for identification and separation from the mouse spermatozoa, an observation which could interfere with the intended use of the inter-species chimera derived rat sperm<sup>139,140</sup>. To circumvent this limitation, in chapter 3 we set out to generate rat-to-mouse chimeras carrying solely donor rat ESC-derived spermatozoa via blastocyst complementation.

By using host blastocysts carrying a mutation in the *Tsc22d3* gene, which renders all non-complemented males sterile, we generated chimeras via injection of mouse ESCs or iPSCs. These intra-species chimeras showed restored testicular morphology, which was confirmed by H&E staining and by the presence of the spermatogonia marker VASA, and exhibited normal testicular weight. The donor cells successfully overcame the meiotic arrest of the host animals, as shown by scRNA-seq of the cauda epididymis, and were



able to sire offspring via natural mating with transmission of the donor cells' transgenes. These findings were in accordance with previous reports<sup>132,134</sup>.

When we injected male rat ESCs into the mutated blastocyst, it resulted in both male and female interspecies mouse-rat chimeras. These chimeras were overall healthy and were able to grow to adulthood. Interestingly, we observed that the generation of interspecies mouse-rat chimeras led to more male than female chimeras. It is known that contribution of XY PSCs can, when injected into an XX blastocyst, push the sex of the animal towards a male phenotype, and the resulting animals can sire offspring, likely due to *Sox9* expression<sup>291-293</sup>. To date, there are no reports about this effect in an interspecies environment, but sex determination both in mice and rats relies on *Sry*, the sex determining region of the Y-Chromosome<sup>294</sup>. This suggests a potential of rat XY PSCs to influence the chimera's sex towards a male phenotype upon contribution to the developing gonads<sup>291,292</sup>.

When analyzing the testes of interspecies chimeras, several of them confirmed our previous intraspecies chimera findings in terms of morphology and weight. The donor rESCs were also able to contribute to spermatogenesis, as the chimeras carried sperm with rat morphology. Further examination of the haploid portion of the cells isolated from the cauda confirmed that all spermatozoa were derived from the donor rESCs.

To better characterize the extent of rat spermatogenesis in a sterile mouse host, we subjected testicular cells to scRNA-seq. However, since the chimeric testes also contained somatic cells from the mouse host, which were not affected by the *Tsc22d3* mutation, we had to generate a custom chimeric reference genome, able to differentiate between transcripts of the two species. When the chimeric sample was mapped against the genome, the mouse cell clusters consisted of somatic cell populations, for example immune and Leydig cells, but surprisingly also formed a cluster termed "Germ cells". This cluster was characterized by the expression of genes indicative of late spermatogonia and early spermatocytes, such as *Dazl*, *Sycp1* and *Sycp2*. Previous reports have described early cell death of the germ cell lineage in *Tsc22d3*-KO animals<sup>135</sup>. Hence, these cells presumably represent a minor mouse germ cell population still surviving, yet, as shown by a lack of later stage spermatocytes, are unable to undergo spermatogenesis. Interestingly, we did not record any somatic cell types of rat origin. Several reasons could account for this; since there is no niche available in somatic tissues, the donor cells are at a competitive disadvantage and cannot contribute to these lineages<sup>135,137</sup>. Alternatively, somatic cells are less abundant in testes than germ cells, and potentially



inefficient isolation of somatic cells from the tissue could affect fidelity, leading to a lack of rat somatic cells during library preparation. Interestingly, we also detected cell clusters consisting of rat cells expressing germ cell markers, yet which did not participate in a pseudotime analysis. We could not conclusively determine the reason for this observation, and if these could be cells not progressing through spermatogenesis due to strict quality checkpoints, as almost 75% of the male germ cells undergo cell death<sup>295</sup>. Analysis of wildtype mouse or rat testes would elucidate whether this is observed more commonly, or whether it is specific to interspecies chimeric testes. Importantly however, the expression of markers for round and elongated spermatids, such as *Dydc1* and *Tnp2*, had similar expression patterns in the rat germ cell fraction of the chimeric testis, and wild-type rats. These findings showed that rat germ cells can undergo spermatogenesis in a xenogeneic environment, however, future experiments might clarify the contribution to the somatic cell population, especially also because we did not capture *Sox9*<sup>+</sup> Sertoli cells. Since this data is based on one chimera, analysis of future chimeras might show contribution to the somatic cell niches. It is important to note that we most likely did not capture any mature spermatozoa. Due to their low RNA content and cell morphology, they are a challenging cell type to perform scRNA-seq on<sup>296</sup>. We did attempt to analyze specifically spermatozoa via scRNA-seq, however, were unsuccessful in establishing the technique, especially given the low sample size available from chimeras.

Since mouse-rat chimeras and female rats cannot be naturally mated, we performed Testicular Sperm Extraction (TESE-) ICSI to evaluate the spermatozoa's fertilization capability. While we observed germ cells in the majority of analyzed male chimeras, which shows a successful complementation in a niche that is only available after birth, not all chimeras developed mature spermatozoa or sufficient numbers to be used for (TESE-) ICSI. Mechanistically, this might be explained by the lack of a niche during development. As a consequence, the injected donor cells face competition with the host's own cells, reducing the probability of a sufficient number of donor cells to contribute to the germ cell lineage. This limitation could be circumvented by interfering with earlier stages of gametogenesis of the host blastocysts, which has previously been shown to be achieved by the introduction of mutations in genes involved in gametogenesis<sup>62,65-67,120,128,129</sup>. Additionally, this would also increase the chances of contribution to the germ line, when only donor PSCs with lower quality are available. Our efforts to establish (TESE-) ICSI for chimera derived rat spermatozoa, which have been frozen-thawed, resulted in the *in vitro* generation of blastocysts. However, after embryo

transfer of fertilized oocytes into surrogate females to assess *in vivo* development, we were not able to detect live births from these trials.

This might be explained by the observation that rat sperm is highly susceptible to freeze-thaw damage, impacting on sperm quality<sup>297,298</sup>. However, this contrasts with previous findings, where TE buffer as freezing medium for wildtype rat spermatozoa intended for ICSI has been shown to be sufficient, and in fact we also successfully performed ICSI with wildtype rat sperm frozen in this way<sup>299</sup>. It is unclear whether rat spermatozoa from an inter-species chimera behave in the same manner. But since rat spermatozoa do not undergo complete maturation in a xenogeneic environment, they may be more susceptible to freezing damage than fully matured spermatozoa<sup>140</sup>. Concluding from that, performing (TESE-) ICSI with freshly isolated spermatozoa might be a superior approach, as has been shown previously<sup>139</sup>. It has been previously reported that round spermatids, a post-meiotic germ cell population preceding spermiogenesis into mature spermatozoa, can give rise to offspring even after freeze-thawing and upon Round Spermatid Injection (ROSI) into rat oocytes<sup>300</sup>. This technique could potentially be employed to store chimera-derived rat germ cells long term and utilize it successfully to generate animals<sup>300</sup>.

In recent years, significant effort has been put towards *in vitro* differentiation from mouse and rat PSCs into male gametes<sup>84,108,112</sup>. Nonetheless, many hurdles remain that yet have to be overcome. For instance, it took over a decade to adapt the findings from the mouse model to another common research model, the rat<sup>108,112</sup>. Currently, all the protocols to generate spermatids capable of fertilization have a major caveat, namely the requirement of either host testes for *in vivo* maturation, or dissociated testes cells to support the development *in vitro*<sup>84,301</sup>. This poses a drawback, since both methods rely on the availability of either suitable allogeneic hosts, or the species' testes. Utilizing xenogeneic testes for transplantations of SSCs did sustain the spermatogonia in the recipient testes, however the resulting spermatozoa exhibited abnormalities, and apart from rat-to-mouse SSC transplantations, no offspring was reported<sup>119,121,125,126,302,303</sup>. This renders *in vitro* gametogenesis a rather slow and inefficient way, which could benefit from ways to directly reprogram somatic cells into PGCLCs. Testes do not only consist of germ cells, but also other cells crucial for the maintenance of germ cells and their subsequent spermatogenesis, such as Sertoli or Leydig cells. Generation of these cells *in vitro*, either from PSCs or somatic cells, might aid in the *in vitro* maturation of PGCLCs, especially for species from which testicular cells or PGCLC/SSC transplantation recipients are not

available. This may help to alleviate the need for embryonic or adult testes for co-culture or aggregation<sup>304-308</sup>.

Recently, Kobayashi and colleagues circumvented xenogeneic *in vitro* gametogenesis by the generation of only mouse derived functional round spermatids, and mouse derived spermatozoa in a *Prdm14*-KO rat host via blastocyst complementation with mouse PSCs. In line with our findings, they also did not observe normal motility in spermatozoa<sup>47,141</sup>. Contrasting with our attempts utilizing spermatozoa, by performing ROSI they were able to generate live mouse offspring<sup>141</sup>. Their study showed feasibility of exclusive generation of xenogeneic germ cells via interspecies chimerism.

For germline chimera-formation it might be warranted to generate mutations not only affecting the germ cells directly, but also niches for the formation of fetal and adult Leydig cells, whose main function is to secrete testosterone, or Sertoli cells, which are commonly described as the 'nurse' cell for spermatogenesis and are reliant on *Sox9* expression<sup>78,81,85,309,310</sup>. Spermatogenesis in mice takes 35d, in comparison to the rat's 54d, and even in mice engrafted with rat spermatogonia, the rat cells keep their distinct cell cycle<sup>311,312</sup>. Thus, gene expression and timing of rat spermatogenesis differs from mouse, potentially causing defects in chimera derived spermatozoa, a hypothesis underscored by severely reduced, or even a complete lack of motility in spermatozoa as observed by us and others<sup>47,141,311</sup>. It could be hypothesized that the formation of mostly donor cell derived testes, potentially providing species-matched hormones and their respective levels and timing could improve the conditions for spermatogenesis and maturation of the spermatozoa in a xenogeneic host. However, new germline- or testicular KO models can only carry mutations in genes not crucial for the formation or maintenance extraembryonic tissues, as otherwise such mutations could not be compensated for by the injected donor PSCs, potentially compromising the embryos development and survival.

In future experiments, chimera derived spermatozoa could be further analyzed for defects present in DNA or epigenetic profiles in order to elucidate to what extent development of xenogeneic germ cells *in vivo* is affected. Also, since we observed more male than female chimeras, it would be interesting to genotype chimeras exhibiting a male phenotype for the presence of female genes, and if there's a correlation between XX/XY males, presence of germ cells and maturation status of the sperm.

Generation of germ cells of species other than rat or mouse via inter-species blastocyst complementation could prove especially promising in respect to endangered

species, with the caveat that PSCs capable of contributing to the germline would need to be generated<sup>142,143,146,313</sup>. Especially regarding the aspect of species conservation, or even de-extinction, male germ cells do not suffice, as the female counterpart in the form of the oocyte is also needed. For this, appropriate models for female germline complementation need to be found, or existing ones evaluated<sup>141</sup>. Currently the problem remains that males can produce several millions of sperm per gram of testis tissue per day, and several methods are available to retrieve sperm from a live male without euthanasia, allowing for a 'near unlimited' amount of spermatozoa available. In contrast, far fewer oocytes can be harvested from a female, making this an even more difficult undertaking for rare species<sup>314-318</sup>. Additionally, artificial reproductive techniques will need to be established to successfully fertilize the oocytes and ensure survival of the embryos. Subsequently, strict controls will have to be established to ensure the health of these animals over several generations, and that no undue mutations have been introduced during interspecies chimeric gametogenesis.

Our study was the first to show rat-to-mouse blastocyst complementation in the germline. While we successfully generated rat spermatozoa in chimeras, they did not allow for complete embryogenesis after transplantation into foster mothers. However, we propose a proof-of-principle, which might serve as a starting point to improve interspecies gamete formation in chimeras.

## 5.2 Interspecies generation of functional muscle stem cells

Generation of therapeutically competent satellite cells holds great promise for the treatment of muscular dystrophies, especially if autologous and gene-edited cells could be transplanted back into patients.

While a number of approaches to generate myogenic cells exist, satellite cells still exhibit the largest propensity to contribute to muscle upon transplantation<sup>204</sup>. However, only small numbers can be isolated from donors, and *in vitro* expansion of satellite cells hampers their potential applicability<sup>204</sup>. To generate large numbers of satellite cells *in vivo*, in chapter 4 we generated iPSCs from a DMD mouse model and gene-corrected the DMD mutation using CRISPR/Cas9 gene editing to utilize the iPSCs for the formation of satellite cells in intra- and inter-species chimeras. We injected these gene-edited DMD iPSCs into *Pax7-CReERT2: R26-LSL-DTA* mouse blastocysts, allowing for selectively ablating host *Pax7* expressing cells upon tamoxifen injections. To our surprise, when we compared the fraction of iPSC derived satellite cells in ablated versus non-ablated

chimeras, as based on the *Pax7*-nGFP reporter present in injected iPSCs, no significant difference was observed. This confirmed robust contribution of donor cells to the satellite cell niche, however, precluded us from observing potential effects in *Pax7* ablated animals. It would be interesting to compare other iPSC clones, and whether they also preferentially contribute to the satellite cell niche. Other ways to unequivocally establish whether the cells expressing *Pax7*-nGFP are of donor origin and are satellite cells are scRNA-seq or spatial transcriptomics, a novel technique allowing for single cell assessment of the transplanted cells in muscle sections<sup>319</sup>. It could be hypothesized that the injected iPSCs preferentially contributed to the myotomes, the muscle's anlage during embryogenesis, and as a result the majority of the myogenic cells would be iPSC derived<sup>320-322</sup>.

We have previously generated a rat *Pax7*-KO (*rPax7*-KO) model (Supplemental Figure 1). The homozygous animals resulting from heterozygous matings showed severely inhibited growth post-partum compared to heterozygous or wildtype littermates, and only survived a few days after birth. We therefore surmised that this model would be suitable to generate inter-species PSC derived satellite cells. Upon performing blastocyst injections with blastocysts from *rPax7*+/- matings, we obtained *rPax7*-KO pups, but none were complemented. However, we did obtain mouse-to-rat inter-species chimeras on a *rPax7*+/- background, several harboring donor iPSC-derived satellite cells which we could culture and characterize *in vitro*, confirming contribution of gene-corrected iPSCs to the satellite cell niche. However, while our approach confirmed feasibility, blastocyst complementation would likely increase the number of satellite cells generated. Transplantation of *in vitro* expanded myoblasts into DMD mouse model muscles showed dystrophin expression *in vivo*. This was in line with previous reports about expanded myoblasts being able to contribute to muscle upon transplantation, but less efficiently than freshly isolated satellite cells<sup>204</sup>. It was also shown that autologous *in vitro* expanded myoblasts were able to largely restore functionality of the urinary sphincter in dogs<sup>323</sup>. Similarly, transplantation of autologous *in vitro* expanded myoblasts into the anal sphincter showed clinical improvements in humans suffering from fecal incontinence, hinting towards therapeutical applications for myoblasts<sup>324</sup>. We also attempted to isolate and directly transplant freshly isolated satellite cells from one interspecies chimera, however, we did not observe dystrophin restoration only in one recipient *Tibialis anterior*, requiring further experimental work.

We also wanted to confirm not only dystrophin expression, since this might only confer short-term results in patients, but also whether the myoblasts contribute to the satellite cell niche. To this end, in an experiment performed after submission of the study manuscript, we FACS purified re-transplanted myoblasts from inter-species chimeras and observed presence of the *Pax7-nGFP* reporter, however this could also be a population of *Pax7-nGFP* expressing myoblasts surviving outside the niche after transplantation (Supplemental Figure 2)<sup>219</sup>. To unequivocally assess contribution of transplanted cells to the satellite cell niche, re-injury of the muscle using cardiotoxin, a snake venom peptide able to destroy myofibers, but leaving satellite cells largely unaffected, would prove superior<sup>325,326</sup>. Serial injury would elucidate whether the contribution of the myoblasts was only to dystrophin expression, or also to the satellite cell niche<sup>326</sup>.

In order to harness the benefits of blastocyst complementation, improvements to the number of blastocysts harboring a *Pax7*-KO should be increased. Since not all injected embryos give rise to chimeras, means of generating *rPax7*-KO embryos other than *rPax7*<sup>+/−</sup> matings might be preferable. For example, pronuclear injections of gRNAs targeting *rPax7* and subsequent embryo culture to the blastocyst stage would ensure that the majority of blastocysts injected are *rPax7*-KO<sup>233,327</sup>. Another salient approach is Somatic Cell Nuclear Transfer (SCNT, colloquially known as ‘cloning’), potentially concomitantly also targeting other myogenic genes to improve donor derived satellite cell or myofiber formation<sup>53</sup>. Combining germ cell blastocyst complementation with this project, *rPax7*-KO PSCs could be injected into rat *PRDM14*-KO blastocysts to exclusively generate *rPax7*-KO spermatozoa in intraspecies chimeras. With these, it would be possible to generate 50% of *rPax7*-KO blastocysts upon matings with heterozygous *rPax7*-KO females. While *Pax7* is crucial for the survival of satellite cells post-partum, a *Pax7*-KO can be compensated to some extent during embryonic development by expression of *Pax3*<sup>157</sup>. Thus, a double Knockout for *Pax3* and *Pax7* in host blastocysts could improve donor cell contribution to the satellite cell pool, and ensure that no competition for the niche is present<sup>328</sup>. It has been reported that a double *Pax3/Pax7*-KO leads to the death of the embryo at mid-gestation<sup>328</sup>. Together with our observation of, so far, no chimeric *rPax7*<sup>-/-</sup> pups having been born, and reports about high chimerism leading to increased embryonic lethality, stringent pilot experiments will be necessary to assess whether double knockouts of *Pax3/Pax7* or other myogenic genes will prevent normal development of the embryo<sup>53,58,59,328</sup>. Alternatively, and similar to the mouse model, generation of a rat *Pax7-CReERT2: R26-LSL-DTA* model would allow for ablation

of satellite post-partum, reducing the risk of embryonic lethality. Additionally, since high chimerism influences the chimera's size and weight, as observed by us and others, long term survival of inter-species chimeras with muscle entirely derived from donor cells on a *Pax7*-KO background remains to be assessed<sup>139,59</sup>. Related to our chapter 3, *Pax7* has been proposed as SSC marker in testes, however a conditional testis *Pax7*-KO did not affect fertility<sup>329</sup>.

In recent years, a number of alternative ways to generate myogenic cells have been devised<sup>193,195-200,202</sup>. For example, overexpression of *MyoD* in mouse embryonic fibroblasts in concert with small molecules treatment directly reprogrammed the cells into iMPCs, containing mononucleated *Pax7*<sup>+</sup> cells<sup>202</sup>. Other promising approaches are harnessing the PSCs amenability by inducing myogenic cells *in vitro* from PSCs via overexpression of myogenic genes or treatment with growth factors and small molecules<sup>193,195-197</sup>. The ability of PSCs to form teratomas *in vivo* can also be capitalized on to generate myogenic cells exhibiting a prominent capacity to expand *in vitro*, yet still engraft into recipient muscles efficiently<sup>198-200</sup>.

Method	Benefits	Drawbacks
<i>In vitro</i> differentiated	+ No need for chimera generation + More rapid than other methods + No risk of zoonoses	- Risk of teratomas - More resembling a late <i>in vivo</i> embryonic development stage - Form heterogeneous population - Limited <i>in vitro</i> expansion potential
Teratoma derived	+ Can be expanded to large numbers <i>in vitro</i> + Maintain robust muscle engraftment upon <i>in vitro</i> expansion + Clonally expandable	- Risk of teratomas - More myoblast like - Potential risk of zoonoses from host animal
iMPC derived	+ Can be expanded to large numbers <i>in vitro</i> + Fibroblasts easily available	- Form heterogeneous population - <i>MyoD</i> overexpression needed - Dependent on small molecules
<i>In vivo</i> chimera derived	+ Cells matured in correct niche <i>in vivo</i> + Isolation of multipotent cells, no risk of teratoma + Satellite cells show robust contribution to muscle upon transplantation + Large numbers of satellite cells generated	- Potential risk of zoonoses from host animal - Chimera with niche preferred - Time consuming - Limited <i>in vitro</i> expansion potential

**Table 1.** Comparison of iPSC, Teratoma, iMPC or *in vivo* chimera derived myogenic progenitor cells<sup>194,195,200,202,210,278,288,330,331</sup>

It will be crucial to compare our approach to generate satellite cells *in vivo* in chimeras with PSC derived myoblasts generated via *in vitro* differentiation or teratomas. The capacity to contribute to the satellite cell niche *in vivo* could be evaluated by employing spatial transcriptomics. Another, more important aspect in human applications is long-term safety after transplantations. It will also be necessary to exclude any contaminating PSCs potentially still present in *in vitro* or teratoma derived myogenic cell populations, in order to avoid the risk associated with PSCs and formation of undesired teratomas *in vivo*.

Regarding DMD patients lacking the dystrophin protein, re-expression of dystrophin in muscle could theoretically cause an immunoreaction against the protein, although rare revertant fibers spontaneously expressing dystrophin are present in many patients, and thus re-expressed dystrophin might not pose a problem<sup>207,208,332</sup>. However, in cases dystrophin is not recognized as self, immunosuppression might be needed<sup>210,332</sup>. Additionally, pre-treatment with the dystrophin specific drug Ataluren, which induces exon-skipping and read-through of the mutated *dystrophin* gene might serve to generate an immunity to dystrophin<sup>333</sup>.

Here, we report on the first study of generation of gene-corrected satellite cells in intra- and inter-species chimeras via blastocyst injections. We were able to show generation of gene-corrected, therapeutically competent satellite cells and myoblasts derived from iPSCs of a DMD mouse via intra-species and mouse-to-rat interspecies chimeras. These findings lay the foundation to further improve the system towards generation of exclusively donor derived satellite cells via blastocyst complementation, and in the future could help in tackling the challenges of currently incurable muscular dystrophies.

### 5.3 Blastocyst complementation in a human context

Globally, there is a dearth of donor organs available for transplantations. Cell therapy holds promise for treatment of a number of diseases, however, donor cells are not always available in sufficient numbers, and may further not be immunologically compatible with a recipient. One strategy proposed to help ameliorate these needs is blastocyst complementation with human PSCs (hPSCs). By generating patient derived iPSCs, and potentially gene-edit mutations, human-animal chimeras might provide a new pool of cells and organs fit for transplantation<sup>212</sup>.



Several key challenges still remain in adopting human-animal chimeras for clinical applications, spanning from biology to ethical considerations. Likely the biggest hurdle to overcome is to increase overall contribution of hPSCs to chimerism. While human-mouse chimerism has been shown to be in the low single digits, human-pig embryonic chimerism has been revealed to be more successful<sup>52,53,57,228</sup>. Several potential causes for this finding which affects all inter-species chimeras to some extent have been proposed. Some, such as evolutionary distance, could only be tackled by using different hosts such as non-human primates. However, this would come with a whole raft of new challenges and ethical considerations<sup>286</sup>. Other barriers are the developmental state of hPSCs and how it relates to the host blastocyst state or cell competition, in which less fit cells are being eliminated<sup>334</sup>. Recent reports demonstrated that a KO of the *Igf1r* gene allows the donor cells to 'outgrow' the host cells, resulting in enhanced tissue contribution<sup>230</sup>. Other means to increase survival of donor cells in a less-than-ideal exogenic environment are KO's in *TP53*, *Myd88* or *P65*, or alternatively ectopic overexpression of the anti-apoptotic gene *Bcl2*<sup>53,228,229</sup>. Of note, while limiting early elimination of hPSCs via genetic alterations might be feasible for proof-of-concept studies and devising solutions to increase chimerism at later stages, applicability for treatment of human diseases is questionable. If it cannot be shown that these mutations do not affect the tissue long term, transplantation of a potentially tumorigenic tissue poses too large of a health risk.

In order to generate human-animal chimeras, suitable hosts will be necessary. Currently, pigs are the most promising candidate, however, are not without their own challenges. For example, porcine endogenous retroviruses (PERVs) remain an issue, requiring animals which have been reared under PERV-free conditions, or animals in which all PERV-copies have been inactivated<sup>284,335</sup>. Since most organs do not consist of only one cell type, but often also contain endothelial or immune cells, animal models with multiple tissue specific mutations will be needed in order to avoid potentially fatal immune reactions<sup>284</sup>. Currently, it is not known to what extent autologous iPSC-derived organs might cause immune reactions upon transplantation, but it is expected to be mild as long as no contaminating host cells are present<sup>31</sup>. However, since satellite cells can be isolated as single cell population, there is hope of autologous cells not eliciting an immunoreaction.

At the same time, unlike the *Pdx1*-KO, organogenesis in many tissues cannot be disabled by mutation of a single gene, requiring further mutations to the host embryo. It is unclear how well a host embryo with a number of organogenesis disabling mutations

would develop, and to what extent complementation by hPSCs would rescue a potentially fatal phenotype.

Besides biological challenges, inter-species chimerism with human PSCs also raises ethical questions. Since donor PSCs can contribute to all the cells in a chimera, there are concerns of contribution of human donor PSCs to the brain or the gametes in chimeras, possibly resulting in some form of abrogated human consciousness<sup>212,285,336</sup>. Although, based on so far overall low contribution of human PSCs to inter-species chimeras, the risk is not very high, yet it is still warranted to eliminate chances of this occurring<sup>31</sup>. It is unclear to what extent, a likely minute, contribution of hPSCs to the chimera's brain would alter consciousness. Since the generation of rat-mouse chimeras is possible, behavioral tests comparing chimeras to non-chimeric animals of the host species might provide some insight. A recent publication described generation of hiPSC derived human cortical organoids (hCO)<sup>337</sup>. After transplantation of the hCOs into the somatosensory cortex of rat pups, the hCOs integrated into the brain, developed cell types not observed in *in vitro* hCOs and affected the rat's reward-seeking behavior. When they were evaluated for learning abilities, they did not differ from non-transplanted rats, indicating the hCOs did not affect cognition<sup>337</sup>. This experiment differs in that the hCOs were in a defined area of the brain, introduced post-partum, in contrast to potentially more heterogeneous contribution in a chimera's brain and integration into its circuitry. However, an altered consciousness or lack thereof would still be hard to prove. Still, as we propose to use a *Pax7*-KO niche in chapter 4, potentially in conjunction with a *Pax3*-KO, it is important to note that both genes are important for neural crest cells, and this could open a niche for human donor cells to populate<sup>157</sup>. Relating to gametes it could also be argued that chimeras will not be used for breeding purposes, and potential formation of human gametes thus is of less concern<sup>338</sup>. In theory, and similar to our first study (chapter 3), human gametes could be generated in chimeras to treat male infertility. Major concerns would arise, since spermatozoa could only be characterized *in vitro*, and predictions about their capacity to generate healthy children could not be made. In addition, the controversy about utilizing CRISPR/Cas9 to generate 'designer children' would be sure to also extend to human gametes from chimeras, deeming this approach socially unacceptable and of questionable scientific benefit, however, may further our understanding of male infertility and its treatment<sup>115,339,340</sup>. A way to circumvent both these concerns could be conceptus complementation<sup>341</sup>. Via careful injection of donor iPSCs or suitable myogenic progenitors into an empty myotome niche for the generation of muscle,

contribution to other tissues could be excluded<sup>53,341,342</sup>. Precluding formation of gametes or neuronal cells can also be achieved via mutations in genes specific for the respective cells, such as *Prdm14* for the germ cells or *Otx2* for neuronal cells<sup>285</sup>. Alternatively, instead of removing the ability to differentiate into specific tissues, the cells could also be pushed to adapt a desired fate. This concept has been shown with *Mixl1* overexpression, prompting donor PSCs to adopt an endodermal fate and significantly reduce contribution to non-endodermal tissues<sup>336</sup>. A further point of consideration is the public's opinion, which might not have the scientific background to assess the impact of human neuronal cells or gametes in chimeras, potentially leading to a public outcry and cessation of public funding<sup>343</sup>. Thus, thorough and unbiased information and ethical assessment will be necessary.

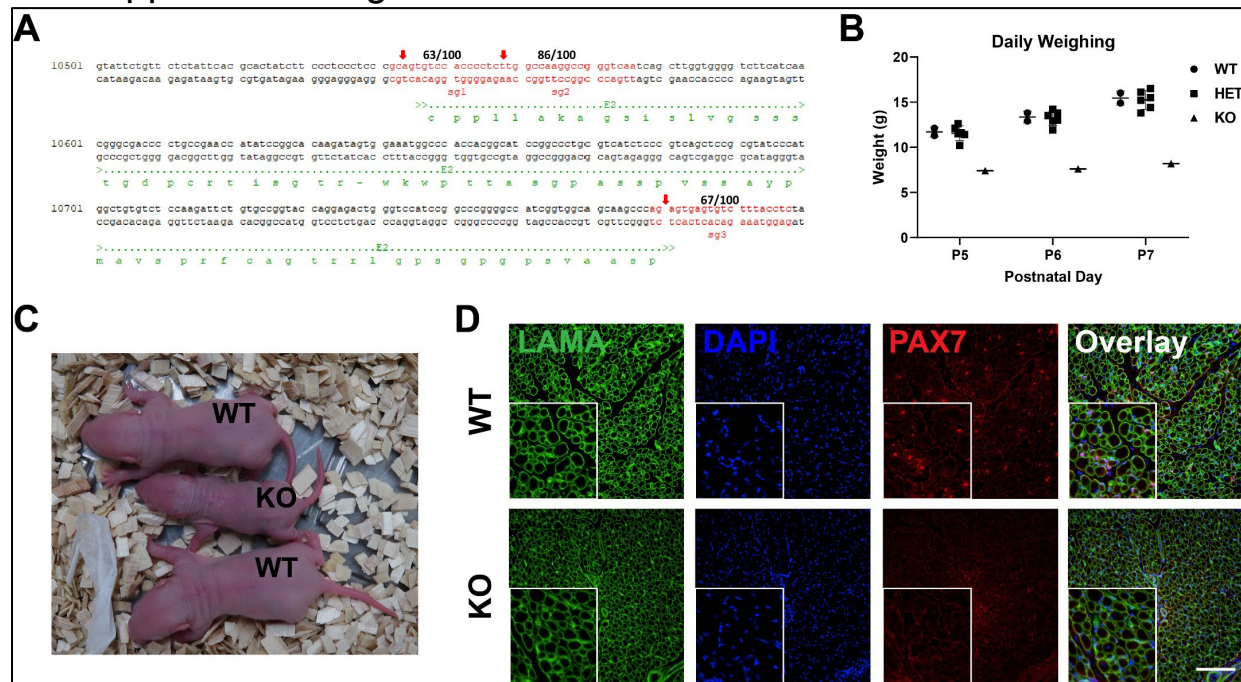
Once human organs have been generated via blastocyst complementation, stringent functionality and safety evaluations will have to be performed. Not only does survival of the chimera need to be assessed, potentially giving clues as to the organ's functionality, but also the organ's morphology, since the host mutations could affect the overall development and functionality of the organ. Harking back at our proposal to generate autologous satellite cells, safety and functionality of the cells would certainly be more facile to assess. Since single cells would be isolated, rather than an entire organ, immunogenicity would likely be mild, and preliminary characterization of the cells *in vitro* or *in vivo* in animals is possible. Additionally, and in contrast to other often transplanted organs such as the heart or liver, transplanted satellite cells are not crucial for immediate survival, allowing assessment without the risk of the patient's early demise due to graft failure.

Generation of autologous iPSCs is labor, time and cost intensive. Until this process will be made more efficient, it might be a more feasible approach to utilize allogeneic cells, rather than autologous cell approaches. This has led to the generation of iPSC cell banks to cover a large portion of the population with a few clinically relevant iPSC lines of a defined HLA haplotype, selected to reduce immune rejection<sup>344</sup>. As an alternative, hiPSCs with an HLA-A/B deletion in combination with an HLA class-II KO has been proposed to cover nearly 90% of the global population<sup>345</sup>. This would have the benefit of 'off-the-shelf' availability of iPSCs, and subsequently treatment times for patients could be reduced, as chimeras harboring specific organs or tissues could be kept for near constant availability, resulting in vastly improved outcomes with more timely treatments.

In summary, we demonstrated germline complementation in interspecies chimeras via blastocyst complementation, resulting in rat spermatozoa carrying fertilization capacity being formed in sterile mouse hosts. Future research will be needed to validate this approach to generate germ cells capable of giving rise to healthy offspring, which could then be tailored for species conservation efforts. In a separate project, we also generated gene-edited iPSCs of a DMD mouse model which gave rise to intra- or inter-species chimeras after injections into mouse or rat blastocysts. These chimeras harbored satellite cells derived from the donor cells, and upon engraftment into recipient DMD mice contributed to re-expression of the dystrophin protein. Next steps would include improvements to the system, in order to generate only donor cell derived xenogeneic satellite cells, and means to adapt and translate the findings for the treatment of human muscular dystrophies.

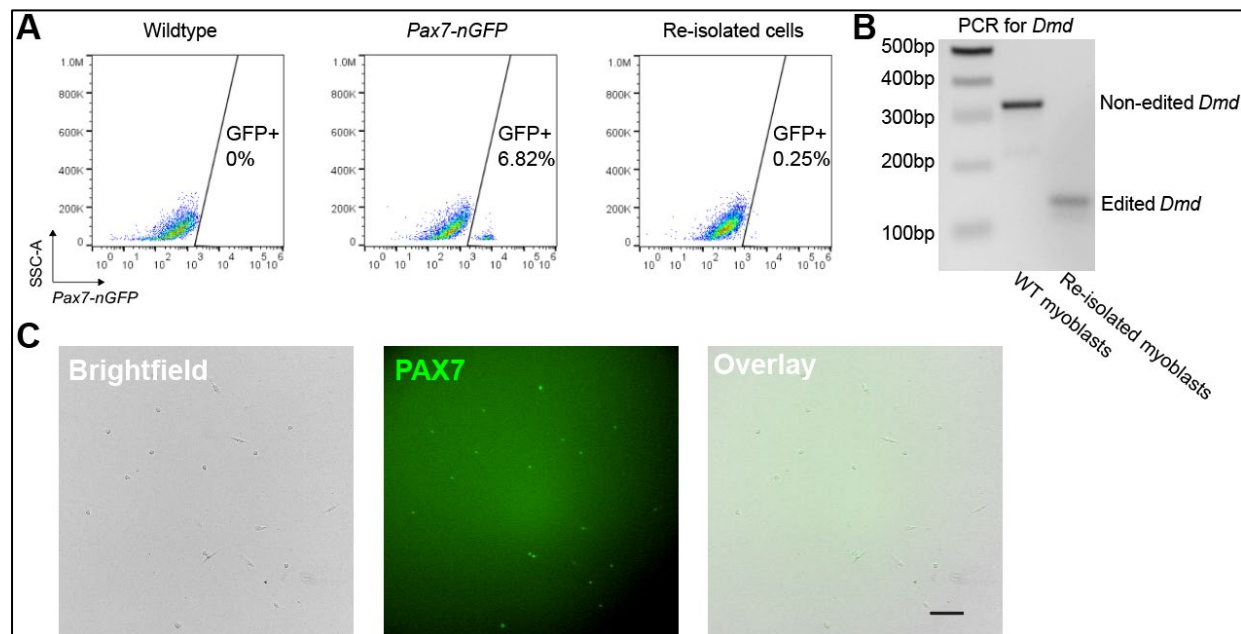
# Chapter 6. Appendix

## 6.1 Supplemental Figures



**Supp. Fig. 1. Generation and preliminary evaluation of a rat *Pax7*-KO model**

(A) Cutting sites of 3 CRISPR/Cas9 gRNAs targeting rat *Pax7* exon 2 indicated by arrows. (B) Weights of pups resulting from mating of *Pax7*<sup>+/-</sup> rats. From postnatal day 5 (P5) to P7. Note lack of weight gain of knockout (KO) animal. n= 1-6 animals. (C) Representative photo of a rat *Pax7*-KO pup with wildtype (WT) littermates. (D) Immunofluorescence image of LAMA, DAPI, and PAX7 in the indicated animals. Note absence of PAX7 in KO animal. Scale bar in non-magnified, 100µm.



**Supp. Fig. 2. Re-isolation of transplanted edited *Dmd*<sup>mdx</sup>; *Pax7*-nGFP myoblasts derived from inter-species chimera #2**

(A) FACS-plots based on nGFP expression for indicated samples. (B) PCR for the presence of edited and non-edited *Dmd*. Note presence of only the edited band in re-isolated myoblasts. (C) Representative images of *Dmd*<sup>mdx</sup>; *Pax7*-nGFP mouse myoblasts re-isolated at P0. Scale bar, 100µm.

## Acknowledgements

---

First of all, I would like to thank my mentor and supervisor, Prof. Ori Bar-Nur. Not only for having given me the opportunity to conduct my doctoral thesis in his newly established lab, but for allowing me to explore, for encouraging me, and supporting me with his creative ideas. It was always great discussing with you, be it science, music, or movies.

I am also thankful to the members of my doctoral committee, Professor Micha Drukker, Professor Saverio Tedesco, and Professor Ferdinand von Meyenn for having taken the time to be on my committee, and for their support and the discussions, both challenging and fruitful.

Everyone working in a team knows how tremendously important and helpful a good vibe is. And a good team we had in the RMB lab! Members both present and past always made it a great environment to work in together, to chat together, and to discuss together. This includes especially my two officemates, Nicola and Seraina. From the early days unpacking boxes, debating over which Eppi tubes to get (obviously, we chose less-than-good ones), all the way to discussing science, random banter, and being there for each other.

I spent quite a number of days in the basement, analyzing chimeras, taking some baby steps towards learning the practical aspects of blastocyst injections and ICSI, and sending out excited messages whenever we found chimera derived sperm. I'd like to thank Monika for her patience during that time, and her support with the experiments.

Many of my experiments would not have worked without the help of the animal caretakers, especially Luci, who always supported me with the animals, be it mouse or rat. Amazing to see how calm the animals were in her hands.

Last, but not even remotely the least, I also thank my friends and family for their unwavering support throughout the whole time, whenever things were going well, and whenever they were not. Thank you.

## Bibliography

---

- 1 Schrode, N. *et al.* Anatomy of a blastocyst: cell behaviors driving cell fate choice and morphogenesis in the early mouse embryo. *Genesis* **51**, 219-233, doi:10.1002/dvg.22368 (2013).
- 2 Cockburn, K. & Rossant, J. Making the blastocyst: lessons from the mouse. *J Clin Invest* **120**, 995-1003, doi:10.1172/JCI41229 (2010).
- 3 Saiz, N. & Plusa, B. Early cell fate decisions in the mouse embryo. *Reproduction* **145**, R65-80, doi:10.1530/REP-12-0381 (2013).
- 4 Christodoulou, N. *et al.* Morphogenesis of extra-embryonic tissues directs the remodelling of the mouse embryo at implantation. *Nat Commun* **10**, 3557, doi:10.1038/s41467-019-11482-5 (2019).
- 5 Smith, A. G. Embryo-derived stem cells: of mice and men. *Annu Rev Cell Dev Biol* **17**, 435-462, doi:10.1146/annurev.cellbio.17.1.435 (2001).
- 6 Martin, G. R. Isolation of a pluripotent cell line from early mouse embryos cultured in medium conditioned by teratocarcinoma stem cells. *Proc Natl Acad Sci U S A* **78**, 7634-7638, doi:10.1073/pnas.78.12.7634 (1981).
- 7 Evans, M. J. & Kaufman, M. H. Establishment in culture of pluripotential cells from mouse embryos. *Nature* **292**, 154-156, doi:10.1038/292154a0 (1981).
- 8 Bradley, A., Evans, M., Kaufman, M. H. & Robertson, E. Formation of germ-line chimaeras from embryo-derived teratocarcinoma cell lines. *Nature* **309**, 255-256, doi:10.1038/309255a0 (1984).
- 9 Tanaka, S., Kunath, T., Hadjantonakis, A. K., Nagy, A. & Rossant, J. Promotion of trophoblast stem cell proliferation by FGF4. *Science* **282**, 2072-2075, doi:10.1126/science.282.5396.2072 (1998).
- 10 Kunath, T. *et al.* Imprinted X-inactivation in extra-embryonic endoderm cell lines from mouse blastocysts. *Development* **132**, 1649-1661, doi:10.1242/dev.01715 (2005).
- 11 Thomson, J. A. *et al.* Embryonic stem cell lines derived from human blastocysts. *Science* **282**, 1145-1147, doi:10.1126/science.282.5391.1145 (1998).
- 12 Li, P. *et al.* Germline competent embryonic stem cells derived from rat blastocysts. *Cell* **135**, 1299-1310, doi:10.1016/j.cell.2008.12.006 (2008).
- 13 Buehr, M. *et al.* Capture of authentic embryonic stem cells from rat blastocysts. *Cell* **135**, 1287-1298, doi:10.1016/j.cell.2008.12.007 (2008).
- 14 De Los Angeles, A. *et al.* Hallmarks of pluripotency. *Nature* **525**, 469-478, doi:10.1038/nature15515 (2015).
- 15 Blum, B. & Benvenisty, N. The tumorigenicity of human embryonic stem cells. *Adv Cancer Res* **100**, 133-158, doi:10.1016/S0065-230X(08)00005-5 (2008).
- 16 Nagy, A. *et al.* Embryonic stem cells alone are able to support fetal development in the mouse. *Development* **110**, 815-821, doi:10.1242/dev.110.3.815 (1990).
- 17 Li, T. D. *et al.* Rat embryonic stem cells produce fertile offspring through tetraploid complementation. *Proc Natl Acad Sci U S A* **114**, 11974-11979, doi:10.1073/pnas.1708710114 (2017).

- 18 Nichols, J. & Smith, A. Naive and primed pluripotent states. *Cell Stem Cell* **4**, 487-492, doi:10.1016/j.stem.2009.05.015 (2009).
- 19 Yagi, M. *et al.* Derivation of ground-state female ES cells maintaining gamete-derived DNA methylation. *Nature* **548**, 224-227, doi:10.1038/nature23286 (2017).
- 20 Mori, M. *et al.* Generation of functional lungs via conditional blastocyst complementation using pluripotent stem cells. *Nat Med* **25**, 1691-1698, doi:10.1038/s41591-019-0635-8 (2019).
- 21 Choi, J. *et al.* Prolonged Mek1/2 suppression impairs the developmental potential of embryonic stem cells. *Nature* **548**, 219-223, doi:10.1038/nature23274 (2017).
- 22 Takahashi, K. & Yamanaka, S. Induction of pluripotent stem cells from mouse embryonic and adult fibroblast cultures by defined factors. *Cell* **126**, 663-676, doi:10.1016/j.cell.2006.07.024 (2006).
- 23 Wernig, M. *et al.* In vitro reprogramming of fibroblasts into a pluripotent ES-cell-like state. *Nature* **448**, 318-324, doi:10.1038/nature05944 (2007).
- 24 Kim, K. *et al.* Epigenetic memory in induced pluripotent stem cells. *Nature* **467**, 285-290, doi:10.1038/nature09342 (2010).
- 25 Okita, K., Ichisaka, T. & Yamanaka, S. Generation of germline-competent induced pluripotent stem cells. *Nature* **448**, 313-317, doi:10.1038/nature05934 (2007).
- 26 Li, H. L. *et al.* Precise correction of the dystrophin gene in duchenne muscular dystrophy patient induced pluripotent stem cells by TALEN and CRISPR-Cas9. *Stem Cell Reports* **4**, 143-154, doi:10.1016/j.stemcr.2014.10.013 (2015).
- 27 Miyagawa, S. *et al.* Case report: Transplantation of human induced pluripotent stem cell-derived cardiomyocyte patches for ischemic cardiomyopathy. *Front Cardiovasc Med* **9**, 950829, doi:10.3389/fcvm.2022.950829 (2022).
- 28 Mandai, M. *et al.* Autologous Induced Stem-Cell-Derived Retinal Cells for Macular Degeneration. *N Engl J Med* **376**, 1038-1046, doi:10.1056/NEJMoa1608368 (2017).
- 29 Loh, Y. H. *et al.* Generation of induced pluripotent stem cells from human blood. *Blood* **113**, 5476-5479, doi:10.1182/blood-2009-02-204800 (2009).
- 30 Robinton, D. A. & Daley, G. Q. The promise of induced pluripotent stem cells in research and therapy. *Nature* **481**, 295-305, doi:10.1038/nature10761 (2012).
- 31 Rashid, T., Kobayashi, T. & Nakauchi, H. Revisiting the flight of Icarus: making human organs from PSCs with large animal chimeras. *Cell Stem Cell* **15**, 406-409, doi:10.1016/j.stem.2014.09.013 (2014).
- 32 Chen, J., Lansford, R., Stewart, V., Young, F. & Alt, F. W. RAG-2-deficient blastocyst complementation: an assay of gene function in lymphocyte development. *Proc Natl Acad Sci U S A* **90**, 4528-4532, doi:10.1073/pnas.90.10.4528 (1993).
- 33 Stanger, B. Z., Tanaka, A. J. & Melton, D. A. Organ size is limited by the number of embryonic progenitor cells in the pancreas but not the liver. *Nature* **445**, 886-891, doi:10.1038/nature05537 (2007).
- 34 Gardner, R. L. & Johnson, M. H. Investigation of early mammalian development using interspecific chimaeras between rat and mouse. *Nat New Biol* **246**, 86-89, doi:10.1038/newbio246086a0 (1973).



- 35 Rossant, J. Investigation of inner cell mass determination by aggregation of isolated rat inner cell masses with mouse morulae. *J Embryol Exp Morphol* **36**, 163-174 (1976).
- 36 Stern, M. S. Letter: Chimaeras obtained by aggregation of mouse eggs with rat eggs. *Nature* **243**, 472-473, doi:10.1038/243472a0 (1973).
- 37 Mystkowska, E. T. Development of mouse-bank vole interspecific chimaeric embryos. *J Embryol Exp Morphol* **33**, 731-744 (1975).
- 38 Rossant, J. & Frels, W. I. Interspecific chimeras in mammals: successful production of live chimeras between *Mus musculus* and *Mus caroli*. *Science* **208**, 419-421, doi:10.1126/science.7367871 (1980).
- 39 Kobayashi, T. *et al.* Generation of rat pancreas in mouse by interspecific blastocyst injection of pluripotent stem cells. *Cell* **142**, 787-799, doi:10.1016/j.cell.2010.07.039 (2010).
- 40 Usui, J. *et al.* Generation of kidney from pluripotent stem cells via blastocyst complementation. *Am J Pathol* **180**, 2417-2426, doi:10.1016/j.ajpath.2012.03.007 (2012).
- 41 Chubb, R. *et al.* In Vivo Rescue of the Hematopoietic Niche By Pluripotent Stem Cell Complementation of Defective Osteoblast Compartments. *Stem Cells* **35**, 2150-2159, doi:10.1002/stem.2670 (2017).
- 42 Chang, A. N. *et al.* Neural blastocyst complementation enables mouse forebrain organogenesis. *Nature* **563**, 126-130, doi:10.1038/s41586-018-0586-0 (2018).
- 43 Matsunari, H. *et al.* Blastocyst complementation generates exogenic pancreas in vivo in apancreatic cloned pigs. *Proc Natl Acad Sci U S A* **110**, 4557-4562, doi:10.1073/pnas.1222902110 (2013).
- 44 Matsunari, H. *et al.* Compensation of Disabled Organogeneses in Genetically Modified Pig Fetuses by Blastocyst Complementation. *Stem Cell Reports* **14**, 21-33, doi:10.1016/j.stemcr.2019.11.008 (2020).
- 45 Zhang, H. *et al.* Rescuing ocular development in an anophthalmic pig by blastocyst complementation. *EMBO Mol Med* **10**, doi:10.15252/emmm.201808861 (2018).
- 46 Ruiz-Estevez, M. *et al.* Liver development is restored by blastocyst complementation of HHEX knockout in mice and pigs. *Stem Cell Res Ther* **12**, 292, doi:10.1186/s13287-021-02348-z (2021).
- 47 Kobayashi, T. *et al.* Germline development in rat revealed by visualization and deletion of Prdm14. *Development* **147**, doi:10.1242/dev.183798 (2020).
- 48 Goto, T. *et al.* Generation of pluripotent stem cell-derived mouse kidneys in Sall1-targeted anephric rats. *Nat Commun* **10**, 451, doi:10.1038/s41467-019-08394-9 (2019).
- 49 Wang, X. *et al.* Generation of rat blood vasculature and hematopoietic cells in rat-mouse chimeras by blastocyst complementation. *J Genet Genomics* **47**, 249-261, doi:10.1016/j.jgg.2020.05.002 (2020).
- 50 Tan, T. *et al.* Chimeric contribution of human extended pluripotent stem cells to monkey embryos ex vivo. *Cell* **184**, 2020-2032 e2014, doi:10.1016/j.cell.2021.03.020 (2021).

- 51 Hu, Z. *et al.* Transient inhibition of mTOR in human pluripotent stem cells enables robust formation of mouse-human chimeric embryos. *Sci Adv* **6**, eaaz0298, doi:10.1126/sciadv.aaz0298 (2020).
- 52 Das, S. *et al.* Generation of human endothelium in pig embryos deficient in ETV2. *Nat Biotechnol* **38**, 297-302, doi:10.1038/s41587-019-0373-y (2020).
- 53 Maeng, G. *et al.* Humanized skeletal muscle in MYF5/MYOD/MYF6-null pig embryos. *Nat Biomed Eng* **5**, 805-814, doi:10.1038/s41551-021-00693-1 (2021).
- 54 Huang, K. *et al.* BMI1 enables interspecies chimerism with human pluripotent stem cells. *Nat Commun* **9**, 4649, doi:10.1038/s41467-018-07098-w (2018).
- 55 Wang, X. *et al.* Human embryonic stem cells contribute to embryonic and extraembryonic lineages in mouse embryos upon inhibition of apoptosis. *Cell Res* **28**, 126-129, doi:10.1038/cr.2017.138 (2018).
- 56 Fu, R. *et al.* Domesticated cynomolgus monkey embryonic stem cells allow the generation of neonatal interspecies chimeric pigs. *Protein Cell* **11**, 97-107, doi:10.1007/s13238-019-00676-8 (2020).
- 57 Wu, J. *et al.* Interspecies Chimerism with Mammalian Pluripotent Stem Cells. *Cell* **168**, 473-486 e415, doi:10.1016/j.cell.2016.12.036 (2017).
- 58 Bozyk, K. *et al.* Mouse<-->rat aggregation chimaeras can develop to adulthood. *Dev Biol* **427**, 106-120, doi:10.1016/j.ydbio.2017.05.002 (2017).
- 59 Yamaguchi, T. *et al.* An interspecies barrier to tetraploid complementation and chimera formation. *Sci Rep* **8**, 15289, doi:10.1038/s41598-018-33690-7 (2018).
- 60 Ginsburg, M., Snow, M. H. & McLaren, A. Primordial germ cells in the mouse embryo during gastrulation. *Development* **110**, 521-528, doi:10.1242/dev.110.2.521 (1990).
- 61 McLaren, A. Primordial germ cells in the mouse. *Dev Biol* **262**, 1-15, doi:10.1016/s0012-1606(03)00214-8 (2003).
- 62 Lawson, K. A. *et al.* Bmp4 is required for the generation of primordial germ cells in the mouse embryo. *Genes Dev* **13**, 424-436, doi:10.1101/gad.13.4.424 (1999).
- 63 Ying, Y., Liu, X. M., Marble, A., Lawson, K. A. & Zhao, G. Q. Requirement of Bmp8b for the generation of primordial germ cells in the mouse. *Mol Endocrinol* **14**, 1053-1063, doi:10.1210/mend.14.7.0479 (2000).
- 64 Saitou, M. & Yamaji, M. Germ cell specification in mice: signaling, transcription regulation, and epigenetic consequences. *Reproduction* **139**, 931-942, doi:10.1530/REP-10-0043 (2010).
- 65 Ohinata, Y. *et al.* Blimp1 is a critical determinant of the germ cell lineage in mice. *Nature* **436**, 207-213, doi:10.1038/nature03813 (2005).
- 66 Yamaji, M. *et al.* Critical function of Prdm14 for the establishment of the germ cell lineage in mice. *Nat Genet* **40**, 1016-1022, doi:10.1038/ng.186 (2008).
- 67 Weber, S. *et al.* Critical function of AP-2 gamma/TCFAP2C in mouse embryonic germ cell maintenance. *Biol Reprod* **82**, 214-223, doi:10.1095/biolreprod.109.078717 (2010).
- 68 Saitou, M. & Yamaji, M. Primordial germ cells in mice. *Cold Spring Harb Perspect Biol* **4**, doi:10.1101/cshperspect.a008375 (2012).

- 69 Saitou, M., Barton, S. C. & Surani, M. A. A molecular programme for the specification of germ cell fate in mice. *Nature* **418**, 293-300, doi:10.1038/nature00927 (2002).
- 70 Anderson, R., Copeland, T. K., Scholer, H., Heasman, J. & Wylie, C. The onset of germ cell migration in the mouse embryo. *Mech Dev* **91**, 61-68, doi:10.1016/s0925-4773(99)00271-3 (2000).
- 71 Molyneaux, K. A., Stallock, J., Schaible, K. & Wylie, C. Time-lapse analysis of living mouse germ cell migration. *Dev Biol* **240**, 488-498, doi:10.1006/dbio.2001.0436 (2001).
- 72 Richardson, B. E. & Lehmann, R. Mechanisms guiding primordial germ cell migration: strategies from different organisms. *Nat Rev Mol Cell Biol* **11**, 37-49, doi:10.1038/nrm2815 (2010).
- 73 Tam, P. P. & Snow, M. H. Proliferation and migration of primordial germ cells during compensatory growth in mouse embryos. *J Embryol Exp Morphol* **64**, 133-147 (1981).
- 74 Gubbay, J. *et al.* A gene mapping to the sex-determining region of the mouse Y chromosome is a member of a novel family of embryonically expressed genes. *Nature* **346**, 245-250, doi:10.1038/346245a0 (1990).
- 75 Lovell-Badge, R., Canning, C. & Sekido, R. Sex-determining genes in mice: building pathways. *Novartis Found Symp* **244**, 4-18; discussion 18-22, 35-42, 253-257 (2002).
- 76 Tanaka, S. S. & Nishinakamura, R. Regulation of male sex determination: genital ridge formation and Sry activation in mice. *Cell Mol Life Sci* **71**, 4781-4802, doi:10.1007/s00018-014-1703-3 (2014).
- 77 Larose, H. *et al.* Gametogenesis: A journey from inception to conception. *Curr Top Dev Biol* **132**, 257-310, doi:10.1016/bs.ctdb.2018.12.006 (2019).
- 78 Schmahl, J., Kim, Y., Colvin, J. S., Ornitz, D. M. & Capel, B. Fgf9 induces proliferation and nuclear localization of FGFR2 in Sertoli precursors during male sex determination. *Development* **131**, 3627-3636, doi:10.1242/dev.01239 (2004).
- 79 Combes, A. N. *et al.* Endothelial cell migration directs testis cord formation. *Dev Biol* **326**, 112-120, doi:10.1016/j.ydbio.2008.10.040 (2009).
- 80 Brennan, J. & Capel, B. One tissue, two fates: molecular genetic events that underlie testis versus ovary development. *Nat Rev Genet* **5**, 509-521, doi:10.1038/nrg1381 (2004).
- 81 Griswold, M. D. The central role of Sertoli cells in spermatogenesis. *Semin Cell Dev Biol* **9**, 411-416, doi:10.1006/scdb.1998.0203 (1998).
- 82 Koubova, J. *et al.* Retinoic acid regulates sex-specific timing of meiotic initiation in mice. *Proc Natl Acad Sci U S A* **103**, 2474-2479, doi:10.1073/pnas.0510813103 (2006).
- 83 Fijak, M. & Meinhardt, A. The testis in immune privilege. *Immunol Rev* **213**, 66-81, doi:10.1111/j.1600-065X.2006.00438.x (2006).
- 84 Saitou, M. & Hayashi, K. Mammalian in vitro gametogenesis. *Science* **374**, eaaz6830, doi:10.1126/science.aaz6830 (2021).

- 85 Wen, Q., Cheng, C. Y. & Liu, Y. X. Development, function and fate of fetal Leydig cells. *Semin Cell Dev Biol* **59**, 89-98, doi:10.1016/j.semcdb.2016.03.003 (2016).
- 86 Western, P. S., Miles, D. C., van den Bergen, J. A., Burton, M. & Sinclair, A. H. Dynamic regulation of mitotic arrest in fetal male germ cells. *Stem Cells* **26**, 339-347, doi:10.1634/stemcells.2007-0622 (2008).
- 87 Yoshida, S. *et al.* The first round of mouse spermatogenesis is a distinctive program that lacks the self-renewing spermatogonia stage. *Development* **133**, 1495-1505, doi:10.1242/dev.02316 (2006).
- 88 Law, N. C., Oatley, M. J. & Oatley, J. M. Developmental kinetics and transcriptome dynamics of stem cell specification in the spermatogenic lineage. *Nat Commun* **10**, 2787, doi:10.1038/s41467-019-10596-0 (2019).
- 89 Tan, K., Song, H. W. & Wilkinson, M. F. Single-cell RNAseq analysis of testicular germ and somatic cell development during the perinatal period. *Development* **147**, doi:10.1242/dev.183251 (2020).
- 90 de Rooij, D. G. & Russell, L. D. All you wanted to know about spermatogonia but were afraid to ask. *J Androl* **21**, 776-798 (2000).
- 91 Oatley, J. M. & Brinster, R. L. The germline stem cell niche unit in mammalian testes. *Physiol Rev* **92**, 577-595, doi:10.1152/physrev.00025.2011 (2012).
- 92 Oatley, J. M. & Brinster, R. L. Regulation of spermatogonial stem cell self-renewal in mammals. *Annu Rev Cell Dev Biol* **24**, 263-286, doi:10.1146/annurev.cellbio.24.110707.175355 (2008).
- 93 Endo, T., Freinkman, E., de Rooij, D. G. & Page, D. C. Periodic production of retinoic acid by meiotic and somatic cells coordinates four transitions in mouse spermatogenesis. *Proc Natl Acad Sci U S A* **114**, E10132-E10141, doi:10.1073/pnas.1710837114 (2017).
- 94 Ogura, A., Matsuda, J. & Yanagimachi, R. Birth of normal young after electrofusion of mouse oocytes with round spermatids. *Proc Natl Acad Sci U S A* **91**, 7460-7462, doi:10.1073/pnas.91.16.7460 (1994).
- 95 O'Donnell, L. Mechanisms of spermiogenesis and spermiation and how they are disturbed. *Spermatogenesis* **4**, e979623, doi:10.4161/21565562.2014.979623 (2014).
- 96 Leblond, C. P. & Clermont, Y. Spermiogenesis of rat, mouse, hamster and guinea pig as revealed by the periodic acid-fuchsin sulfuric acid technique. *Am J Anat* **90**, 167-215, doi:10.1002/aja.1000900202 (1952).
- 97 Cho, C. *et al.* Protamine 2 deficiency leads to sperm DNA damage and embryo death in mice. *Biol Reprod* **69**, 211-217, doi:10.1095/biolreprod.102.015115 (2003).
- 98 Jodar, M. Sperm and seminal plasma RNAs: what roles do they play beyond fertilization? *Reproduction* **158**, R113-R123, doi:10.1530/REP-18-0639 (2019).
- 99 Corral-Vazquez, C. *et al.* The RNA content of human sperm reflects prior events in spermatogenesis and potential post-fertilization effects. *Mol Hum Reprod* **27**, doi:10.1093/molehr/gaab035 (2021).

- 100 Lehti, M. S. & Sironen, A. Formation and function of sperm tail structures in association with sperm motility defects. *Biol Reprod* **97**, 522-536, doi:10.1093/biolre/iox096 (2017).
- 101 Gervasi, M. G. & Visconti, P. E. Molecular changes and signaling events occurring in spermatozoa during epididymal maturation. *Andrology* **5**, 204-218, doi:10.1111/andr.12320 (2017).
- 102 Yoshimizu, T., Obinata, M. & Matsui, Y. Stage-specific tissue and cell interactions play key roles in mouse germ cell specification. *Development* **128**, 481-490, doi:10.1242/dev.128.4.481 (2001).
- 103 Ying, Y., Qi, X. & Zhao, G. Q. Induction of primordial germ cells from murine epiblasts by synergistic action of BMP4 and BMP8B signaling pathways. *Proc Natl Acad Sci U S A* **98**, 7858-7862, doi:10.1073/pnas.151242798 (2001).
- 104 Toyooka, Y., Tsunekawa, N., Akasu, R. & Noce, T. Embryonic stem cells can form germ cells in vitro. *Proc Natl Acad Sci U S A* **100**, 11457-11462, doi:10.1073/pnas.1932826100 (2003).
- 105 Ohinata, Y. *et al.* A signaling principle for the specification of the germ cell lineage in mice. *Cell* **137**, 571-584, doi:10.1016/j.cell.2009.03.014 (2009).
- 106 Kimura, Y. & Yanagimachi, R. Intracytoplasmic sperm injection in the mouse. *Biol Reprod* **52**, 709-720, doi:10.1095/biolreprod52.4.709 (1995).
- 107 Nakaki, F. *et al.* Induction of mouse germ-cell fate by transcription factors in vitro. *Nature* **501**, 222-226, doi:10.1038/nature12417 (2013).
- 108 Hayashi, K., Ohta, H., Kurimoto, K., Aramaki, S. & Saitou, M. Reconstitution of the mouse germ cell specification pathway in culture by pluripotent stem cells. *Cell* **146**, 519-532, doi:10.1016/j.cell.2011.06.052 (2011).
- 109 Zhou, Q. *et al.* Complete Meiosis from Embryonic Stem Cell-Derived Germ Cells In Vitro. *Cell Stem Cell* **18**, 330-340, doi:10.1016/j.stem.2016.01.017 (2016).
- 110 Ishikura, Y. *et al.* In vitro reconstitution of the whole male germ-cell development from mouse pluripotent stem cells. *Cell Stem Cell* **28**, 2167-2179 e2169, doi:10.1016/j.stem.2021.08.005 (2021).
- 111 Ishikura, Y. *et al.* In Vitro Derivation and Propagation of Spermatogonial Stem Cell Activity from Mouse Pluripotent Stem Cells. *Cell Rep* **17**, 2789-2804, doi:10.1016/j.celrep.2016.11.026 (2016).
- 112 Oikawa, M. *et al.* Functional primordial germ cell-like cells from pluripotent stem cells in rats. *Science* **376**, 176-179, doi:10.1126/science.abl4412 (2022).
- 113 Hirabayashi, M. *et al.* Offspring derived from intracytoplasmic injection of transgenic rat sperm. *Transgenic Res* **11**, 221-228, doi:10.1023/a:1015210604906 (2002).
- 114 Hirabayashi, M., Kato, M., Aoto, T., Ueda, M. & Hochi, S. Rescue of infertile transgenic rat lines by intracytoplasmic injection of cryopreserved round spermatids. *Mol Reprod Dev* **62**, 295-299, doi:10.1002/mrd.10127 (2002).
- 115 Daley, G. Q. Gametes from embryonic stem cells: a cup half empty or half full? *Science* **316**, 409-410, doi:10.1126/science.1138772 (2007).

- 116 Sasaki, K. *et al.* Robust In Vitro Induction of Human Germ Cell Fate from Pluripotent Stem Cells. *Cell Stem Cell* **17**, 178-194, doi:10.1016/j.stem.2015.06.014 (2015).
- 117 Hwang, Y. S. *et al.* Reconstitution of prospermatogonial specification in vitro from human induced pluripotent stem cells. *Nat Commun* **11**, 5656, doi:10.1038/s41467-020-19350-3 (2020).
- 118 Brinster, R. L. & Avarbock, M. R. Germline transmission of donor haplotype following spermatogonial transplantation. *Proc Natl Acad Sci U S A* **91**, 11303-11307, doi:10.1073/pnas.91.24.11303 (1994).
- 119 Kubota, H. & Brinster, R. L. Spermatogonial stem cells. *Biol Reprod* **99**, 52-74, doi:10.1093/biolre/i0y077 (2018).
- 120 Ciccarelli, M. *et al.* Donor-derived spermatogenesis following stem cell transplantation in sterile NANOS2 knockout males. *Proc Natl Acad Sci U S A* **117**, 24195-24204, doi:10.1073/pnas.2010102117 (2020).
- 121 Shinohara, T. *et al.* Rats produced by interspecies spermatogonial transplantation in mice and in vitro microinsemination. *Proc Natl Acad Sci U S A* **103**, 13624-13628, doi:10.1073/pnas.0604205103 (2006).
- 122 Honaramooz, A. *et al.* Fertility and germline transmission of donor haplotype following germ cell transplantation in immunocompetent goats. *Biol Reprod* **69**, 1260-1264, doi:10.1095/biolreprod.103.018788 (2003).
- 123 Herrid, M. *et al.* Irradiation enhances the efficiency of testicular germ cell transplantation in sheep. *Biol Reprod* **81**, 898-905, doi:10.1095/biolreprod.109.078279 (2009).
- 124 Zhang, Z., Renfree, M. B. & Short, R. V. Successful intra- and interspecific male germ cell transplantation in the rat. *Biol Reprod* **68**, 961-967, doi:10.1095/biolreprod.102.009480 (2003).
- 125 Clouthier, D. E., Avarbock, M. R., Maika, S. D., Hammer, R. E. & Brinster, R. L. Rat spermatogenesis in mouse testis. *Nature* **381**, 418-421, doi:10.1038/381418a0 (1996).
- 126 Ogawa, T., Dobrinski, I., Avarbock, M. R. & Brinster, R. L. Xenogeneic spermatogenesis following transplantation of hamster germ cells to mouse testes. *Biol Reprod* **60**, 515-521, doi:10.1095/biolreprod60.2.515 (1999).
- 127 Kanatsu-Shinohara, M. *et al.* Regeneration of spermatogenesis by mouse germ cell transplantation into allogeneic and xenogeneic testis primordia or organoids. *Stem Cell Reports* **17**, 924-935, doi:10.1016/j.stemcr.2022.02.013 (2022).
- 128 Tsuda, M. *et al.* Conserved role of nanos proteins in germ cell development. *Science* **301**, 1239-1241, doi:10.1126/science.1085222 (2003).
- 129 Brinster, R. L. & Zimmermann, J. W. Spermatogenesis following male germ-cell transplantation. *Proc Natl Acad Sci U S A* **91**, 11298-11302, doi:10.1073/pnas.91.24.11298 (1994).
- 130 Suarez, P. E. *et al.* The glucocorticoid-induced leucine zipper (gilz/Tsc22d3-2) gene locus plays a crucial role in male fertility. *Mol Endocrinol* **26**, 1000-1013, doi:10.1210/me.2011-1249 (2012).

- 131 Geissler, E. N., Ryan, M. A. & Housman, D. E. The dominant-white spotting (W) locus of the mouse encodes the c-kit proto-oncogene. *Cell* **55**, 185-192, doi:10.1016/0092-8674(88)90020-7 (1988).
- 132 Taft, R. A. *et al.* The perfect host: a mouse host embryo facilitating more efficient germ line transmission of genetically modified embryonic stem cells. *PLoS One* **8**, e67826, doi:10.1371/journal.pone.0067826 (2013).
- 133 Miura, K., Matoba, S., Hirose, M. & Ogura, A. Generation of chimeric mice with spermatozoa fully derived from embryonic stem cells using a triple-target CRISPR method for Nanos3dagger. *Biol Reprod* **104**, 223-233, doi:10.1093/biolre/iaaa176 (2021).
- 134 Koentgen, F. *et al.* Exclusive transmission of the embryonic stem cell-derived genome through the mouse germline. *Genesis* **54**, 326-333, doi:10.1002/dvg.22938 (2016).
- 135 Bruscoli, S. *et al.* Long glucocorticoid-induced leucine zipper (L-GILZ) protein interacts with ras protein pathway and contributes to spermatogenesis control. *J Biol Chem* **287**, 1242-1251, doi:10.1074/jbc.M111.316372 (2012).
- 136 Romero, Y. *et al.* The Glucocorticoid-induced leucine zipper (GILZ) Is essential for spermatogonial survival and spermatogenesis. *Sex Dev* **6**, 169-177, doi:10.1159/000338415 (2012).
- 137 Ngo, D. *et al.* Glucocorticoid-induced leucine zipper (GILZ) regulates testicular FOXO1 activity and spermatogonial stem cell (SSC) function. *PLoS One* **8**, e59149, doi:10.1371/journal.pone.0059149 (2013).
- 138 Isotani, A., Hatayama, H., Kaseda, K., Ikawa, M. & Okabe, M. Formation of a thymus from rat ES cells in xenogeneic nude mouse<-->rat ES chimeras. *Genes Cells* **16**, 397-405, doi:10.1111/j.1365-2443.2011.01495.x (2011).
- 139 Isotani, A., Yamagata, K., Okabe, M. & Ikawa, M. Generation of Hprt-disrupted rat through mouse<-->rat ES chimeras. *Sci Rep* **6**, 24215, doi:10.1038/srep24215 (2016).
- 140 Tsukiyama, T., Kato-Itoh, M., Nakauchi, H. & Ohinata, Y. A comprehensive system for generation and evaluation of induced pluripotent stem cells using piggyBac transposition. *PLoS One* **9**, e92973, doi:10.1371/journal.pone.0092973 (2014).
- 141 Kobayashi, T. *et al.* Blastocyst complementation using Prdm14-deficient rats enables efficient germline transmission and generation of functional mouse spermatids in rats. *Nat Commun* **12**, 1328, doi:10.1038/s41467-021-21557-x (2021).
- 142 Ceballos, G. *et al.* Accelerated modern human-induced species losses: Entering the sixth mass extinction. *Sci Adv* **1**, e1400253, doi:10.1126/sciadv.1400253 (2015).
- 143 Honda, A. Applying iPSCs for Preserving Endangered Species and Elucidating the Evolution of Mammalian Sex Determination. *Bioessays* **40**, e1700152, doi:10.1002/bies.201700152 (2018).
- 144 Honda, A. *et al.* Flexible adaptation of male germ cells from female iPSCs of endangered Tokudaia osimensis. *Sci Adv* **3**, e1602179, doi:10.1126/sciadv.1602179 (2017).

- 145 Hildebrandt, T. B. *et al.* Embryos and embryonic stem cells from the white rhinoceros. *Nat Commun* **9**, 2589, doi:10.1038/s41467-018-04959-2 (2018).
- 146 Ben-Nun, I. F. *et al.* Induced pluripotent stem cells from highly endangered species. *Nat Methods* **8**, 829-831, doi:10.1038/nmeth.1706 (2011).
- 147 Saragusty, J. *et al.* Rewinding the process of mammalian extinction. *Zoo Biol* **35**, 280-292, doi:10.1002/zoo.21284 (2016).
- 148 Dumont, N. A., Bentzinger, C. F., Sincennes, M. C. & Rudnicki, M. A. Satellite Cells and Skeletal Muscle Regeneration. *Compr Physiol* **5**, 1027-1059, doi:10.1002/cphy.c140068 (2015).
- 149 Relaix, F. & Zammit, P. S. Satellite cells are essential for skeletal muscle regeneration: the cell on the edge returns centre stage. *Development* **139**, 2845-2856, doi:10.1242/dev.069088 (2012).
- 150 Mauro, A. Satellite cell of skeletal muscle fibers. *J Biophys Biochem Cytol* **9**, 493-495 (1961).
- 151 Sacco, A., Doyonnas, R., Kraft, P., Vitorovic, S. & Blau, H. M. Self-renewal and expansion of single transplanted muscle stem cells. *Nature* **456**, 502-506, doi:10.1038/nature07384 (2008).
- 152 Collins, C. A. *et al.* Stem cell function, self-renewal, and behavioral heterogeneity of cells from the adult muscle satellite cell niche. *Cell* **122**, 289-301, doi:10.1016/j.cell.2005.05.010 (2005).
- 153 Seale, P. *et al.* Pax7 is required for the specification of myogenic satellite cells. *Cell* **102**, 777-786 (2000).
- 154 Rodgers, J. T. *et al.* mTORC1 controls the adaptive transition of quiescent stem cells from G0 to G(Alert). *Nature* **510**, 393-396, doi:10.1038/nature13255 (2014).
- 155 Rocheteau, P., Gayraud-Morel, B., Siegl-Cachedenier, I., Blasco, M. A. & Tajbakhsh, S. A subpopulation of adult skeletal muscle stem cells retains all template DNA strands after cell division. *Cell* **148**, 112-125, doi:10.1016/j.cell.2011.11.049 (2012).
- 156 Kuang, S., Kuroda, K., Le Grand, F. & Rudnicki, M. A. Asymmetric self-renewal and commitment of satellite stem cells in muscle. *Cell* **129**, 999-1010, doi:10.1016/j.cell.2007.03.044 (2007).
- 157 Mansouri, A., Stoykova, A., Torres, M. & Gruss, P. Dysgenesis of cephalic neural crest derivatives in Pax7<sup>-/-</sup> mutant mice. *Development* **122**, 831-838, doi:10.1242/dev.122.3.831 (1996).
- 158 von Maltzahn, J., Jones, A. E., Parks, R. J. & Rudnicki, M. A. Pax7 is critical for the normal function of satellite cells in adult skeletal muscle. *Proc Natl Acad Sci U S A* **110**, 16474-16479, doi:10.1073/pnas.1307680110 (2013).
- 159 Domenig, S. A., Palmer, A. S. & Bar-Nur, O. in *Organ Tissue Engineering* Ch. Chapter 19-1, 1-62 (2020).
- 160 Proskorovski-Ohayon, R. *et al.* PAX7 mutation in a syndrome of failure to thrive, hypotonia, and global neurodevelopmental delay. *Hum Mutat* **38**, 1671-1683, doi:10.1002/humu.23310 (2017).



- 161 Marg, A. *et al.* Human muscle-derived CLEC14A-positive cells regenerate muscle independent of PAX7. *Nat Commun* **10**, 5776, doi:10.1038/s41467-019-13650-z (2019).
- 162 Feichtinger, R. G. *et al.* Biallelic variants in the transcription factor PAX7 are a new genetic cause of myopathy. *Genet Med* **21**, 2521-2531, doi:10.1038/s41436-019-0532-z (2019).
- 163 Furrer, R. & Handschin, C. Muscle Wasting Diseases: Novel Targets and Treatments. *Annu Rev Pharmacol Toxicol* **59**, 315-339, doi:10.1146/annurev-pharmtox-010818-021041 (2019).
- 164 Duan, D., Goemans, N., Takeda, S., Mercuri, E. & Aartsma-Rus, A. Duchenne muscular dystrophy. *Nat Rev Dis Primers* **7**, 13, doi:10.1038/s41572-021-00248-3 (2021).
- 165 Mercuri, E. & Muntoni, F. Muscular dystrophies. *Lancet* **381**, 845-860, doi:10.1016/S0140-6736(12)61897-2 (2013).
- 166 Gao, Q. Q. & McNally, E. M. The Dystrophin Complex: Structure, Function, and Implications for Therapy. *Compr Physiol* **5**, 1223-1239, doi:10.1002/cphy.c140048 (2015).
- 167 Ervasti, J. M. & Campbell, K. P. Membrane organization of the dystrophin-glycoprotein complex. *Cell* **66**, 1121-1131, doi:10.1016/0092-8674(91)90035-w (1991).
- 168 Bladen, C. L. *et al.* The TREAT-NMD DMD Global Database: analysis of more than 7,000 Duchenne muscular dystrophy mutations. *Hum Mutat* **36**, 395-402, doi:10.1002/humu.22758 (2015).
- 169 Brioschi, S. *et al.* Genetic characterization in symptomatic female DMD carriers: lack of relationship between X-inactivation, transcriptional DMD allele balancing and phenotype. *BMC Med Genet* **13**, 73, doi:10.1186/1471-2350-13-73 (2012).
- 170 Song, T. J., Lee, K. A., Kang, S. W., Cho, H. & Choi, Y. C. Three cases of manifesting female carriers in patients with Duchenne muscular dystrophy. *Yonsei Med J* **52**, 192-195, doi:10.3349/ymj.2011.52.1.192 (2011).
- 171 Muntoni, F., Torelli, S. & Ferlini, A. Dystrophin and mutations: one gene, several proteins, multiple phenotypes. *Lancet Neurol* **2**, 731-740, doi:10.1016/s1474-4422(03)00585-4 (2003).
- 172 Chang, N. C. *et al.* The Dystrophin Glycoprotein Complex Regulates the Epigenetic Activation of Muscle Stem Cell Commitment. *Cell Stem Cell* **22**, 755-768 e756, doi:10.1016/j.stem.2018.03.022 (2018).
- 173 Heslop, L., Morgan, J. E. & Partridge, T. A. Evidence for a myogenic stem cell that is exhausted in dystrophic muscle. *J Cell Sci* **113 ( Pt 12)**, 2299-2308, doi:10.1242/jcs.113.12.2299 (2000).
- 174 Wang, Y. X. *et al.* EGFR-Aurka Signaling Rescues Polarity and Regeneration Defects in Dystrophin-Deficient Muscle Stem Cells by Increasing Asymmetric Divisions. *Cell Stem Cell* **24**, 419-432 e416, doi:10.1016/j.stem.2019.01.002 (2019).

- 175 Dumont, N. A. *et al.* Dystrophin expression in muscle stem cells regulates their polarity and asymmetric division. *Nat Med* **21**, 1455-1463, doi:10.1038/nm.3990 (2015).
- 176 Theadom, A. *et al.* Prevalence of muscular dystrophies: a systematic literature review. *Neuroepidemiology* **43**, 259-268, doi:10.1159/000369343 (2014).
- 177 Tabebordbar, M., Wang, E. T. & Wagers, A. J. Skeletal muscle degenerative diseases and strategies for therapeutic muscle repair. *Annu Rev Pathol* **8**, 441-475, doi:10.1146/annurev-pathol-011811-132450 (2013).
- 178 Birnkrant, D. J. *et al.* Diagnosis and management of Duchenne muscular dystrophy, part 2: respiratory, cardiac, bone health, and orthopaedic management. *Lancet Neurol* **17**, 347-361, doi:10.1016/S1474-4422(18)30025-5 (2018).
- 179 Birnkrant, D. J. *et al.* Diagnosis and management of Duchenne muscular dystrophy, part 1: diagnosis, and neuromuscular, rehabilitation, endocrine, and gastrointestinal and nutritional management. *Lancet Neurol* **17**, 251-267, doi:10.1016/S1474-4422(18)30024-3 (2018).
- 180 Tremblay, J. P. *et al.* Results of a triple blind clinical study of myoblast transplantations without immunosuppressive treatment in young boys with Duchenne muscular dystrophy. *Cell Transplant* **2**, 99-112, doi:10.1177/096368979300200203 (1993).
- 181 Miller, R. G. *et al.* Myoblast implantation in Duchenne muscular dystrophy: the San Francisco study. *Muscle Nerve* **20**, 469-478, doi:10.1002/(sici)1097-4598(199704)20:4<469::aid-mus10>3.0.co;2-u (1997).
- 182 Skuk, D. & Tremblay, J. P. Clarifying misconceptions about myoblast transplantation in myology. *Mol Ther* **22**, 897-898, doi:10.1038/mt.2014.57 (2014).
- 183 Skuk, D. *et al.* Dystrophin expression in muscles of duchenne muscular dystrophy patients after high-density injections of normal myogenic cells. *J Neuropathol Exp Neurol* **65**, 371-386, doi:10.1097/01.jnen.0000218443.45782.81 (2006).
- 184 Perie, S. *et al.* Autologous myoblast transplantation for oculopharyngeal muscular dystrophy: a phase I/IIa clinical study. *Mol Ther* **22**, 219-225, doi:10.1038/mt.2013.155 (2014).
- 185 Ng, M. Y., Li, H., Ghelfi, M. D., Goldman, Y. E. & Cooperman, B. S. Ataluren and aminoglycosides stimulate read-through of nonsense codons by orthogonal mechanisms. *Proc Natl Acad Sci U S A* **118**, doi:10.1073/pnas.2020599118 (2021).
- 186 Eser, G. & Topaloglu, H. Current Outline of Exon Skipping Trials in Duchenne Muscular Dystrophy. *Genes (Basel)* **13**, doi:10.3390/genes13071241 (2022).
- 187 Duan, D. Systemic AAV Micro-dystrophin Gene Therapy for Duchenne Muscular Dystrophy. *Mol Ther* **26**, 2337-2356, doi:10.1016/j.ymthe.2018.07.011 (2018).
- 188 Bulcha, J. T., Wang, Y., Ma, H., Tai, P. W. L. & Gao, G. Viral vector platforms within the gene therapy landscape. *Signal Transduct Target Ther* **6**, 53, doi:10.1038/s41392-021-00487-6 (2021).
- 189 Lim, K. R. Q., Yoon, C. & Yokota, T. Applications of CRISPR/Cas9 for the Treatment of Duchenne Muscular Dystrophy. *J Pers Med* **8**, doi:10.3390/jpm8040038 (2018).

- 190 Doudna, J. A. & Gersbach, C. A. Genome editing: the end of the beginning. *Genome Biol* **16**, 292, doi:10.1186/s13059-015-0860-5 (2015).
- 191 Tabebordbar, M. *et al.* In vivo gene editing in dystrophic mouse muscle and muscle stem cells. *Science* **351**, 407-411, doi:10.1126/science.aad5177 (2016).
- 192 Long, C. *et al.* Postnatal genome editing partially restores dystrophin expression in a mouse model of muscular dystrophy. *Science* **351**, 400-403, doi:10.1126/science.aad5725 (2016).
- 193 Darabi, R. *et al.* Functional skeletal muscle regeneration from differentiating embryonic stem cells. *Nat Med* **14**, 134-143, doi:10.1038/nm1705 (2008).
- 194 Kim, J. *et al.* Expansion and Purification Are Critical for the Therapeutic Application of Pluripotent Stem Cell-Derived Myogenic Progenitors. *Stem Cell Reports* **9**, 12-22, doi:10.1016/j.stemcr.2017.04.022 (2017).
- 195 Chal, J. *et al.* Differentiation of pluripotent stem cells to muscle fiber to model Duchenne muscular dystrophy. *Nat Biotechnol* **33**, 962-969, doi:10.1038/nbt.3297 (2015).
- 196 Kodaka, Y., Rabu, G. & Asakura, A. Skeletal Muscle Cell Induction from Pluripotent Stem Cells. *Stem Cells Int* **2017**, 1376151, doi:10.1155/2017/1376151 (2017).
- 197 Darabi, R. *et al.* Human ES- and iPS-derived myogenic progenitors restore DYSTROPHIN and improve contractility upon transplantation in dystrophic mice. *Cell Stem Cell* **10**, 610-619, doi:10.1016/j.stem.2012.02.015 (2012).
- 198 Chan, S. S. *et al.* Skeletal Muscle Stem Cells from PSC-Derived Teratomas Have Functional Regenerative Capacity. *Cell Stem Cell* **23**, 74-85 e76, doi:10.1016/j.stem.2018.06.010 (2018).
- 199 Pappas, M. P., Xie, N., Penaloza, J. S. & Chan, S. S. K. Defining the Skeletal Myogenic Lineage in Human Pluripotent Stem Cell-Derived Teratomas. *Cells* **11**, doi:10.3390/cells11091589 (2022).
- 200 Xie, N. *et al.* In vitro expanded skeletal myogenic progenitors from pluripotent stem cell-derived teratomas have high engraftment capacity. *Stem Cell Reports* **16**, 2900-2912, doi:10.1016/j.stemcr.2021.10.014 (2021).
- 201 Davis, R. L., Weintraub, H. & Lassar, A. B. Expression of a single transfected cDNA converts fibroblasts to myoblasts. *Cell* **51**, 987-1000, doi:10.1016/0092-8674(87)90585-x (1987).
- 202 Bar-Nur, O. *et al.* Direct Reprogramming of Mouse Fibroblasts into Functional Skeletal Muscle Progenitors. *Stem Cell Reports* **10**, 1505-1521, doi:10.1016/j.stemcr.2018.04.009 (2018).
- 203 Domenig, S. A. *et al.* CRISPR/Cas9 editing of directly reprogrammed myogenic progenitors restores dystrophin expression in a mouse model of muscular dystrophy. *Stem Cell Reports* **17**, 321-336, doi:10.1016/j.stemcr.2021.12.003 (2022).
- 204 Montarras, D. *et al.* Direct isolation of satellite cells for skeletal muscle regeneration. *Science* **309**, 2064-2067, doi:10.1126/science.1114758 (2005).

- 205 Garcia, S. M. *et al.* High-Yield Purification, Preservation, and Serial Transplantation of Human Satellite Cells. *Stem Cell Reports* **10**, 1160-1174, doi:10.1016/j.stemcr.2018.01.022 (2018).
- 206 Greising, S. M., Weiner, J. I., Garry, D. J., Sachs, D. H. & Garry, M. G. Human muscle in gene edited pigs for treatment of volumetric muscle loss. *Front Genet* **13**, 948496, doi:10.3389/fgene.2022.948496 (2022).
- 207 Ferrer, A., Wells, K. E. & Wells, D. J. Immune responses to dystropin: implications for gene therapy of Duchenne muscular dystrophy. *Gene Ther* **7**, 1439-1446, doi:10.1038/sj.gt.3301259 (2000).
- 208 Maffioletti, S. M., Noviello, M., English, K. & Tedesco, F. S. Stem cell transplantation for muscular dystrophy: the challenge of immune response. *Biomed Res Int* **2014**, 964010, doi:10.1155/2014/964010 (2014).
- 209 Gilchrist, S. C., Ontell, M. P., Kochanek, S. & Clemens, P. R. Immune response to full-length dystrophin delivered to Dmd muscle by a high-capacity adenoviral vector. *Mol Ther* **6**, 359-368, doi:10.1006/mthe.2002.0675 (2002).
- 210 Selvaraj, S., Kyba, M. & Perlingeiro, R. C. R. Pluripotent Stem Cell-Based Therapeutics for Muscular Dystrophies. *Trends Mol Med* **25**, 803-816, doi:10.1016/j.molmed.2019.07.004 (2019).
- 211 Saitou, M. & Miyachi, H. Gametogenesis from Pluripotent Stem Cells. *Cell Stem Cell* **18**, 721-735, doi:10.1016/j.stem.2016.05.001 (2016).
- 212 Wu, J. *et al.* Stem cells and interspecies chimaeras. *Nature* **540**, 51-59, doi:10.1038/nature20573 (2016).
- 213 Chen, J. *et al.* Generation of normal lymphocyte populations by Rb-deficient embryonic stem cells. *Curr Biol* **3**, 405-413, doi:10.1016/0960-9822(93)90347-q (1993).
- 214 Kitahara, A. *et al.* Generation of Lungs by Blastocyst Complementation in Apneumatic Fgf10-Deficient Mice. *Cell Rep* **31**, 107626, doi:10.1016/j.celrep.2020.107626 (2020).
- 215 Hamanaka, S. *et al.* Generation of Vascular Endothelial Cells and Hematopoietic Cells by Blastocyst Complementation. *Stem Cell Reports* **11**, 988-997, doi:10.1016/j.stemcr.2018.08.015 (2018).
- 216 Yamaguchi, T. *et al.* Interspecies organogenesis generates autologous functional islets. *Nature* **542**, 191-196, doi:10.1038/nature21070 (2017).
- 217 Miura, K., Matoba, S., Hirose, M. & Ogura, A. Generation of chimeric mice with spermatozoa fully derived from embryonic stem cells using a triple-target CRISPR method for Nanos3dagger. *Biol Reprod*, doi:10.1093/biolre/ioaa176 (2020).
- 218 Beard, C., Hochedlinger, K., Plath, K., Wutz, A. & Jaenisch, R. Efficient method to generate single-copy transgenic mice by site-specific integration in embryonic stem cells. *Genesis* **44**, 23-28, doi:10.1002/gene.20180 (2006).
- 219 Sambasivan, R. *et al.* Distinct regulatory cascades govern extraocular and pharyngeal arch muscle progenitor cell fates. *Dev Cell* **16**, 810-821, doi:10.1016/j.devcel.2009.05.008 (2009).

- 220 Bar-Nur, O. *et al.* Small molecules facilitate rapid and synchronous iPSC generation. *Nat Methods* **11**, 1170-1176, doi:10.1038/nmeth.3142 (2014).
- 221 Sommer, C. A. *et al.* Induced pluripotent stem cell generation using a single lentiviral stem cell cassette. *Stem Cells* **27**, 543-549, doi:10.1634/stemcells.2008-1075 (2009).
- 222 Tong, C., Li, P., Wu, N. L., Yan, Y. & Ying, Q. L. Production of p53 gene knockout rats by homologous recombination in embryonic stem cells. *Nature* **467**, 211-213, doi:10.1038/nature09368 (2010).
- 223 Hirabayashi, M. *et al.* Offspring derived from intracytoplasmic injection of transgenic rat sperm. *Transgenic Res* **11**, 221-228, doi:10.1023/a:1015210604906 (2002).
- 224 Men, H. & Bryda, E. C. Derivation of a germline competent transgenic Fischer 344 embryonic stem cell line. *PLoS One* **8**, e56518, doi:10.1371/journal.pone.0056518 (2013).
- 225 Lois, C., Hong, E. J., Pease, S., Brown, E. J. & Baltimore, D. Germline transmission and tissue-specific expression of transgenes delivered by lentiviral vectors. *Science* **295**, 868-872, doi:10.1126/science.1067081 (2002).
- 226 Zheng, C., Ballard, E. B. & Wu, J. The road to generating transplantable organs: from blastocyst complementation to interspecies chimeras. *Development* **148**, doi:10.1242/dev.195792 (2021).
- 227 Ballard, E. B. & Wu, J. Growth Competition in Interspecies Chimeras: A New Paradigm for Blastocyst Complementation. *Cell Stem Cell* **28**, 3-5, doi:10.1016/j.stem.2020.12.011 (2021).
- 228 Zheng, C. *et al.* Cell competition constitutes a barrier for interspecies chimerism. *Nature* **592**, 272-276, doi:10.1038/s41586-021-03273-0 (2021).
- 229 Masaki, H. *et al.* Inhibition of Apoptosis Overcomes Stage-Related Compatibility Barriers to Chimera Formation in Mouse Embryos. *Cell Stem Cell* **19**, 587-592, doi:10.1016/j.stem.2016.10.013 (2016).
- 230 Nishimura, T. *et al.* Generation of Functional Organs Using a Cell-Competitive Niche in Intra- and Inter-species Rodent Chimeras. *Cell Stem Cell* **28**, 141-149 e143, doi:10.1016/j.stem.2020.11.019 (2021).
- 231 Chen, Y., Spitzer, S., Agathou, S., Karadottir, R. T. & Smith, A. Gene Editing in Rat Embryonic Stem Cells to Produce In Vitro Models and In Vivo Reporters. *Stem Cell Reports* **9**, 1262-1274, doi:10.1016/j.stemcr.2017.09.005 (2017).
- 232 Ostermeier, G. C., Wiles, M. V., Farley, J. S. & Taft, R. A. Conserving, Distributing and Managing Genetically Modified Mouse Lines by Sperm Cryopreservation. *PLOS ONE* **3**, e2792, doi:10.1371/journal.pone.0002792 (2008).
- 233 Men, H., Stone, B. J. & Bryda, E. C. Media optimization to promote rat embryonic development to the blastocyst stage in vitro. *Theriogenology* **151**, 81-85, doi:10.1016/j.theriogenology.2020.03.007 (2020).
- 234 Ogura, A. & Yanagimachi, R. Round spermatid nuclei injected into hamster oocytes from pronuclei and participate in syngamy. *Biol Reprod* **48**, 219-225, doi:10.1095/biolreprod48.2.219 (1993).

- 235 Griffin, J. Methods of sperm DNA extraction for genetic and epigenetic studies. *Methods Mol Biol* **927**, 379-384, doi:10.1007/978-1-62703-038-0\_32 (2013).
- 236 Hatakeyama, M. *et al.* SUSHI: an exquisite recipe for fully documented, reproducible and reusable NGS data analysis. *BMC Bioinformatics* **17**, 228, doi:10.1186/s12859-016-1104-8 (2016).
- 237 Qi, W., Schlapbach, R. & Rehrauer, H. RNA-Seq Data Analysis: From Raw Data Quality Control to Differential Expression Analysis. *Methods Mol Biol* **1669**, 295-307, doi:10.1007/978-1-4939-7286-9\_23 (2017).
- 238 Chen, S., Zhou, Y., Chen, Y. & Gu, J. fastp: an ultra-fast all-in-one FASTQ preprocessor. *Bioinformatics* **34**, i884-i890, doi:10.1093/bioinformatics/bty560 (2018).
- 239 Dobin, A. *et al.* STAR: ultrafast universal RNA-seq aligner. *Bioinformatics* **29**, 15-21, doi:10.1093/bioinformatics/bts635 (2013).
- 240 Liao, Y., Smyth, G. K. & Shi, W. The Subread aligner: fast, accurate and scalable read mapping by seed-and-vote. *Nucleic Acids Res* **41**, e108, doi:10.1093/nar/gkt214 (2013).
- 241 Robinson, M. D., McCarthy, D. J. & Smyth, G. K. edgeR: a Bioconductor package for differential expression analysis of digital gene expression data. *Bioinformatics* **26**, 139-140, doi:10.1093/bioinformatics/btp616 (2010).
- 242 Zheng, G. X. *et al.* Massively parallel digital transcriptional profiling of single cells. *Nat Commun* **8**, 14049, doi:10.1038/ncomms14049 (2017).
- 243 Butler, A., Hoffman, P., Smibert, P., Papalexi, E. & Satija, R. Integrating single-cell transcriptomic data across different conditions, technologies, and species. *Nat Biotechnol* **36**, 411-420, doi:10.1038/nbt.4096 (2018).
- 244 Stuart, T. *et al.* Comprehensive Integration of Single-Cell Data. *Cell* **177**, 1888-1902 e1821, doi:10.1016/j.cell.2019.05.031 (2019).
- 245 Franzen, O., Gan, L. M. & Bjorkegren, J. L. M. PanglaoDB: a web server for exploration of mouse and human single-cell RNA sequencing data. *Database (Oxford)* **2019**, doi:10.1093/database/baz046 (2019).
- 246 Han, X. *et al.* Mapping the Mouse Cell Atlas by Microwell-Seq. *Cell* **173**, 1307, doi:10.1016/j.cell.2018.05.012 (2018).
- 247 Rinaldi, V. D. *et al.* An atlas of cell types in the mouse epididymis and vas deferens. *Elife* **9**, doi:10.7554/eLife.55474 (2020).
- 248 Valli, H. *et al.* Fluorescence- and magnetic-activated cell sorting strategies to isolate and enrich human spermatogonial stem cells. *Fertil Steril* **102**, 566-580 e567, doi:10.1016/j.fertnstert.2014.04.036 (2014).
- 249 Tan, G. *et al.* uzh/ezRun: v3.14.1 for Bioconductor 3.14 (3.14.1). doi:https://doi.org/10.5281/zenodo.5760369 (2021).
- 250 Green, C. D. *et al.* A Comprehensive Roadmap of Murine Spermatogenesis Defined by Single-Cell RNA-Seq. *Dev Cell* **46**, 651-667 e610, doi:10.1016/j.devcel.2018.07.025 (2018).
- 251 Grive, K. J. *et al.* Dynamic transcriptome profiles within spermatogonial and spermatocyte populations during postnatal testis maturation revealed by single-

- cell sequencing. *PLoS Genet* **15**, e1007810, doi:10.1371/journal.pgen.1007810 (2019).
- 252 Cao, J. *et al.* The single-cell transcriptional landscape of mammalian organogenesis. *Nature* **566**, 496-502, doi:10.1038/s41586-019-0969-x (2019).
- 253 Qiu, X. *et al.* Reversed graph embedding resolves complex single-cell trajectories. *Nat Methods* **14**, 979-982, doi:10.1038/nmeth.4402 (2017).
- 254 Trapnell, C. *et al.* The dynamics and regulators of cell fate decisions are revealed by pseudotemporal ordering of single cells. *Nat Biotechnol* **32**, 381-386, doi:10.1038/nbt.2859 (2014).
- 255 Almada, A. E. & Wagers, A. J. Molecular circuitry of stem cell fate in skeletal muscle regeneration, ageing and disease. *Nat Rev Mol Cell Biol* **17**, 267-279, doi:10.1038/nrm.2016.7 (2016).
- 256 Yin, H., Price, F. & Rudnicki, M. A. Satellite cells and the muscle stem cell niche. *Physiol Rev* **93**, 23-67, doi:10.1152/physrev.00043.2011 (2013).
- 257 Hoffman, E. P., Brown, R. H., Jr. & Kunkel, L. M. Dystrophin: the protein product of the Duchenne muscular dystrophy locus. *Cell* **51**, 919-928 (1987).
- 258 Koenig, M. *et al.* Complete cloning of the Duchenne muscular dystrophy (DMD) cDNA and preliminary genomic organization of the DMD gene in normal and affected individuals. *Cell* **50**, 509-517 (1987).
- 259 Dowling, J. J., Weihl, C. C. & Spencer, M. J. Molecular and cellular basis of genetically inherited skeletal muscle disorders. *Nat Rev Mol Cell Biol* **22**, 713-732, doi:10.1038/s41580-021-00389-z (2021).
- 260 Yiu, E. M. & Kornberg, A. J. Duchenne muscular dystrophy. *J Paediatr Child Health* **51**, 759-764, doi:10.1111/jpc.12868 (2015).
- 261 Hanlon, K. S. *et al.* High levels of AAV vector integration into CRISPR-induced DNA breaks. *Nat Commun* **10**, 4439, doi:10.1038/s41467-019-12449-2 (2019).
- 262 Nelson, C. E. *et al.* Long-term evaluation of AAV-CRISPR genome editing for Duchenne muscular dystrophy. *Nat Med* **25**, 427-432, doi:10.1038/s41591-019-0344-3 (2019).
- 263 Li, A. *et al.* AAV-CRISPR Gene Editing Is Negated by Pre-existing Immunity to Cas9. *Mol Ther* **28**, 1432-1441, doi:10.1016/j.ymthe.2020.04.017 (2020).
- 264 Riviere, C., Danos, O. & Douar, A. M. Long-term expression and repeated administration of AAV type 1, 2 and 5 vectors in skeletal muscle of immunocompetent adult mice. *Gene Ther* **13**, 1300-1308, doi:10.1038/sj.gt.3302766 (2006).
- 265 Judson, R. N. & Rossi, F. M. V. Towards stem cell therapies for skeletal muscle repair. *NPJ Regen Med* **5**, 10, doi:10.1038/s41536-020-0094-3 (2020).
- 266 Partridge, T. A., Morgan, J. E., Coulton, G. R., Hoffman, E. P. & Kunkel, L. M. Conversion of mdx myofibres from dystrophin-negative to -positive by injection of normal myoblasts. *Nature* **337**, 176-179, doi:10.1038/337176a0 (1989).
- 267 Partridge, T. The current status of myoblast transfer. *Neurol Sci* **21**, S939-942, doi:10.1007/s100720070007 (2000).

- 268 Skuk, D. *et al.* Dystrophin expression in myofibers of Duchenne muscular dystrophy patients following intramuscular injections of normal myogenic cells. *Mol Ther* **9**, 475-482, doi:10.1016/j.ymthe.2003.11.023 (2004).
- 269 Ito, N., Kii, I., Shimizu, N., Tanaka, H. & Takeda, S. Direct reprogramming of fibroblasts into skeletal muscle progenitor cells by transcription factors enriched in undifferentiated subpopulation of satellite cells. *Sci Rep* **7**, 8097, doi:10.1038/s41598-017-08232-2 (2017).
- 270 Shelton, M. *et al.* Derivation and expansion of PAX7-positive muscle progenitors from human and mouse embryonic stem cells. *Stem Cell Reports* **3**, 516-529, doi:10.1016/j.stemcr.2014.07.001 (2014).
- 271 Sherwood, R. I. *et al.* Isolation of adult mouse myogenic progenitors: functional heterogeneity of cells within and engrafting skeletal muscle. *Cell* **119**, 543-554, doi:10.1016/j.cell.2004.10.021 (2004).
- 272 Zvick, J. *et al.* Exclusive generation of rat spermatozoa in sterile mice utilizing blastocyst complementation with pluripotent stem cells. *Stem Cell Reports*, doi:10.1016/j.stemcr.2022.07.005 (2022).
- 273 Murphy, M. M., Lawson, J. A., Mathew, S. J., Hutcheson, D. A. & Kardon, G. Satellite cells, connective tissue fibroblasts and their interactions are crucial for muscle regeneration. *Development* **138**, 3625-3637, doi:10.1242/dev.064162 (2011).
- 274 Voehringer, D., Liang, H. E. & Locksley, R. M. Homeostasis and effector function of lymphopenia-induced "memory-like" T cells in constitutively T cell-depleted mice. *J Immunol* **180**, 4742-4753, doi:10.4049/jimmunol.180.7.4742 (2008).
- 275 Neal, A., Boldrin, L. & Morgan, J. E. The satellite cell in male and female, developing and adult mouse muscle: distinct stem cells for growth and regeneration. *PLoS One* **7**, e37950, doi:10.1371/journal.pone.0037950 (2012).
- 276 Maesner, C. C., Almada, A. E. & Wagers, A. J. Established cell surface markers efficiently isolate highly overlapping populations of skeletal muscle satellite cells by fluorescence-activated cell sorting. *Skelet Muscle* **6**, 35, doi:10.1186/s13395-016-0106-6 (2016).
- 277 Bulfield, G., Siller, W. G., Wight, P. A. & Moore, K. J. X chromosome-linked muscular dystrophy (mdx) in the mouse. *Proc Natl Acad Sci U S A* **81**, 1189-1192, doi:10.1073/pnas.81.4.1189 (1984).
- 278 Chal, J. *et al.* Recapitulating early development of mouse musculoskeletal precursors of the paraxial mesoderm in vitro. *Development* **145**, doi:10.1242/dev.157339 (2018).
- 279 Kim, I. *et al.* Integrative molecular roadmap for direct conversion of fibroblasts into myocytes and myogenic progenitor cells. *Sci Adv* **8**, eabj4928, doi:10.1126/sciadv.abj4928 (2022).
- 280 Chapman, V. M., Miller, D. R., Armstrong, D. & Caskey, C. T. Recovery of induced mutations for X chromosome-linked muscular dystrophy in mice. *Proc Natl Acad Sci U S A* **86**, 1292-1296, doi:10.1073/pnas.86.4.1292 (1989).



- 281 Im, W. B. *et al.* Differential expression of dystrophin isoforms in strains of mdx mice with different mutations. *Hum Mol Genet* **5**, 1149-1153, doi:10.1093/hmg/5.8.1149 (1996).
- 282 Wang, G. *et al.* Generation of Pulmonary Endothelial Progenitor Cells for Cell-based Therapy Using Interspecies Mouse-Rat Chimeras. *Am J Respir Crit Care Med* **204**, 326-338, doi:10.1164/rccm.202003-0758OC (2021).
- 283 Yang, Y. *et al.* Derivation of Pluripotent Stem Cells with In Vivo Embryonic and Extraembryonic Potency. *Cell* **169**, 243-257 e225, doi:10.1016/j.cell.2017.02.005 (2017).
- 284 Kano, M., Mizutani, E., Homma, S., Masaki, H. & Nakauchi, H. Xenotransplantation and interspecies organogenesis: current status and issues. *Front Endocrinol (Lausanne)* **13**, 963282, doi:10.3389/fendo.2022.963282 (2022).
- 285 Hashimoto, H. *et al.* Development of blastocyst complementation technology without contributions to gametes and the brain. *Exp Anim* **68**, 361-370, doi:10.1538/expanim.18-0173 (2019).
- 286 De Los Angeles, A. *et al.* Why it is important to study human-monkey embryonic chimeras in a dish. *Nat Methods* **19**, 914-919, doi:10.1038/s41592-022-01571-7 (2022).
- 287 Han, L. *et al.* Distinctive Clinical and Pathologic Features of Immature Teratomas Arising from Induced Pluripotent Stem Cell-Derived Beta Cell Injection in a Diabetes Patient. *Stem Cells Dev* **31**, 97-101, doi:10.1089/scd.2021.0255 (2022).
- 288 Xi, H. *et al.* A Human Skeletal Muscle Atlas Identifies the Trajectories of Stem and Progenitor Cells across Development and from Human Pluripotent Stem Cells. *Cell Stem Cell* **27**, 158-176 e110, doi:10.1016/j.stem.2020.04.017 (2020).
- 289 Bray, N. L., Pimentel, H., Melsted, P. & Pachter, L. Near-optimal probabilistic RNA-seq quantification. *Nat Biotechnol* **34**, 525-527, doi:10.1038/nbt.3519 (2016).
- 290 Oji, A. *et al.* CRISPR/Cas9 mediated genome editing in ES cells and its application for chimeric analysis in mice. *Sci Rep* **6**, 31666, doi:10.1038/srep31666 (2016).
- 291 Onishi, A. & Mikami, H. [The reproductive performance of XX/XY male chimeric mice]. *Jikken Dobutsu* **34**, 433-437, doi:10.1538/expanim1978.34.4\_433 (1985).
- 292 Koopman, P., Gubbay, J., Vivian, N., Goodfellow, P. & Lovell-Badge, R. Male development of chromosomally female mice transgenic for Sry. *Nature* **351**, 117-121, doi:10.1038/351117a0 (1991).
- 293 Vidal, V. P., Chaboissier, M. C., de Rooij, D. G. & Schedl, A. Sox9 induces testis development in XX transgenic mice. *Nat Genet* **28**, 216-217, doi:10.1038/90046 (2001).
- 294 Prokop, J. W. *et al.* Transcriptional analysis of the multiple Sry genes and developmental program at the onset of testis differentiation in the rat. *Biol Sex Differ* **11**, 28, doi:10.1186/s13293-020-00305-8 (2020).
- 295 Shaha, C., Tripathi, R. & Mishra, D. P. Male germ cell apoptosis: regulation and biology. *Philos Trans R Soc Lond B Biol Sci* **365**, 1501-1515, doi:10.1098/rstb.2009.0124 (2010).

- 296 Tomoiaga, D. *et al.* Single-cell sperm transcriptomes and variants from fathers of children with and without autism spectrum disorder. *NPJ Genom Med* **5**, 14, doi:10.1038/s41525-020-0117-4 (2020).
- 297 Nakagata, N., Mikoda, N., Nakao, S., Nakatsukasa, E. & Takeo, T. Establishment of sperm cryopreservation and in vitro fertilisation protocols for rats. *Sci Rep* **10**, 93, doi:10.1038/s41598-019-57090-7 (2020).
- 298 Seita, Y., Sugio, S., Ito, J. & Kashiwazaki, N. Generation of live rats produced by in vitro fertilization using cryopreserved spermatozoa. *Biol Reprod* **80**, 503-510, doi:10.1095/biolreprod.108.072918 (2009).
- 299 Kaneko, T., Kimura, S. & Nakagata, N. Offspring derived from oocytes injected with rat sperm, frozen or freeze-dried without cryoprotection. *Theriogenology* **68**, 1017-1021, doi:10.1016/j.theriogenology.2007.07.017 (2007).
- 300 Hayama, T. *et al.* Practical selection methods for rat and mouse round spermatids without DNA staining by flow cytometric cell sorting. *Mol Reprod Dev* **83**, 488-496, doi:10.1002/mrd.22644 (2016).
- 301 Saitou, M. & Miyauchi, H. Gametogenesis from Pluripotent Stem Cells. *Cell Stem Cell* **18**, 721-735, doi:10.1016/j.stem.2016.05.001 (2016).
- 302 Dobrinski, I., Avarbock, M. R. & Brinster, R. L. Transplantation of germ cells from rabbits and dogs into mouse testes. *Biol Reprod* **61**, 1331-1339, doi:10.1095/biolreprod61.5.1331 (1999).
- 303 Nagano, M., McCarrey, J. R. & Brinster, R. L. Primate spermatogonial stem cells colonize mouse testes. *Biol Reprod* **64**, 1409-1416, doi:10.1095/biolreprod64.5.1409 (2001).
- 304 Zhang, L. *et al.* Reprogramming of Sertoli cells to fetal-like Leydig cells by Wt1 ablation. *Proc Natl Acad Sci U S A* **112**, 4003-4008, doi:10.1073/pnas.1422371112 (2015).
- 305 Xu, C. *et al.* Differentiation roadmap of embryonic Sertoli cells derived from mouse embryonic stem cells. *Stem Cell Res Ther* **10**, 81, doi:10.1186/s13287-019-1180-6 (2019).
- 306 Seol, D. W., Park, S., Shin, E. Y., Chang, J. H. & Lee, D. R. In Vitro Derivation of Functional Sertoli-Like Cells from Mouse Embryonic Stem Cells. *Cell Transplant* **27**, 1523-1534, doi:10.1177/0963689718797053 (2018).
- 307 Liang, J. *et al.* Induction of Sertoli-like cells from human fibroblasts by NR5A1 and GATA4. *Elife* **8**, doi:10.7554/eLife.48767 (2019).
- 308 Li, Z. H., Lu, J. D., Li, S. J., Chen, H. L. & Su, Z. J. Generation of Leydig-like cells: approaches, characterization, and challenges. *Asian J Androl* **24**, 335-344, doi:10.4103/aja202193 (2022).
- 309 Sarraj, M. A. *et al.* Fetal testis dysgenesis and compromised Leydig cell function in Tgfbr3 (beta glycan) knockout mice. *Biol Reprod* **82**, 153-162, doi:10.1095/biolreprod.109.078766 (2010).
- 310 Barrionuevo, F. *et al.* Homozygous inactivation of Sox9 causes complete XY sex reversal in mice. *Biol Reprod* **74**, 195-201, doi:10.1095/biolreprod.105.045930 (2006).

- 311 Franca, L. R., Ogawa, T., Avarbock, M. R., Brinster, R. L. & Russell, L. D. Germ cell genotype controls cell cycle during spermatogenesis in the rat. *Biol Reprod* **59**, 1371-1377, doi:10.1095/biolreprod59.6.1371 (1998).
- 312 Clermont, Y. & Harvey, S. C. Duration of the Cycle of the Seminiferous Epithelium of Normal, Hypophysectomized and Hypophysectomized-Hormone Treated Albino Rats. *Endocrinology* **76**, 80-89, doi:10.1210/endo-76-1-80 (1965).
- 313 O'Donnell, L., Nicholls, P. K., O'Bryan, M. K., McLachlan, R. I. & Stanton, P. G. Spermiation: The process of sperm release. *Spermatogenesis* **1**, 14-35, doi:10.4161/spmg.1.1.14525 (2011).
- 314 Fayomi, A. P. & Orwig, K. E. Spermatogonial stem cells and spermatogenesis in mice, monkeys and men. *Stem Cell Res* **29**, 207-214, doi:10.1016/j.scr.2018.04.009 (2018).
- 315 Snyder, R. L. Collection of mouse semen by electroejaculation. *Anat Rec* **155**, 11-14, doi:10.1002/ar.1091550103 (1966).
- 316 Boersma, A., Olszanska, O., Walter, I. & Rulicke, T. Microsurgical and Percutaneous Epididymal Sperm Aspiration for Sperm Collection from Live Mice. *J Am Assoc Lab Anim Sci* **54**, 471-477 (2015).
- 317 Inoue, R., Harada, K., Wakayama, S., Ooga, M. & Wakayama, T. Improvement of a twice collection method of mouse oocytes by surgical operation. *J Reprod Dev* **66**, 427-433, doi:10.1262/jrd.2020-059 (2020).
- 318 Byers, S. L., Wiles, M. V. & Taft, R. A. Surgical oocyte retrieval (SOR): a method for collecting mature mouse oocytes without euthanasia. *J Am Assoc Lab Anim Sci* **48**, 44-51 (2009).
- 319 McKellar, D. W. *et al.* Large-scale integration of single-cell transcriptomic data captures transitional progenitor states in mouse skeletal muscle regeneration. *Commun Biol* **4**, 1280, doi:10.1038/s42003-021-02810-x (2021).
- 320 Akhlaghpour, A. *et al.* Chicken Interspecies Chimerism Unveils Human Pluripotency. *Stem Cell Reports* **16**, 39-55, doi:10.1016/j.stemcr.2020.11.014 (2021).
- 321 Tajbakhsh, S. Skeletal muscle stem cells in developmental versus regenerative myogenesis. *J Intern Med* **266**, 372-389, doi:10.1111/j.1365-2796.2009.02158.x (2009).
- 322 Sambasivan, R. & Tajbakhsh, S. Skeletal muscle stem cell birth and properties. *Semin Cell Dev Biol* **18**, 870-882, doi:10.1016/j.semcdb.2007.09.013 (2007).
- 323 Eberli, D., Aboushwareb, T., Soker, S., Yoo, J. J. & Atala, A. Muscle precursor cells for the restoration of irreversibly damaged sphincter function. *Cell Transplant* **21**, 2089-2098, doi:10.3727/096368911X623835 (2012).
- 324 Boyer, O. *et al.* Autologous Myoblasts for the Treatment of Fecal Incontinence: Results of a Phase 2 Randomized Placebo-controlled Study (MIAS). *Ann Surg* **267**, 443-450, doi:10.1097/SLA.0000000000002268 (2018).
- 325 Hardy, D. *et al.* Comparative Study of Injury Models for Studying Muscle Regeneration in Mice. *PLoS One* **11**, e0147198, doi:10.1371/journal.pone.0147198 (2016).

- 326 Gross, J. G. & Morgan, J. E. Muscle precursor cells injected into irradiated mdx mouse muscle persist after serial injury. *Muscle Nerve* **22**, 174-185, doi:10.1002/(sici)1097-4598(199902)22:2<174::aid-mus5>3.0.co;2-s (1999).
- 327 Ittner, L. M. & Gotz, J. Pronuclear injection for the production of transgenic mice. *Nat Protoc* **2**, 1206-1215, doi:10.1038/nprot.2007.145 (2007).
- 328 Relaix, F., Rocancourt, D., Mansouri, A. & Buckingham, M. A Pax3/Pax7-dependent population of skeletal muscle progenitor cells. *Nature* **435**, 948-953, doi:10.1038/nature03594 (2005).
- 329 Aloisio, G. M. *et al.* PAX7 expression defines germline stem cells in the adult testis. *J Clin Invest* **124**, 3929-3944, doi:10.1172/JCI75943 (2014).
- 330 Suchy, F., Yamaguchi, T. & Nakauchi, H. iPSC-Derived Organs In Vivo: Challenges and Promise. *Cell Stem Cell* **22**, 21-24, doi:10.1016/j.stem.2017.12.003 (2018).
- 331 Miyagoe-Suzuki, Y. & Takeda, S. Skeletal muscle generated from induced pluripotent stem cells - induction and application. *World J Stem Cells* **9**, 89-97, doi:10.4252/wjsc.v9.i6.89 (2017).
- 332 Mendell, J. R. *et al.* Dystrophin immunity in Duchenne's muscular dystrophy. *N Engl J Med* **363**, 1429-1437, doi:10.1056/NEJMoa1000228 (2010).
- 333 Berger, J. *et al.* Effect of Ataluren on dystrophin mutations. *J Cell Mol Med* **24**, 6680-6689, doi:10.1111/jcmm.15319 (2020).
- 334 Amoyel, M. & Bach, E. A. Cell competition: how to eliminate your neighbours. *Development* **141**, 988-1000, doi:10.1242/dev.079129 (2014).
- 335 Niu, D. *et al.* Inactivation of porcine endogenous retrovirus in pigs using CRISPR-Cas9. *Science* **357**, 1303-1307, doi:10.1126/science.aan4187 (2017).
- 336 Kobayashi, T., Kato-Itoh, M. & Nakauchi, H. Targeted organ generation using Mixl1-inducible mouse pluripotent stem cells in blastocyst complementation. *Stem Cells Dev* **24**, 182-189, doi:10.1089/scd.2014.0270 (2015).
- 337 Revah, O. *et al.* Maturation and circuit integration of transplanted human cortical organoids. *Nature* **610**, 319-326, doi:10.1038/s41586-022-05277-w (2022).
- 338 Hyun, I. *et al.* ISSCR guidelines for the transfer of human pluripotent stem cells and their direct derivatives into animal hosts. *Stem Cell Reports* **16**, 1409-1415, doi:10.1016/j.stemcr.2021.05.005 (2021).
- 339 Suter, S. M. In vitro gametogenesis: just another way to have a baby? *J Law Biosci* **3**, 87-119, doi:10.1093/jlb/lsv057 (2016).
- 340 Nagamatsu, G. & Hayashi, K. Stem cells, in vitro gametogenesis and male fertility. *Reproduction* **154**, F79-F91, doi:10.1530/REP-17-0510 (2017).
- 341 Nagashima, H. & Matsunari, H. Growing human organs in pigs-A dream or reality? *Theriogenology* **86**, 422-426, doi:10.1016/j.theriogenology.2016.04.056 (2016).
- 342 Cohen, M. A. *et al.* Human neural crest cells contribute to coat pigmentation in interspecies chimeras after in utero injection into mouse embryos. *Proc Natl Acad Sci U S A* **113**, 1570-1575, doi:10.1073/pnas.1525518113 (2016).
- 343 Vogel, G. STEM CELLS. NIH debates human-animal chimeras. *Science* **350**, 261-262, doi:10.1126/science.350.6258.261 (2015).

- 344 Umekage, M., Sato, Y. & Takasu, N. Overview: an iPS cell stock at CiRA. *Inflamm Regen* **39**, 17, doi:10.1186/s41232-019-0106-0 (2019).
- 345 Xu, H. *et al.* Targeted Disruption of HLA Genes via CRISPR-Cas9 Generates iPSCs with Enhanced Immune Compatibility. *Cell Stem Cell* **24**, 566-578 e567, doi:10.1016/j.stem.2019.02.005 (2019).